การเพิ่มการละลายของเมลอกซิแคมโดยการพ่นแห้งและการทำให้แห้งแบบเย็นเยือกแข็งร่วมกับเบต้าไซโคลเด็กซ์ตริน

นางสาว เพชรรัตน์ กรอนันต์สิริ

วิทยานิพนธ์นี้เป็นส่วนหนึ่งของการศึกษาตามหลักสูตรปริญญาเภสัชศาสตรมหาบัณฑิต
สาขาวิชาเภสัชอุตสาหกรรม ภาควิชาเภสัชอุตสาหกรรม
คณะเภสัชศาสตร์ จุฬาลงกรณ์มหาวิทยาลัย
ปีการศึกษา 2547

ISBN 974-53-1890-6

DISSOLUTION ENHANCEMENT OF MELOXICAM BY CO-SPRAY DRYING AND CO-FREEZE DRYING WITH β-CYCLODEXTRIN

Miss Petcharat Kornanansiri

A Thesis Submitted in Partial Fulfillment of the Requirements
for the Degree of Master of Science in Pharmacy
Department of Manufacturing Pharmacy
Faculty of Pharmaceutical Sciences
Chulalongkorn University
Academic Year 2004

ISBN 974-53-1890-6

Thesis Title	DISSOLUTION ENHANCEMENT OF MELOXICAM BY CO-SPRAY DRYING AND CO-FREEZE DRYING WITH β-CYCLODEXTRIN
By	Miss Petcharat Kornanansiri
Field of study	Manufacturing Pharmacy
Thesis Advisor	Associate Professor Poj Kulvanich, Ph.D.

Accepted by the Faculty of Pharmacuetical Sciences, Chulalongkorn University in Partial Fulfillment of the Requirements for the Master's Degree

……Dean of the Faculty of Pharmaceutical Sciences
(Associate Professor Boonyong Tantisira, Ph.D.)

THESIS COMMITTEE

…… Chairman
(Associate Professor Parunee Thanomkiat, M. Pharm. St.)

…… Thesis Advisor
(Associate Professor Poj Kulvanich, Ph.D.)

……. Member
(Associate Professor Suchada Chutimaworapan, Ph.D.)

……. Member
(Narueporn Sutanthavibul, Ph.D.)

…….. Member
(Jittima Chatchawalsaisin, Ph.D.)

เพชรรัตน์ กรอนันต์สิริ : การเพิ่มการละลายของเมลอกซิแคม โดยการพ่นแห้ง และการทำให้แห้งแบบเย็นเยือกแข็งร่วมกับเบต้าไซโคลเด็กซ์ตริน (DISSOLUTION ENHANCEMENT OF MELOXICAM BY CO-SPRAY DRYING AND CO-FREEZE DRYING WITH β-CYCLODEXTRIN) อ.ที่ปรึกษา: รศ. ดร. พจน์ กุลวานิช. 109 หน้า. ISBN 974-53-1890-6

วัตถุประสงค์ของงานวิจัยนี้คือ การศึกษาการเพิ่มการละลายของเมลอกซิแคมซึ่งเป็นยาที่มีค่าการละลายต่ำโดยการพ่นแห้งและการทำให้แห้งแบบเย็นเยือกแข็งร่วมกับเบต้าไซโคลเด็กซ์ตรินในอัตราส่วน 1:1 และ 1:2 โมล (เมลอกซิแคม : เบต้าไซโคลเด็กซ์ตริน) จากการศึกษาวัฏภาคการละลายพบว่าการละลายของเมลอกซิแคมในสารละลายเบต้าไซโคลเด็กซ์ตรินเป็นชนิด B_S คือการละลายของเมลอกซิแคมเพิ่มขึ้นตามความเข้มข้นของเบต้าไซโคลเด็กซ์ตรินที่เพิ่มขึ้นจนคงที่แล้วกลับลดลงซึ่งคาดว่าเกิดจากขีดจำกัดในการละลายน้ำของสารประกอบเชิงซ้อนที่เกิดขึ้น การศึกษาคุณสมบัติทางเคมีกายภาพของผงพ่นแห้งและผงแห้งแบบเย็นเยือกแข็งระหว่างเมลอกซิแคมกับเบต้าไซโคลเด็กซ์ตรินโดยวิธีเอกซ์เรย์ดิฟแฟรกโทเมตรี ฟูเรียร์ทรานฟอร์มอินฟราเรดสเปกโทรสโกปีและดิฟเฟอเรนเชียลสแกนนิงแคลอริเมตรีพบว่าสารประกอบเชิงซ้อนที่ได้จากกระบวนการพ่นแห้งอยู่ในรูปอสัณฐานโดยคาดว่าเกิดจากผลของกระบวนการพ่นแห้ง ในขณะที่รูปผลึกของสารประกอบเชิงซ้อนระหว่างเมลอกซิแคมและเบต้าไซโคลเด็กซ์ตรินที่เตรียมโดยวิธีการทำให้แห้งแบบเย็นเยือกแข็งอยู่ในรูปอสัณฐานไม่แท้ โดยอาจเกิดจากการที่โมเลกุลของโซเดียมไฮดรอกไซด์ เข้าไปแทรกในกระบวนการจัดเรียงตัวของโมเลกุลระหว่างเมลอกซิแคมและเบต้าไซโคลเด็กซ์ตริน ในการศึกษาการละลายของยาเม็ดเมลอกซิแคมในน้ำ กรดไฮโดรคลอริก 0.1 N พีเอช1.2 และสารละลายฟอสเฟตบัฟเฟอร์พีเอช6.8 พบว่าการพ่นแห้งและการทำให้แห้งแบบเย็นเยือกแข็งของยาร่วมกับเบต้าไซโคลเด็กซ์ตริน ในอัตราส่วน 1:1 และ 1:2 สามารถเพิ่มการละลายในตัวกลางดังกล่าวเมื่อเปรียบเทียบกับตัวยาเม็ดเมลอกซิแคมธรรมดาและยาเม็ดเมลอกซิแคมที่มีขายในท้องตลาดได้อย่างมีนัยสำคัญทางสถิติ

ภาควิชา.....เภสัชอุตสาหกรรม..... ลายมือชื่อนิสิต.....

สาขาวิชา.....เภสัชอุตสาหกรรม..... ลายมือชื่ออาจารย์ที่ปรึกษา.....

ปีการศึกษา.....2547..... ลายมือชื่ออาจารย์ที่ปรึกษาร่วม.....-.....

4576586633: MAJOR MANUFACTURING PHARMACY
KEY WORD: meloxicam / β-cyclodextrin / solubility / spray drying / freeze drying / lyophilization

PETCHARAT KORNANANSIRI: DISSOLUTION ENHANCEMENT OF MELOXICAM BY CO-SPRAY DRYING AND CO-FREEZE DRYING WITH β-CYCLODEXTRIN. THESIS ADVISOR: ASSOC. PROF. POJ KULVANICH, Ph.D., 109 pp. ISBN 974-53-1890-6

The purpose of this study was to enhance the solubility of meloxicam, which was sparingly soluble in water, by co-spray drying and co-freeze drying with β-cyclodextrin in the molar ratio 1:1 and 1:2 (meloxicam: β-cyclodextrin). From the phase solubility study, it was found that the phase solubility diagram of meloxicam in the presence of β-cyclodextrin could be classified as B_S-type which the solubility of meloxicam increased as the increasing concentration of β-cyclodextrin until reached the plateau and then decreased by the limited solubility of complexes. The physicochemical properties were characterized by X-ray diffractometry, Fourier transform Infrared spectroscopy, and differential scanning calorimetry. The results indicated that the meloxicam-β-cyclodextrin complex prepared by spray drying technique, existed in an amorphous form which might be caused by the spray drying process. The meloxicam-β-cyclodextrin complex prepared by freeze drying technique, expressed an amorphous form which might be attributed to the interruption of sodium hydroxide in a rearrangement of the complex. The dissolution studies which operated in deionized water, 0.1 N HCl pH 1.2, and phosphate buffer solutions pH 6.8 revealed that the use of co-spray drying and co-freeze drying with β-cyclodextrin in the molar ratio 1:1 and 1:2 could significantly enhance the dissolution of meloxicam tablet in those media in comparison to plain meloxicam tablet and commercial meloxicam tablet.

Department…….Manufacturing Pharmacy.. Student's name……..
Field of study…..…..Industrial Pharmacy…. Advisor's name…….
Academic year……..2004……. Co-advisor's name……-……

ACKNOWLEDGEMENT

First, and foremost, I would like to express my sincere gratitude to my thesis advisor, Associated Professor Poj Kulvanich, Ph.D. for not only his invaluable advice, guidance, encouragement, hearten and understanding but also his kindness and cheerfulness that make me feel deeply appreciated.

Special thanks are also extended to the Graduate School, Chulalongkorn University for granting partial financial support, Rama Production Co. Ltd., for their supplying β-cyclodextrin, and United Drug Co. Ltd, Siam Bhaesach Co. Ltd., for their supplying meloxicam in this study.

My gratitude is given to the staffs of laboratory group of Professor Yamamoto Keiji, Department of pharmaceutical technology, Chiba University; Sarintip Sooksai, Ph.D. and the staffs working in the Institute of Biotechnology and Genetic Engineering for the permission to use the equipments and their helpful, kindness and encouragement.

I wish to express deep appreciation for her kindness and encouragement to Narueporn Sutanthavibul, Ph.D. for spending her valuable time, comments, and suggestion.

The other special thanks were expressed to the staffs; my friends and my senior graduate student of the Department of Manufacturing Pharmacy and other people whose names have not mentioned for their assistance and encouragement firmly deserve acknowledgements.

Ultimately, I would like to express my infinite thanks and deepest gratitude to my family especially my parents for their endless love, care, understanding, encouragement, and support throughout these past years.

CONTENTS

Page

LIST OF TABLES

LIST OF FIGURES

LIST OF ABBREVIATIONS

%	percentage
β	beta
° C	degree Celsius (centrigrade)
CD	cyclodextrin
cm	centimeter(s)
DSC	differential scanning calorimetry
e.g.	for example, exempli gratia
et.al.	et alli, and others
FD	freeze dried meloxicam-β-cyclodextrin (in 0.05 N NaOH solution) powder
FD 1:1	freeze dried meloxicam-β-cyclodextrin (in 0.05 N NaOH solution) powder in the molar ratio 1:1 (meloxicam:β-cyclodextrin)
FD 1:2	freeze dried meloxicam-β-cyclodextrin (in 0.05 N NaOH solution) powder in the molar ratio 1:2 (meloxicam:β-cyclodextrin)
FDCD	freeze dried β-cyclodextrin (in deionized water) powder
FDCD/NaOH	freeze dried β-cyclodextrin (in 0.05 N NaOH solution) powder
FDRM/NaOH	freeze dried meloxicam (in 0.05 N NaOH solution) powder
g	gram(s)
hr	hour(s)
IR	infrared
K_c	stability or equilibrium constant
K_d	dissociation constant
kp	kilopond(s)
L	litre(s)
lb	pound(s)
mg	milligram(s)
min	minute(s)

ml	milliliter(s)
mm	millimeter(s)
mM	millimolar
mp	melting point
MW	molecular weight
N	normality
NMR	nuclear magnetic resonance
nm	nanometer
PBS pH 6.8	phosphate buffer pH 6.8
pH	the negative logarithm of the dissolution constant
PM	physical mixture of meloxicam and β-cyclodextrin
psi	pound per square inch
PXRD	Powder X-ray diffractrometry
RM	meloxicam intact
rpm	round per minute
SEM	scanning electron microscope
SP	spray dried meloxicam-β-cyclodextrin (in 30% ammonium hydroxide solution) powder
SP 1:1	spray dried meloxicam-β-cyclodextrin (in 30% ammonium hydroxide solution) powder in the molar ratio 1:1 (meloxicam:β-cyclodextrin)
SP 1:2	spray dried meloxicam-β-cyclodextrin (in 30% ammonium hydroxide solution) powder in the molar ratio 1:2 (meloxicam:β-cyclodextrin)
SPRM	spray dried meloxicam (in 30% ammonium hydroxide solution) powder
tRM	meloxicam tablets prepared from meloxicam intact
tSPRM	meloxicam tablets prepared from spray dried meloxicam (in 30% ammonium hydroxide solution) powder

tPM 1:1	meloxicam tablets prepared from physical mixture meloxicam-β-cyclodextrin powder in the molar ratio 1:1 (meloxicam:β-cyclodextrin)
tPM 1:2	meloxicam tablets prepared from physical mixture meloxicam-β-cyclodextrin powder in the molar ratio 1:2 (meloxicam:β-cyclodextrin)
tSP 1:1	meloxicam tablets prepared from spray dried meloxicam-β-cyclodextrin (in 30% ammonium hydroxide solution) powder in the molar ratio 1:1 (meloxicam:β-cyclodextrin)
tSP 1:2	meloxicam tablets prepared from spray dried meloxicam-β-cyclodextrin (in 30% ammonium hydroxide solution) powder in the molar ratio 1:2 (meloxicam:β-cyclodextrin)
tFD 1:1	meloxicam tablets prepared from freeze dried meloxicam-β-cyclodextrin (in 0.05 N NaOH solution) powder in the molar ratio 1:1 (meloxicam:β-cyclodextrin)
tFD 1:2	meloxicam tablets prepared from freeze dried meloxicam-β-cyclodextrin (in 0.05 N NaOH solution) powder in the molar ratio 1:2 (meloxicam:β-cyclodextrin)
USP	The United State Pharmacopoeia
UV	ultraviolet
w/v	weight by volume
v/v	volume by volume
μm	micrometer(s)

CHAPTER I

INTRODUCTION

Nowadays, new drug discoveries are being continuously grown up. Most new compounds usually have a wide variety of their physicochemical properties, especially their solubility. Subsequently, the bioavailability of their oral dosage form may be altered. In general, solubility is the rate determining step for poorly water soluble drugs. On the other hand, the intestinal absorption process is the rate determining step for highly aqueous solubility drugs. Therefore, the increasing of aqueous solubility of a poorly water soluble drug may be an approach to solving the above problem.

Meloxicam is a new generation of nonsteroidal anti-inflammatory drug which has the characteristic of being poorly water soluble. It has both a high potency on the reduction of COX2 and lower gastrointestinal effect. Nonetheless, its dissolution rate in acid media is not adequate enough to provide the effective amount of drug dissolved which affects its bioavailability. Recently, a few studies have investigated the effect of cyclodextrin on improving the solubility, dissolution rate, and bioavailability of meloxicam. (Naidu et al., 2004; Baboota, 2002; Nath et al., 2000). They found that cyclodextrin can be employed as a solubility enhancer via inclusion complex phenomena.

Due to the fact that, the outside of CD is hydrophilic, on the other hand, the inside of the cavity is hydrophobic. Among the three types of natural CD, β-CD is the most accessible, the lowest-priced, and generally the most useful. Moreover, the cavity size of β-CD appears to optimal for the entrapment of meloxicam and results in the greatest solubilization effect. The preparation of drug-CD complexes may be gained from different approaches. One of the most popular methods is spray drying which is especially suitable for the thermo labile materials. The advantage of this

method is the controllable size and shape of obtained powder which directly affects the content uniformity of solid dosage form. Another outstanding advantage is the acquired fine particles which have a higher surface area, resulting in a higher dissolution rate. Freeze drying is also a method for drying which produces high porosity particles. The higher the porosity, the larger the surface area. According that both spray and freeze drying themselves can improve the physical properties of drug when comparing with the former.

Kurozumi et al. (1975) prepared the inclusion compounds of the non-steroidal anti-inflammatory drugs and other slightly water soluble water drugs with α-CD and β-CD in powdered form by the freeze-drying and the coprecipitation methods. It was found that the freeze-drying method was successful in obtaining the inclusion compounds of all the test drugs with β-CD.

Lin and Kao (1989) studied the inclusion complexes between piroxicam and β-CD by spray-drying technique. It was found that spray drying could be used to prepare drug inclusion complexes in an amorphous state. It was found that the spray drying could be used to prepare drug inclusion complexes in amorphous state. Moreover, the dissolution rates of tablets made from spray-dried powder were faster than those of the pure drug and the physical mixture of drug and β-CD, respectively. The enhanced dissolution rate of spray-dried products might be attributed to the decrease in particle size, the high-energetic amorphous state and inclusion complex formation.

Acerbi et al. (1990a) investigated the dissolution rate and physicochemical properties of piroxicam-β-CD inclusion complex prepared by spray-drying and freeze drying techniques. They found that the spray-dried powder has a high surface area and a small particle size. Meanwhile, the freeze-dried powder has a high over saturation pattern in the solubilization kinetics as well.

Both techniques had a high efficiency on dissolution improvement. Furthermore, Acerbi et al. (1990b) observed that the oral absorption profile of piroxicam from it's β-CD complex in tablet and sachet formulations which prepared by freeze drying method are more rapidly absorbed than piroxicam capsule.

Baboota and Agarwal (2002) studied the inclusion complexes of meloxicam with β-CD prepared by grinding, kneading, solid dispersion, and the freeze drying method. They investigated that the in vitro dissolution rate of drug-β-CD was faster than those of drug alone. In the other words, Naidu et al. (2004) also investigated that the physicochemical and dissolution properties of meloxicam-CD binary systems prepared by physical mixture, kneaded, and coevaporated system were superior when compared to pure meloxicam.

An attempt to enhance the dissolution rate of meloxicam by using the co-spray drying and co-freeze drying with β-CD, were studied and evaluated on the possible applications. In this study, the co-spray drying with β-CD was defined as the combination of the effect of spray drying technique and β-CD; the co-freeze drying with β-CD was defined as the combination of the effect of freeze drying technique and β-CD.

The objectives of this study are followed

1. To study the preparation of meloxicam by co-spray drying and co-freeze drying with β-CD
2. To compare the physicochemical properties especially the dissolution of spray and freeze dried products
3. To investigate the preparation of meloxicam tablets by using spray and freeze dried powder and compare their dissolution properties with the prototype product.

CHAPTER II

LITERATURE REVIEWS

1. **Spray Drying Technique** (Killeen , 1996)

Spray drying is the formation of a droplet normally containing a suspended material which is coated by a substance, either melted or dissolved in the droplet's medium. The energy is applied to the droplet, forcing evaporation of the medium resulting in both energy and mass transfer through the droplet. The production of powdered particles by means of spray drying offers many advantages. Such particles can be manufactured with a fixed configuration, composition, and size. Thus spray drying can avoid uniformity problems and enhance dissolution, while making the most of selected raw material properties.

Examples of this approach are:

- ❖ Excipient production, where spray drying can be on a continuous basis easily resulting in free-flowing powders.
- ❖ Pharmaceutical tablet granulation, where a binder forms a shell around the active granule, enhancing compressibility, dissolution, and stability.
- ❖ In microencapsulation, solids and liquids are encapsulated in a shell of specified material by spray drying emulsions or suspensions. This method may be used for taste masking as with some vitamins or to protect a drug from oxidation.

The spray drying process consists of the following steps:

1) Formation of slurry to be sprayed: this slurry may be a simple concentrated solution or a dispersion of an insoluble material in a vehicle or medium.

2) The liquid is atomized into droplets: this action is critical as the droplet size and spray pattern dictate the equipment size as well as the final product size.
3) The droplet is exposed to a heated gas flow, normally air; inert gases may be used to prevent oxidation. The heated gas supplies the energy required to vaporize the solvent.
4) The dry free-flowing powder or encapsulated liquid or solid is collected.

Particles produced by a spray drying technique are usually spherically or regularly shaped with a narrow size distribution and content uniformity. Particle size can range form 1 μm to 1 mm. In general, it averages between 50 and 350 μm. Other desired properties like porosity, bulk and tapped densities, moisture, and friability are influenced by the dryer's design and operations.

2. Freeze Drying Technique (Pikal et al.; Rey and May, 1999)

The freeze-drying or lyophilization is a multistage operation to dry a delicate product from the frozen state under moderate vacuum.

The freeze-drying cycle

1. The material is hardened by low temperature throughout the freezing step. During this critical period, all present fluid become solid bookies, either crystalline, amorphous, or glass. Most often, water gives rise to a complex ice network but it might also be imbedded in glassy structures or remain more or less firmly bound within the interstitial structures. Solutes do concentrate and might finally crystallize out. At the same time, the volumetric expansion of the system might induce powerful mechanical stresses that combine with the osmotic shock given by the increasing concentration of interstitial fluids.

2. The sublimation phase or primary drying will follow when the frozen material, placed under vacuum, is progressively heated to deliver enough energy for the ice to sublimate. During this very critical period a correct balance has to be adjusted between heat input (heat transfer) and water sublimation (mass transfer) so that drying can proceed without inducing adverse reactions in the frozen material such as back melting puffing, or collapse. A continuous and precise adjustment of the operating pressure is then compulsory in order to link the heat input to the evaporative possibilities in the frozen material.

The determination of the end of the main drying can be done by several methods. Measuring the temperature increase in the product when the ice is mostly sublimated is only possible with sensors in the product. Their reading will vary by 10°C or more in this phase and at least 1 or 2 hr has to be added as a safety margin. The drop in pressure can also be used, but only if no pressure control by gas injection has been used during main drying and again with a loss of 1 or 2 hr. Another method used is to measure the pressure rise in the chamber after closing the valve between chamber and condenser, called barometric temperature measurement (BMT)

3. The desorption phase or secondary drying starts when ice is being distilled away and a higher vacuum allows the progressive extraction of bound water at above zero temperatures. This again is not an easy task since overdrying might be as bad as underdrying. For each product, appropriate residual moisture has to be reached under given temperatures and pressures.

The secondary drying can be monitored by measuring the amount of water desorbed per time in percent of the solid content, called desorption rate in %/h. The desorption rate is a characteristic function of time for a given product at a given temperature. Only water is measured, which can be desorbed at that temperature. This depends on the energy by which the water molecule is bound to the structure of solid.

4. Final condition and storage begins with the extraction of the product from the equipment. During this operation great care has to be taken to not lose the refined qualities that have been achieved during the preceding steps. Thus for vials, stoppering under vacuum or neutral gas within the chamber is the current practice.

For products in bulk or in ampoules, extraction might be done in a tight gas chamber through remote operation. Water, oxygen, light, and contaminants are all important threats that must be monitored and controlled.

5. Ultimate storage has to be carried out according to the specific "sensitivities" of the products (at room temperature, + 4°C, - 20°C). Again uncontrolled exposures to water vapor, oxygen (air), light, excess heat, or nonsterile environment are major factors to be considered. This obviously includes the composition and quality of the container itself, i.e., glass, elastomers of the stoppers, plastic or organic membranes.

3. Meloxicam

Meloxicam is a non-steroidal, anti-inflammatory drug (NSAID) which is used in the treatment of osteoarthritis and rheumatoid arthritis. Its molecular structure and weight are shown below.

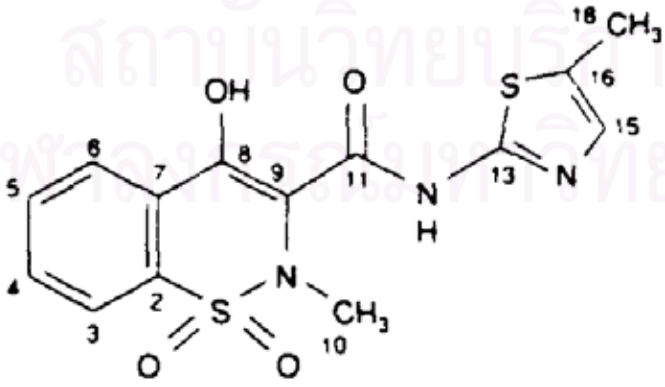

Figure 1 Structure of meloxicam (enol) with atomic numbering. (Luger et al., 1996)

Meloxicam is a yellow, odourless, crystalline powder which melts and degrades at 254°C. Its molecular weight is 351.41. The partition coefficient of meloxicam in n-octanol-buffer at pH 2, 3, 4, 5, 6, 7.4, and 12 are 2.43, 2.68, 2.34, 1.91, 1.01, 0.07, and -0.13, respectively. Meloxicam is practically insoluble in water (0.012 mg/ml at 25 °C: Seedher and Bhatia, 2003), slightly soluble in acetone, very slightly soluble in ethanol (96%) and in methanol, and soluble in dimethylformamide.

Ruey-Shiuan Tsai et al. (1993) studied the physicochemical and structural properties of non-steroidal anti-inflammatory oxicams, i.e. piroxicam, tenoxicam, lornoxicam, isoxicam, and meloxicam. They found that the replacement of a pyridine-2-yl ring of piroxicam with a 5-methylthiazol-2-yl ring yielding meloxicam appears to be “isolipophilic”, since the lipophilicity of 5-methylthiazol-2-yl (log P_{oct} = 0.71) is similar to that of pyridine (log P_{oct} = 0.65). Apparently, this substitution also leads to a dramatic decrease in the basicity of the N-atom of the carboxamide-substituting heterocycle and hence a change in electronic features. The study of acid-base behavior of meloxicam showed that the dissociation constants of meloxicam in H_2O, H_2O /EtOH 1:1 (v/v), and H_2O /EtOH 1:4(v/v) were 4.08, 4.24 (±0.01), and 4.63 (±0.03), respectively. The pK_a values of acidic meloxicam increased in H_2O /EtOH. Moreover, they found that an enhanced acidity of the enolic OH group is observed due to the presence of the charged ammonium group which exerts electrostatic effects upon the enolic OH group. It is noted that the log value of isoxicam meloxciam is relatively higher than the maximal distribution coefficient of piroxicam, tenoxicam, and lornoxicam. Clearly, the isosteric replacements among oxicams have changed their acid-base behavior as well as their partitioning behavior in biphasic systems.

Luger et al. (1996) investigated the structure and physicochemical properties of meloxicam. Solubility of meloxicam at various pH values was presented in Table 1. Meloxicam was soluble at neutral pH but become rapidly insoluble with decreasing pH. At very low pH its solubility increased, indicating a second pKa value and the existence of cation species. Meloxicam crystallized in four different prototropic forms: the anion, the acidic enol, the zwitterions and the cation forms. As determined by ^{1}H- and ^{13}C-NMR, meloxicam in neutral or weakly basic solution exists in the

anion form. The equilibrium between the enol and zwitterions forms depends on solvent polarity. The distribution coefficients of isoxicam and tenoxicam were comparable at all pH examined, implying the similar lipophilic expression of their charged. The distribution coefficients of isoxicam and meloxicam decreased significantly when the pH is increased from 4.17 to 5.24 due to the deprotonation of the enolic OH. It must be noted that the enolic group is completely ionized in highly basic solution (1.0 M NaOH, pH 13), and hence the anionic species would be the only one partitioning into the octanol phase in the form of an ion pair. At pH near the isoelectric point, the species of zwitterionic oxicams partitioning into the octanol phase could well be a mixture of neutral and zwitterionic forms. The enolic group of meloxicam remained neutral when partitioning into the octan-1-ol phase from a highly acidic solution (0.1 N HCl, pH 1). Meloxicam appeared to partition overwhelmingly as anions into the octanol phase at pH 7.4. This result might be relevant to their pharmacological activity since a negative charge is an important structural requirement for binding to cyclooxygenase. The $\Delta\log P_{\text{oct-hep}}$ value of meloxicam implied a weak H-bond donating capacity, probably because the two strong H-bond donor groups (enolic OH and amide NH) are internally bonded.

Table 1 Meloxicam solubility at various pH values. (Luger et al., 1996)

pH value (start)	Substance conc. used (g/100ml)	pH value (filtrate)	Solubility (mg/100 ml intact substance)
1.0 (0.1 M HCl)	10	1.10	0.086
1.0 (buffer)	10	1.02	0.093
2.0 (buffer)	10	1.99	0.037
3.0 (buffer)	10	2.99	0.038
4.0 (buffer)	10	3.97	0.049
5.0 (buffer)	10	4.96	0.213
6.0 (buffer)	10	5.99	2.70
7.0 (buffer)	10	7.00	26.6
8.0 (buffer)	10	7.73	155
9.0 (buffer)	10	7.96	195
10.0 (buffer)	10	8.07	231

4. Cyclodextrin

4.1 Structure and physicochemical properties of cyclodextrins

Cyclodextrins are cyclic oligosaccharides, comprised of a variable number of α-D-glucopyranose units attached by α-1,4-linkages. The most common cyclodextrins are α-CD, β-CD, and γ-CD, consisting of 6, 7, and 8 glucose units, respectively. According to the lack of free rotation around glycosidic bonds and the C1-conformation of the α-D-glucopyranosyl residues, the shape of CDs are not completely cylindrical but are toroidal or cone in shape (Figure 2). The primary hydroxyl groups are located on the narrow side of the ring, while the secondary hydroxyl groups are located on the wider edge. In addition, the apolar C3, C5 hydrogen and ether-like oxygen are at the inside of the molecules. The inside of the cavity is hydrophobic whereas the outside is hydrophilic. As a result of this architecture, CDs are able to form an inclusion complex with hydrophobic drug molecules provided the minimum requirement is met, which is geometric compatibility. The drug molecules must fit entirely or at least partially with the cavity of cyclodextrins. The complex formation not only depends on the stereochemistry but also the polarity of drug molecules. Basically, the more hydrophobic are molecules, the higher affinity to the cavity of CDs. Moreover, the unionized drugs usually form a more stable complex than that of ionized species.

Physicochemical properties of α-, β-, and γ-CD are given in Table 2. The solubility of β-CD is the least among three types of common CD which due to intramolecular hydrogen bonding between secondary hydroxyl groups as shown in Figure 2. This formation effects directly inhibit the hydrogen bond formation between outer surface reactive groups and surrounding water molecules, lead to less negative heats of hydration. Consequently, β-CD turns to a rigid structure which explain the limited aqueous solubility. However, chemical modification by substitution of hydroxyl group with methoxy and ethoxy functional groups, will overcome this problem.

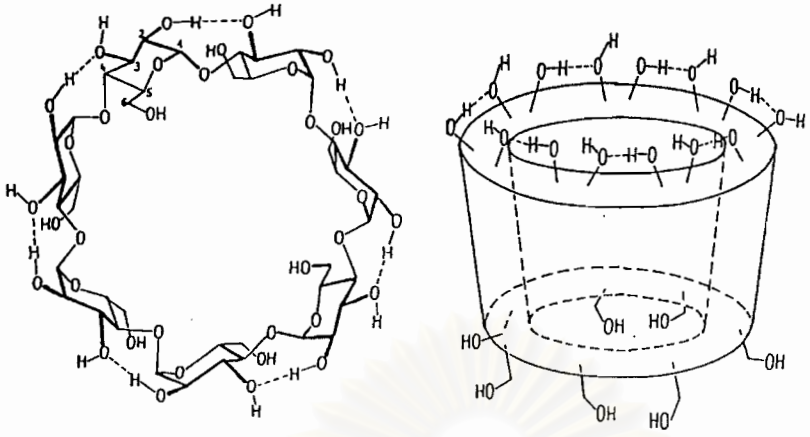

Figure 2 Chemical structures of β-CD (Barcza A.B., and Barcza L., 2000)

Table 2 Physicochemical properties of α-, β-, and γ-CD. (Bekers et al., 1991)

Properties	α-CD	β-CD	γ-CD
Number of glucopyranose unit	6	7	8
Cavity diameter (A°)	5	6	8
Height of torus (A°)	7.9	7.9	7.9
Diameter of periphery (A°)	14.6	15.4	17.5
Molecular weight (g/mole)	972	1135	1297
Aqueous solubility [1)]	14.5	1.85	23.2
Melting point (°C)	275	280	275
pKa [2)]	12.3	12.2	12.1
Half-life of ring opening [3)] (hr)	6.2	5.4	3.0
Hydrolysis [4)]	negligible	slow	rapid

1) in grams per 100 ml water at ambient temperature

2) pKa: by potentiometry at 25 °C

3) Half-life of ring opening in 1 N HCl at 60 °

4) By *Aspergillus oryzae* α-amylase

4.2 Pharmaceutical applications of cyclodextrins (Davis and Brewster, 2004; Martin, 2004)

Due to the fact that each guest molecule is individually surrounded by a CD, the molecule is micro-encapsulated from microscopically points of view which lead to advantageous changes in the chemical and physical properties of the guest molecules. CDs can be used to achieve the following:

- ❖ Enhance solubility
- ❖ Enhance bioavailability
- ❖ Enhance stability
- ❖ Convert liquids and oils to free-flowing powders
- ❖ Reduce evaporation and stabilize flavors
- ❖ Reduce odors and tastes
- ❖ Reduce haemolysis
- ❖ Prevent admixture incompatibilities

The main interest in CDs lies in their ability to form inclusion complexes with several compounds as followed:

Shan-Yang Lin and Yuh-Horng Kao (1989) investigated the inclusion complexes of acetaminophen, indomethacin, piroxicam, and warfarin with β-CD prepared by using a spray drying technique. It was found that the spray-drying technique could be used to prepare the amorphous state of drug inclusion complexes. The flowability and compressibility of the spray-dried products were poor, due to the small particles size formed by the spray drying process. However, the dissolution rates of drugs from tablets made by the spray-dried products were faster than those of the pure drug and the physical mixture of drug and β-CD. The enhanced dissolution rate of spray-dried products might be attributed to the decreased particle size, the high-energetic amorphous state, and inclusion complex formation.

Nath and Shivakumar (1999) used a 2^3 factorial design of experiment, the effect of factors on aqueous solubility of meloxicam β-CD complex prepared by solvent evaporation method. *In vitro* dissolution tests in acid (pH 1.2) revealed that only 38 % of the drug was released from tablets of meloxicam; whereas, 77 % to 93 % of the drug was released from tablets of meloxicam β-CD complexes over a period of one hour following first order rate kinetics.

Sanoferjan et al. (1999) studied the effect of tenoxicam β-CD complexation on the enhancement of drug solubility. The complex prepared in 1:1 molar ratio by kneading, common solvent, and neutralization complex techniques was characterized by infrared spectroscopy and X-ray diffraction studies and evaluated for its dissolution profile, thermal stability and photostability. The complex prepared by neutralization method was found to yield very reliable and best results over that of the common solvent and kneading methods.

Mamdouh M. Ghorab (2004) investigated the evaluation of β-CD as a vehicle, either singly or in blends with lactose (spray-dried or monohydrate), for preparing a meloxicam tablet. The tablets were prepared by direct compression and wet granulation techniques. It was found that all tablet formations showed acceptable mechanical properties. This dissolution rate of meloxicam was significantly enhanced by inclusion of β-CD in the formulations up to 30 %. Moreover, the mean pharmacokinetic parameters were significantly increased in presence of β-CD

4.3 **Inclusion complex formation** (Szetjli, 1998; Martin, 2004)

The outstanding property of CDs is their ability to form solid inclusion complexes with a variety of solid, liquid and gaseous compounds by a molecular complexation. In these complexes (Figure 3), a guest molecule is held within the cavity of the CD host molecule. Complex formation is a dimensional fit between host cavity and guest molecule. The lipophilic cavity of CD molecules provides a

microenvironment into which appropriately sized non-polar moieties can enter to form inclusion complexes. During formation of inclusion complex, the formation or breaking of covalent bond is not occurring. The main driving force of complex formation is the release of enthalpy-rich water molecules from the cavity. Water molecules are displaced by more hydrophobic guest molecules present in the solution to attain an apolar–apolar association and decrease of CD ring strain resulting in a more stable lower energy state.

The binding of guest molecules within the host CD is not fixed or permanent but rather is a dynamic equilibrium. Binding strength depends on how well the 'host–guest' complex fits together and on specific local interactions between surface atoms. Complexes can be formed either in solution or in the crystalline state and water is typically the solvent of choice. Inclusion complexation can be accomplished in a co-solvent system and in the presence of any non-aqueous solvent.

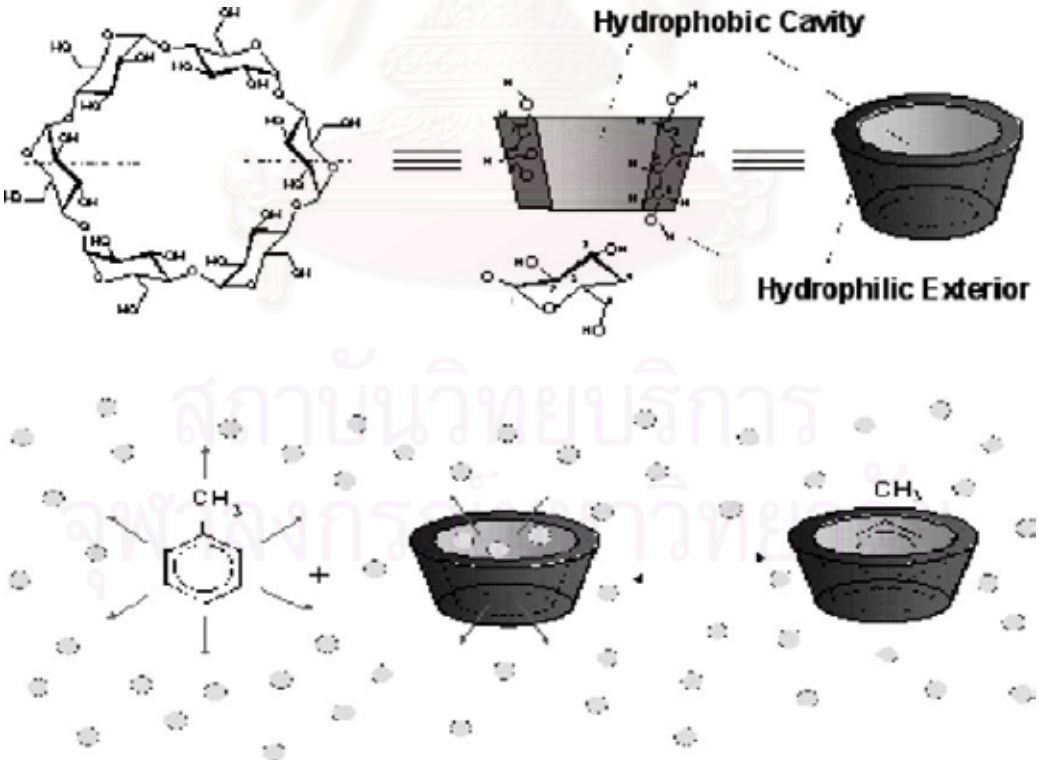

Figure 3 CD inclusion complex formations. (Martin, 2004)

Seedhler and Bhatia (2003) studied the solubility enhancement of COX-2 inhibitors using various solvent systems. They found that the solubility of meloxicam increased significantly with increase in pH value. Moreover, physicochemical properties of the solvent such as polarity, intermolecular interactions, and the ability of the solvent to form hydrogen bond with the drug molecules were the major factors involved in the dissolution of drugs by pure solvents. The greater the difference in the polarity of the two solvents in a given mixed solvent, the greater was the solubilization power

CD architecture confers upon these molecules a wide range of chemical properties markedly different from those exhibited by non-cyclic carbohydrates in the same molecular weight range. Inclusion in CDs exerts a profound effect on the physicochemical properties of guest molecules as they are temporarily locked or caged within the host cavity giving rise to beneficial modifications of guest molecules, which are not achievable otherwise.

The potential guest list for molecular encapsulation in CDs is quite varied and includes such compounds as straight or branched chain aliphatics, aldehydes, ketones, alcohols, organic acids, fatty acids, aromatics, gases, and polar compounds such as halogens, oxyacids and amines. Due to the availability of multiple reactive hydroxyl groups, the functionality of CDs is greatly increased by chemical modification. Through modification, the applications of CDs are expanded. CDs are modified through substituting various functional compounds on the primary and/or secondary face of the molecule. Modified CDs are useful as enzyme mimics because the substituted functional groups act in molecular recognition. The same property is used for targeted drug delivery and analytical chemistry as modified CDs show increased enantioselectivity over native CDs.

The ability of a CD to form an inclusion complex with a guest molecule is a function of two key factors. The first is steric and depends on the relative size of the CD to the size of the guest molecule or certain key functional groups within the guest. If the guest is the wrong size, it will not fit properly into the CD cavity.

The second critical factor is the thermodynamic interactions between the different components of the system (CD, guest, solvent). For a complex to form there must be a favorable net energetic driving force that pulls the guest into the CD. While the height of the CD cavity is the same for all three types, the number of glucose units determines the internal diameter of the cavity and its volume. Based on these dimensions, α-cyclodextrin can typically complex low molecular weight molecules or compounds with aliphatic side chains, β-CD will complex aromatics and heterocycles and γ- CD can accommodate larger molecules such as acrocycles and steroids.

In general, therefore, there are four energetically favorable interactions that help shift the equilibrium to form the inclusion complex:

1) The displacement of polar water molecules from the apolar CD cavity.
2) The increased number of hydrogen bonds formed as the displaced water returns to the larger pool.
3) A reduction of the repulsive interactions between the hydrophobic guest and the aqueous environment.
4) An increase in the hydrophobic interactions as the guest inserts itself into the apolar CD cavity.

While this initial equilibrium to form the complex is very rapid (often within minutes); the final equilibrium can take much longer to reach. Once inside the CD cavity, the guest molecule makes conformational adjustments to take maximum advantage of the weak van der Waals forces that exist.

Complexes can be formed by a variety of techniques that depend on the properties of the active material, the equilibrium kinetics, the other formulation ingredients and processes and the final dosage form desired. However, each of these processes depends on a small amount of water to help drive the thermodynamics. Among the methods used are simple dry mixing, mixing in solutions and suspensions followed by a suitable separation, the preparation of pastes and several thermo-mechanical techniques.

Dissociation of the inclusion complex is a relatively rapid process usually driven by a large increase in the number of water molecules in the surrounding environment. The resulting concentration gradient shifts the equilibrium in Figure 3 to the left. In highly dilute and dynamic systems like the body, the guest has difficulty finding another CD to reform the complex and is left free in solution.

Hamada et al. (1975) studied the interaction of α- and β- CDs with several non-steroidal anti-inflammatory drugs and observed the solubility and stability of the drugs in aqueous solution. The solubility of all kinds of drugs increased with the addition of β-CD due mainly to the inclusion complex formation. The dissolution rate of drug increased with β-CD as similar as in tendency to the solubility data.

Redenti et al. (1996) studied the differentiation between amorphous piroxicam: β-CD complex and a mixture of the two amorphous components by differential scanning calorimetry and near-infrared Fourier transform Raman spectroscopy. It was found that the liophylization yielded a partially amorphous product indicated the high tendency of piroxicam to crystalline; whereas, the completely amorphization was successfully obtained by rapidly cooling after melting. Thermal analysis could be used to evaluate the inclusion complex purity with regard to crystalline and/or amorphous free piroxicam content.

Braibanti et al. (1998) examined the complexation between β-CD and piroxicam and investigated the thermodynamics of this interaction using a flow microcalorimetric study. The results confirmed the formation of a complex between β-CD and piroxicam and allow the evaluation of the equilibrium constant of the process, assuming the formation of a 1:1 complex.

Guo Xiliang et al. (2003) investigated the inclusion behavior of piroxicam with β- CD, hydroxypropyl-β-CD, and carboxymethyl-β-CD by using steady-state fluorescence and nuclear magnetic resonance techniques. The remarkable fluorescence emission enhancement upon addition of cyclodextrins suggested that

CDs were most suitable for inclusion of the uncharged species of piroxicam. The stoichiometry of the piroxicam-CDs inclusion complexes was 1:1, except for *β*-CD where a 1:2 inclusion complex was formed. The formation constants showed the strongest inclusion capacity of *β*-CD. NMR showed the inclusion mode of piroxicam with CDs.

4.4 **Determination of complex stability constants** (Martin, 2004)

Measurements of stability or equilibrium constants (K_c) or the dissociation constants (K_d) of the drug–CD complexes are important since this is an index of changes in physicochemical properties of a compound upon inclusion. Most methods for determining the K-values are based on titrating changes in the physicochemical properties of the guest molecule, i.e. the drug molecule, with the CD and then analysing the concentration dependencies. Additive properties that can be titrated in this way to provide information on the K-values include aqueous solubility, chemical reactivity, molar absorptivity and other optical properties (e.g. optical rotation dispersion), phase solubility measurements, nuclear magnetic resonance chemical shifts, pH-metric methods, calorimetric titration, freezing point depression, and liquid chromatography chromatographic retention times. While it is possible to use both guest or host changes to generate equilibrium constants, guest properties are usually most easily assessed.

$$D + CD \Leftrightarrow DCD$$

$$K_c = \frac{[DCD]}{[D][CD]} \qquad \ldots(1)$$

Connors (1965) has evaluated the population characteristics of CD complex stabilities in aqueous solution. The stability constant (K_c) is better expressed as $K_{m:n}$ to indicate the stoichiometric ration of the complex. It can be written:

$$\underset{(a-mx)(b-nx)}{mL+nS} \xleftrightarrow{K_{m:n}} \underset{(X)}{L_m S_n}$$

:so that, $$K_{m:n} = \frac{[x]}{[a-mx]^m [b-nx]^n} \qquad \ldots(2)$$

In addition, dissociation constant can also be defined:

$$K_d = \frac{[a-mx]^m [b-nx]^n}{[x]} = \frac{1}{K_c} \text{ or } \frac{1}{K_{m:n}} \qquad \ldots(3)$$

One of the most useful and widely applied analytical approaches in this context is the Phase–solubility method described by Higuchi and Connors (1965). Phase–solubility analysis involves an examination of the effect of a solubilizer, i.e. cyclodextrin or ligand on the drug being solubilized, i.e. the substrate.

Experimentally, the drug of interest is added to several vials such that it is always in excess. The presence of solid drug in these systems is necessary to maximize the thermodynamic activity of the dissolved substrate. To the drug or substrate (S) a constant volume of water containing successively larger concentrations of the CD or ligand (L) is added. The vials are mixed at constant temperature until equilibrium is established (which frequently takes about 1 week). The solid drug is then removed and the solution assayed for the total concentration of S.

A Phase–solubility diagram is constructed by plotting the total molar concentration of S on the y-axis and the total molar concentration of L added on the x-axis (Figure 3). Phase–solubility diagrams prepared in this way fall into two main categories: A- and B-types. A-type (Figure 3(A)) curves are indicative for the formation of soluble inclusion complexes while B-type (Figure 3(B)) behaviors are suggestive of the formation of inclusion complexes of poor solubility.

While A-curves are subdivided into A_L (linear increases of drug solubility as a function of CD concentration), A_P (positively deviating isotherm) and A_N (negatively deviating isotherms) subtypes, B-curves are subdivided into B_S which response denotes complexes of limited solubility and B_I subtypes which are indicative of insoluble complexes. A_L-type diagrams are first order with respect to the CD (L) and may be first or higher order with respect to the drug (S), i.e. SL, S_2L, S_3L, . . ., S_mL. If the slope of an A_L-type system is greater than one, higher order complexes are indicated. A slope of less than one does not necessarily exclude higher order complexation but 1:1 complexation is usually assumed in the absence of other information. A_P-type systems suggest the formation of higher order complexes with respect to the ligand at higher ligand concentrations, i.e. SL_2, SL_3. . . SL_n. The stoichiometry of A_P-type systems can be evaluated by curve fitting. A_N-type systems are problematic and difficult to interpret. The negative deviation from linearity may be associated with ligand-induced changes in the dielectric constant of the solvent or self-association of the ligands at high CD concentrations.

These phase solubility systems not only allows a qualitative assessment of the complexes formed but may also be used to derive equilibrium constants. The equilibrium constant (K) for the formation of $[S_mL_n]$ can be represented by:

$$K = \frac{[S_mL_n]}{[S]^m[L]^n} \qquad \ldots(4)$$

where,

$$[S] = S_0 \qquad \ldots(5)$$

$$[S]_t = S_0 + m[S_mL_n] \qquad \ldots(6)$$

$$[L] = [L] + n[S_mL_n] \qquad \ldots(7)$$

Therefore, the values of $[S_mL_n]$, [S] and [L] can be obtained:

$$[S] = S_0 \qquad \ldots(5)$$

$$[S_m L_n] = \frac{[S]_t - S_0}{m} \qquad \ldots(8)$$

$$[L] = [L]_t - n\,[S_m L_n], \qquad \ldots.(9)$$

If *m* is known, *K* can be calculated. If *m* = 1 (i.e. a 1:1 drug:cyclodextrin complex forms), the following equation can be applied:

$$K_{1:1} = \frac{slope}{S_o(1 - slope)} \qquad \ldots(10)$$

While the chemically modified CDs including HP-*β*-CD and SBE-*β*-CD usually produce soluble complexes (i.e. A-type systems), *β*-CD often gives rise to B-type curves due to the poor water solubility of the ligand itself. From S_o to point a in figure 3(B), the apparent solubility of S is increased due to soluble complex formation between S and L. At point a, however, the solubility limit of this complex is reached. Addition of further L results in formation of more complexes which must, of course, precipitate, the concentration of uncomplexed S is maintained constant by dissolution of solid S. At point b, the entire solid S has been consumed in this manner and further addition of S results in depletion of S in the solution by complex formation and concomitant precipitation of the insoluble complex. The dotted segment a-d represents supersaturation of the solution with respect to the initially formed complex. The curve B_I is interpreted in the same manner, with the difference that the complex formed is so insoluble that the initial rise in the concentration of S is not detectable.

If the complex responsible for the initial rise in the Type B_S diagram is the same complex finally precipitated along the b-c curve, evidently the increase in S concentration from S_O to a must be equal to the final S concentration at c. This condition is not often observed; however, suggesting that often the system must involve formation of two or more distinct complexes.

One of these being responsible for the initial rise in solubility, while another is precipitated in the latter stages of the diagram. Another feature sometimes seen is an increase insolubility beyond point c, apparently due to formation of another complex species which is more soluble that the one responsible for the descending portion of the curve, b-c.

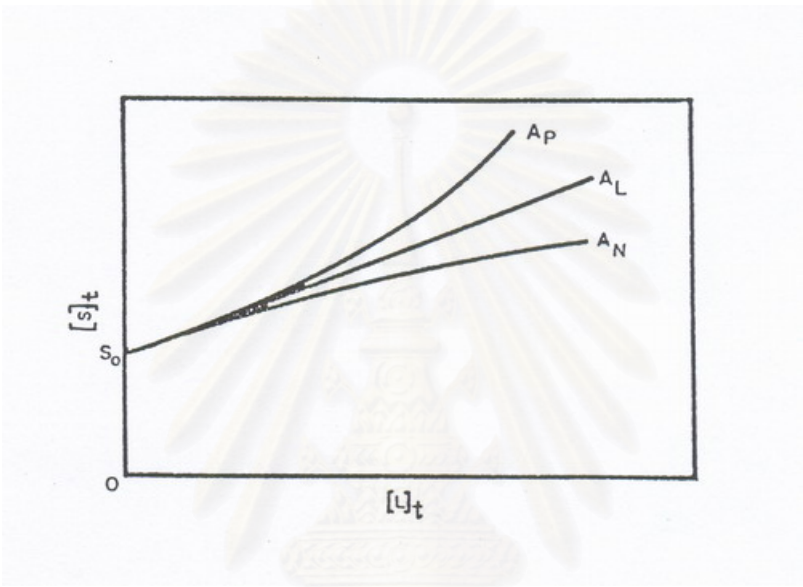

(A)

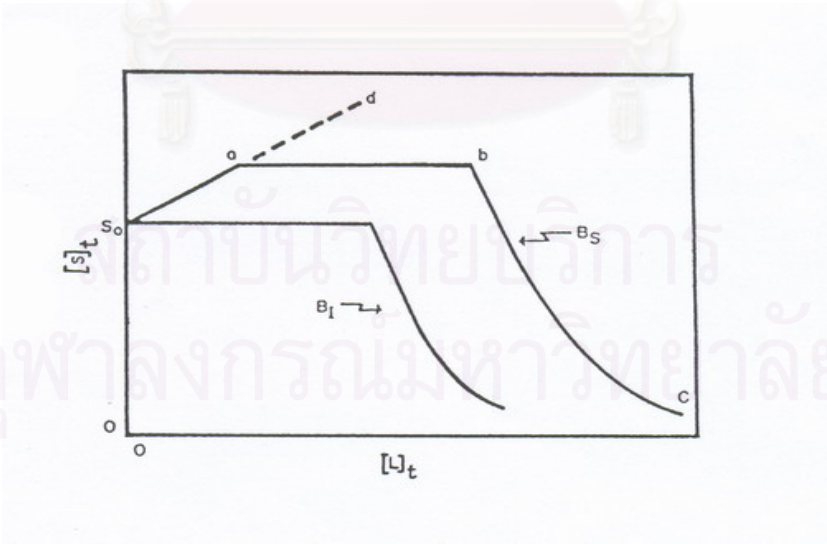

(B)

Figure 4 Phase-solubility relationships (A) A-type, and (B) B-type. (Higuchi and Conners, 1965)

CHAPTER III

EXPERIMENTAL

Materials

Raw materials were used as received without further purification

1. Drug substance

- Meloxicam (MW: 351.41)
  (Lot No. MX/005/3003, supplied by Siam Bhaesach Co. Ltd., Thailand)

2. Carrier

- β-cyclodextrin : Ringdex- B® (MW: 1135)
  (Lot No. 23273, supplied by Rama Production Co. Ltd., Thailand)

3. Excipients

- Microcrystalline cellulose : Avicel® pH 102
  (Lot No. 2155, Asahi Kasei Corporation, Japan)

- Spray-dried lactose : Tablettose®
  (Lot No. L0021A4003, Meggle GMBH, Germany)

- Sodium starch glycolate: Explotab®
  (Lot No. 4111034027, Rama Production Co. Ltd., Thailand)

- Talcum
  (Lot No. 201023-010701, The People's Republic of China, China)

- Magnesium stearate
  (Lot No. F1G253, Faci Asia Pacific Pte Ltd., Australia)

4. Reagents

- 30% Ammonium hydroxide
  (Lot No. 60785PEN, Panreac, E.U.)

- Dimethylformamide
  (Lot No. 0305636, Fischer Scientific, U.K.)

- Hydrochloric acid solution 37%, AR grade
  (Lot No. 03 02 0186, Lab Scan Analytical Sciences, Ireland)

- Isopropyl myristate
  (Lot No. 407065, S. Tong Chemicals Co. Ltd., Thailand)

- Monobasic potassium phosphate, AR grade
  (Lot No. B/NO.F2H145, UNIVAR, Australia)

- Sodium hydroxide pellets, AR grade
  (Lot No. B 191998 230, Merck, Germany)

Methods

1. UV analysis

1.1 Calibration curve of meloxicam in deionized water

The stock solution of meloxicam was prepared in dimethylformamide. The appropriate dilutions of 0.002595, 0.005190, 0.007785, 0.010380, and 0.012975 mg/ml meloxicam concentration were made in deionized water. There was no interfering of used dimethylformamide in this study. The calibration curve was plotted between meloxicam concentration in mg/ml and absorbance at 361 nm.

1.2 Calibration curve of meloxicam in 0.1 N HCl pH 1.2

The stock solution of meloxicam was prepared in dimethylformamide. The appropriate dilutions of 0.002770, 0.005540, 0.008310, 0.011080, 0.013850, 0.016620, and 0.019390 mg/ml meloxicam concentration were made in 0.1 N HCl pH 1.2. There was no interfering of used dimethylformamide in this study. The calibration curve was plotted between meloxicam concentration in mg/ml and absorbance at 361 nm.

1.3 Calibration curve of meloxicam in phosphate buffer pH 6.8

The stock solution of meloxicam was prepared in dimethylformamide. The appropriate dilutions of 0.002770, 0.005540, 0.008310, 0.011080, 0.013850, 0.016620, and 0.019390 mg/ml meloxicam concentration were made in phosphate buffer pH 6.8. There was no interfering of used dimethylformamide in this study. The calibration curve was plotted between meloxicam concentration in mg/ml and absorbance at 361 nm.

1.4 Calibration curve of meloxicam in 1 N NaOH

The stock solution of meloxicam was prepared in 1 N NaOH. The appropriate dilutions of 0.00228, 0.00456, 0.00684, 0.00912, 0.01140, 0.01368, 0.01596, 0.01824, 0.02052, and 0.02280 mg/ml meloxicam concentration were made in 1 N NaOH. The calibration curve was plotted between meloxicam concentration in mg/ml and absorbance at 361 nm.

1.5 Calibration curve of meloxicam in dimethylformamide

The stock solution of meloxicam was prepared in dimethylformamide. The appropriate dilutions of 0.002595, 0.005190, 0.007785, 0.010380, and 0.0112975 mg/ml meloxicam concentration were made in dimethylformamide. The calibration curve was plotted between meloxicam concentration in mg/ml and absorbance at 361 nm.

2. Phase solubility study

Phase solubility studies were carried out according to Higuchi and Conners (1965). An excess amount of meloxicam was added into various concentrations of aqueous β-CD solution (0-14 mM). The mixture was equilibrated in the top-to-bottom rotating machine at 37 ± 1 ºC for 7 days. The suspensions were filtered through 0.45 μm nylon membrane filter. The filtrates were analyzed spectrophotometrically at a wavelength of 361 nm (Ultraviolet/visible recording spectrophotometer, Model V-530, Jasco, Japan) in which no absorption of β-CD was detected. The experiment was performed in triplicate.

3. Preparation of meloxicam sample

3.1 SPRM: Spray dried meloxicam (in 30% ammonium hydroxide solution) powder

The spray drying of meloxicam in 30% ammonium hydroxide solution was done in order to investigate the effect of spray drying process and ammonium hydroxide on the physicochemical properties of meloxicam. First, 10.5470 g of meloxicam was dissolved in 2.470 L of 30% ammonium hydroxide solution on magnetic stirrer for 60 minutes. According to the acidity of meloxicam, it was practically soluble in the neutral pH. Hence, the 30% ammonium hydroxide solution was added to increase the basicity of preparation. The solution was then sprayed (Spray dryer, Buchi, Japan) under the optimum condition as shown in Table 3. This condition was done by adjustment of the inlet air temperature, outlet air temperature, feed rate, and aspirating rate during the spray drying process.

3.2 FDRM/NaOH: Freeze dried meloxicam (in 1 N sodium hydroxide solution) powder

The freeze drying of meloxicam in 1 N sodium hydroxide solution was done in order to investigate the effect of freeze drying process and sodium hydroxide on the physicochemical properties of meloxicam. In this case, the 1 N sodium hydroxide was used instead of 30% ammonium hydroxide on an account of the limit of the freeze dryer. This equipment could not resist the erosion of ammonium hydroxide. The preliminary studies expressed that meloxicam could not dissolve in 0.05 N sodium hydroxide as used in the other preparations.

First, the 0.5273 g of meloxicam was dissolved in 100 ml of 1 N sodium hydroxide solution on magnetic stirrer for 60 minutes. Then the freeze dried product was prepared by freezing at -40ºC, 500 millitorr. During the primary drying, the temperature started at -30°C and then gradually 10°C increased until it reached 20°C; the temperatures at each point were held for 3 hr. The pressure used in this step was controlled at 200 millitorr. The secondary drying was performed at 25°C, 100 millitorr for 5 hr. (LYO-LAB, Lyophilization Systems, Inc., USA).

4. Preparation of *β*-cyclodextrin sample

4.1 SPCD: Spray dried *β*-CD (in 30% ammonium hydroxide solution) powder

The spray drying of *β*-CD in 30% ammonium hydroxide was done in order to investigate the effect of spray drying process and ammonium hydroxide on the physicochemical properties of *β*-CD. First, 34.10 g of *β*-CD was dissolved in 482 ml of 30% ammonium hydroxide solution on magnetic stirrer for 60 minutes. The solution was then sprayed under the optimum condition as shown in Table 3.

4.2 FDCD: Freeze dried β-CD (in deionized water) powder

The freeze drying of β-CD in deionized water was done in order to investigate the effect of freeze drying process on the physicochemical properties of β-CD. First, 6.8094 g of β-CD was dissolved in 397 ml of deionized water on magnetic stirrer for 60 minutes. The freeze dried product was prepared by freezing at -40ºC, 500 millitorr. During the primary drying, the temperature started at -30°C and then gradually 10°C increased until it reached 20°C; the temperatures at each point were held for 3 hr. The pressure used in this step was controlled at 200 millitorr. The secondary drying was performed at 25°C, 100 millitorr for 5 hr. (LYO-LAB, Lyophilization Systems, Inc., USA). The freeze dried products were sieved through mesh No. 60.

4.3 FDCD/NaOH: Freeze dried β-CD (in 0.05 N sodium hydroxide solution) powder

The freeze drying of β-CD in 0.05 N sodium hydroxide was done in order to investigate the effect of sodium hydroxide on the physicochemical properties of β-CD. First, 8.5141 g of β-cyclodextrin was dissolved in 470 ml of deionized water on magnetic stirrer for 60 minutes. The 25 ml of 1 N sodium hydroxide solution was added and mixed for 60 minutes.

The freeze dried product was prepared by freezing at -40ºC, 500 millitorr. During the primary drying, the temperature started at -30°C and then gradually 10°C increased until it reached 20°C; the temperatures at each point were held for 3 hr. The pressure used in this step was controlled at 200 millitorr. The secondary drying was performed at 25°C, 100 millitorr for 5 hr. (LYO-LAB, Lyophilization Systems, Inc., USA). The freeze dried products were sieved through mesh No. 60.

5. Preparation of meloxicam and β-cyclodextrin systems

5.1 SP: Spray dried meloxicam-β-cyclodextrin (in 30% ammonium hydroxide solution) powder

The SP 1:1 was prepared by dissolving 5.3044 g of meloxicam and 23 g of β-CD in 485 ml of 30% concentrated ammonium hydroxide solution on a magnetic stirrer for 60 minutes. The SP 1:2 was prepared by dissolving 5.3078 g of meloxicam and 34.10 g of β-CD in 480 ml of 30% concentrated ammonium hydroxide solution on a magnetic stirrer for 60 minutes. The solutions were then sprayed under the optimum condition as shown in Table 3.

5.2 FD: Freeze dried meloxicam-β-cyclodextrin (in 0.05 N NaOH solution) powder

FD 1:1 was prepared by dissolving 6.8032 g of β-CD in 375 ml of deionized water on magnetic stirrer for 60 minutes and then 2.1101 g of meloxicam was dissolved in β-CD solution on magnetic stirrer for another 60 minutes. The 20 ml of 1 N sodium hydroxide solution was added and mixed for 60 minutes. FD 1:2 was prepared by dissolving 6.8054 g of β-CD in 376 ml of deionized water on magnetic stirrer for 60 minutes and then 1.0538 g of meloxicam was dissolved in β-CD solution on magnetic stirrer for another 60 minutes. The 20 ml of 1 N sodium hydroxide solution was added and mixed for 60 minutes. The solutions were operated in the freeze dryer (LYO-LAB, Lyophilization Systems, Inc., USA). The freeze dried product was prepared by freezing at -40ºC, 500 millitorr. During the primary drying, the temperature started at -30°C and then gradually 10°C increased until it reached 20°C; the temperatures at each point were held for 3 hr. The pressure used in this step was controlled at 200 millitorr. The secondary drying was performed at 25°C, 100 millitorr for 5 hr. The freeze dried products were sieved through mesh No. 60.

5.3 PM: Physical mixture of meloxicam and β-cyclodextrin

Meloxicam and β-CD were physically mixed in a plastic bag for 15 minutes and kept in the closed containers for further investigation. The amount of used materials was show in Table 4.

Table 3 The spray drying parameter of each preparation.

Parameter	SPRM	SPCD	SP 1:1	SP 1:2
Inlet air temperature (ºC)	125	125	120	120
Outlet air temperature (ºC)	70	70	70	70
Feed rate (ml/min)	5	5	5	5

6. Preparation of meloxicam tablets

The tablets containing 7.5 mg of meloxicam were prepared by direct compression on a hydraulic press using a round flat faced punch-die assembly diameter of 10 mm. Each preparation was performed with different pressure in order to control the hardness of tablet. The used pressure throughout the study was as followed:

Preparations		**Pressure (psi)**
RM	:	600
SPRM	:	500
PM 1:1	:	500
PM 1:2	:	400
FD 1:1	:	350
FD 1:2	:	300
SP 1:1	:	300
SP 1:2	:	200

The tablet hardness was controlled in the range from 3-5 kp. Tabletting was operated at least 50 tablets per batch with 180 mg weight per tablet. The compositions of meloxicam tablet are shown in Table 5. In case of RM; Avicel® pH 102 first was mixed with meloxicam intact in a plastic bag for 2 min. then Tablettose® was added and mixed for 2 min., after that Explotab® was added and mixed for 2 min. The mixture was sieved through mesh No.60 in order to overcome the aggregation of powder, and then the mixture was mixed with talcum for 1 min. then was mixed with magnesium stearate for 1 min. In case of PM; meloxicam intact was first mixed with β-cyclodextrin in a plastic bag for 2 min., and then Avicel® pH 102 was added and mixed for 2 min. Then Tablettose® was added and mixed for 2 min., after that Explotab® was added and mixed for 2 min. The mixture was sieved through mesh No.60 in order to overcome the aggregation of powder, and then the mixture was mixed with talcum for 1 min. then was mixed with magnesium stearate for 1 min. In case of SPRM, SP, and FD; Avicel® pH 102 first was mixed with SPRM or SP or FD powder in a plastic bag for 2 min. then Tablettose® was added and mixed for 2 min., after that Explotab® was added and mixed for 2 min. The mixture was mixed with talcum for 1 min. then was mixed with magnesium stearate for 1 min.

Table 4 The composition of meloxicam tablet. (180 mg/tablet)

Ingredient (g)	tRM	tSPRM	tPM1:1	tPM1:2	tSP 1:1	tSP1:2	tFD 1:1	tFD1:2
meloxicam-*β*-CD powder	-	-	-	-	0.0400	0.0559	0.0400	0.0559
meloxicam spray dried powder	-	0.0075	-	-	-	-	-	-
meloxicam	0.0075	-	0.0075	0.0075	-	-	-	-
β-CD	-	-	0.0325	0.0484	-	-	-	-
Avicel® pH 102	0.0469	0.0469	0.0371	0.0313	0.0371	0.0313	0.0371	0.0313
Tablettose®	0.1094	0.1094	0.0867	0.0766	0.0866	0.0766	0.0866	0.0766
Explotab®	0.0090	0.0090	0.0090	0.0090	0.0090	0.0090	0.0090	0.0090
Talcum	0.0054	0.0054	0.0054	0.0054	0.0054	0.0054	0.0054	0.0054
Mg stearate	0.0018	0.0018	0.0018	0.0018	0.0018	0.0018	0.0018	0.0018

7. Characterization of the samples

7.1 Scanning electron microscopy

The surface morphology of pure materials, physical mixtures, spray dried powders, and freeze dried powder was observed by scanning electron microscope (JSM-5800LV, Jeol Ltd., Japan). The samples were coated with gold using ion sputtering prior to the microscopic examination.

7.2 Particle size analysis

The powder was dispersed in isopropyl myristate. Particle size was measured by the light scattering method using laser particle size analyzer (Mastersizer S, Malvern Instrument Ltd., UK; Measurement range, 0.05-880 μm). The experiment was performed in triplicate.

7.3 True density

The density of pure materials, physical mixtures, spray dried powders, and freeze dried powder was determined by using helium pycnometer (Ultrapycnometer 1000, Quantachrome). The mean of five determinations of each preparation was calculated. A known quantity of helium was first introduced into the empty apparatus (dead space). Then a weighed amount of powder was introduced into the sample tube. The adsorbed gas was removed from the powder by an out-gassing procedure. After that helium, which was not adsorbed by the material, was again introduced. The pressure was read on a mercury manometer, and by application of the gas laws, the volume of helium surrounding the particles and pores was calculated. The difference between the volume of helium filling the empty apparatus and the volume of helium in the presence of the powder sample yields the volume occupied by the powder. Since helium penetrates into the smallest pores and crevices, it is generally conceded that the helium method gives the closet approximation to true density.

7.4 Moisture content determination

All samples were investigated the moisture content by Karl Fischer method

7.5 Fourier transform Infrared spectrophotometry

Infrared spectra of pure materials, physical mixture, spray dried powders, and freeze dried powders were measured using the potassium bromide disc method in the range of 4000 - 400 cm^{-1} (Infrared spectrometer Model FT-IR 1760X, Perkin Elmer, Germany).

7.6 Differential scanning calorimetry

DSC thermograms were obtained from Differential scanning calorimeter (DSC 822e, Mettler Toledo, USA.). All samples were examined using 4-6 mg of samples in aluminium pan and crimp. Scanning was carried out from 30-300 ºC with scanning rate at 10 ºC/min. Purged nitrogen gas was used at the rate of 60 ml/min.

7.7 Powder X-ray diffractrometry (PXRD)

X-ray diffraction patterns of pure materials, physical mixture, spray dried powder, and freeze dried powder were investigated by using an X-ray diffractometer (Model JDX-8030, Jeol, Japan). The samples were irradiated with monochromatized Cu Kβ radiation and analyzed between 2θ angles of 2 and 35º. The voltage, and current used were 30 Kv, and 15 mA, respectively.

7.8 Quantitation of spray dried and freeze dried meloxicam powders

The exact amounts of spray dried and freeze dried meloxicam powders were weighed into a volumetric flask and adjusted to 100 ml with 1 N NaOH. The mixtures were sonicated for 60 minutes and filtered through 0.45 μm nylon filter. The filtrates were analyzed spectrophotometrically at wavelength 361 nm.

8. Evaluation of meloxicam tablets

8.1 Tablet weight

Twenty tablets of each preparation were individually weighed using analytical balance. The average weight and standard deviation were calculated.

8.2 Thickness

The thickness of meloxicam tablet was measured using a micrometer. The mean of ten determinations was calculated.

8.3 Hardness

The hardness of meloxicam tablets was controlled in the range of 3-5 kp. The hardness was measured using hardness tester (Schleuniger-2E, Switzerland). Mean of five determinations was calculated.

8.4 Friability

Twenty tablets were weighed before operating in a friabilator (Erweka, Western Germany) for 4 minutes. All tablets were weighed after the process and then the percentage of friability was calculated.

8.5 Disintegration time

Disintegration time was investigated followed USP method using a disintegration tester (Erweka ZT 31, Germany). Disintegration time was recorded when all six tablets absolutely disintegrated.

8.6 The percentage labeled amount of meloxicam tablets

Ten tablets of each preparation were weighed and ground in mortar and pestle. An exact amount of the powder containing 7.5 mg of meloxicam was weighed into 50 ml volumetric flask then added about 35 ml dimethylformamide. After sonication for 30 minutes, the mixtures were adjusted with dimethylformamide. The mixtures were filtered through Whatman No. 1 membrane filter. One milliliter of filtrate was pipetted into 10 ml volumetric flask and adjusted with dimethylformamide. The solutions were determined using a UV/visible spectrophotometer at 361 nm. The percentage labeled amount of meloxicam tablet was observed duplicate.

8.7 Dissolution studies of meloxicam tablets

In vitro dissolution studies of all samples were carried out in 900 ml of deionized water, 0.1 N hydrochloric acid pH 1.2, and phosphate buffer pH 6.8 solutions according to the USP method using paddle. All samples were investigated with a speed of 100 rpm and a temperature of 37 ± 1ºC. A 10 ml of aliquot was withdrawn at different time intervals. While the tRM, tPM1:1, and tPM1:2 preparations were sampling at 5, 10, 15, 20, 30,40, 50, 60, 90, and 120 minutes, the tSPRM, tSP1:1, tSP1:2, tFD1:1, and tFD1:2 preparations were sampling at 1, 3, 5, 7, 10, 13, 15, 17, 20, 30, 60, 90, and 120 minutes. The time intervals were different according to the rate of drug release. The medium was replaced with 10 ml of fresh medium solution. The sampling was filtered using a 0.45 μm nylon filter. The filtrates were analyzed by UV spectrophotometer at 361 nm. The dissolution studies were performed in triplicate.

CHAPTER IV

RESULTS AND DISCUSSION

1. Phase solubility study

Phase solubility diagram of meloxicam-β-CD system at 37 ± 1°C is illustrated in Figure 5. Considering this curve, the apparent solubility of meloxicam increased which due to the formation of soluble meloxicam-β-CD inclusion complex. While the solubility limit of this complex reached at 8 mM β-CD concentration, the complex formation continued in the plateau region. The further addition of β-CD over 12 mM β-CD concentration resulted in the precipitation of a microcrystalline complex. This condition was not often observed, nevertheless, suggesting that the system must involve formation of two or more distinct complexes, one of these being responsible for the initial rise in solubility while another was precipitated in the latter stages of the diagram. The phase solubility diagram of meloxicam-β-CD system was classified as B_S-type according to Higuchi and Connors (1965). The stoichiometric ratio could be evaluated because the amount of β-CD represented by the plateau is equal to that entering into the complex in this interval, and the corresponding amount of meloxicam being converted to complex is equal to that present as free undissolved meloxicam at point a. The stoichiometric ratio was calculated by the following equation:

Meloxicam content of complex formed in the plateau region

= Total meloxicam added to system – Meloxicam concentration at point a

= 8.9070 - 0.3342 = 8.5728 mM

β-CD content of complex formed in the same region

= β-CD concentration at point b – β-CD concentration at point a

= 12 - 8 = 4 mM

The stoichiometric ratio

= Meloxicam content of complex formed in the plateau region

β-CD content of complex formed in the same region

= 8.5728 / 4 = 2.1432 mM

The calculating indicated that the stoichiometric ratio of meloxicam and β-CD was 1:2.

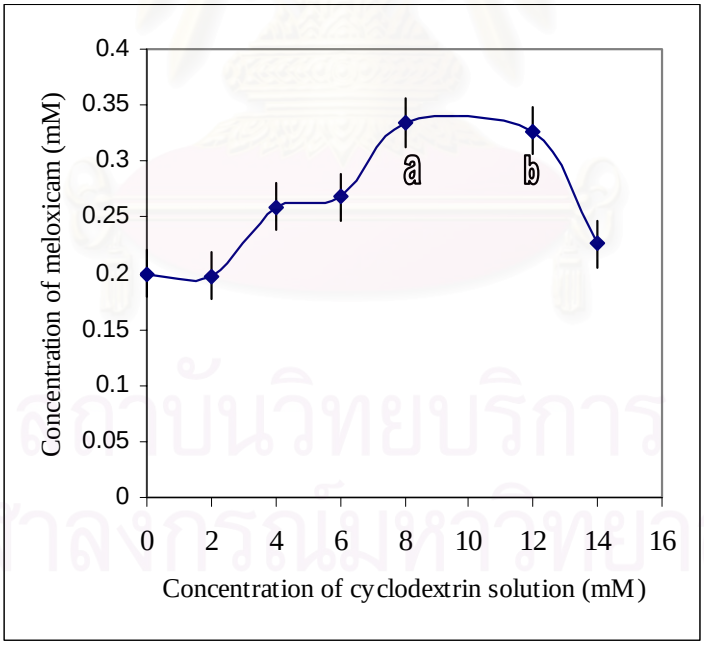

Figure 4 Phase solubility diagram of meloxicam in 0-14 mM β-CD concentration.

Table 5 Solubility of meloxicam in 0-14 mM β-CD concentration.

Concentration of β-CD (mM)	Solubility of meloxicam (mM) (average ± SD)
0	0.1999 ± 0.05
2	0.1978 ± 0.06
4	0.2597 ± 0.07
6	0.2677 ± 0.11
8	0.3342 ± 0.12
12	0.3267 ± 0.18
14	0.2262 ± 0.06

2. Characterization of the samples

2.1 Scanning electron microscope

The photomicrographs of the powder are shown in Figure 5 and 6. RM was irregular in shape with different sizes; whereas spray dried meloxicam powder SPRM was round in shape with a rough surface. CD shows an irregular shape and its sizes were bigger than RM. In contrast, SPCD were smaller and more spherical in shape than CD. Basically, the particles produced by a spray drying technique are usually spherically or regularly shaped (Killeen, 1996). FDCD/NaOH was in the shape of broken flakes which might be attributed to the presence of the solid bookies occurred during the freeze drying process (Pikal et al.; Rey and May, 1999). The photomicrograph of the PM presented the characterization of each component without modification in shape or size. The photomicrographs of SP 1:1 and SP 1:2 revealed the effect of spray drying process on their physical characterizations. FD 1:1 and FD 1:2 were broken flakes The physical characterization of freeze dried powder was also affected by the freeze drying process.

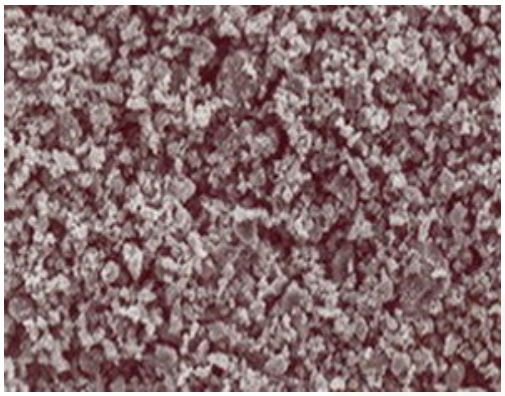

(A)

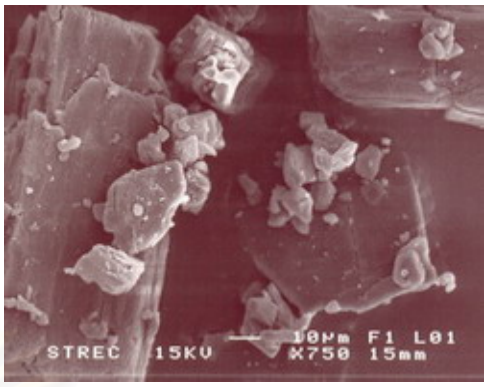

(B)

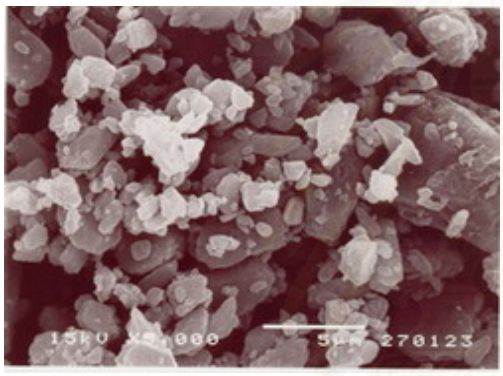

(C)

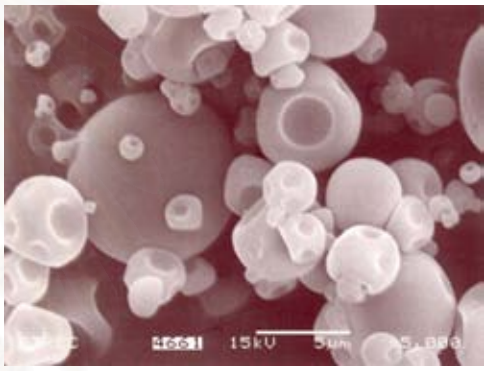

(D)

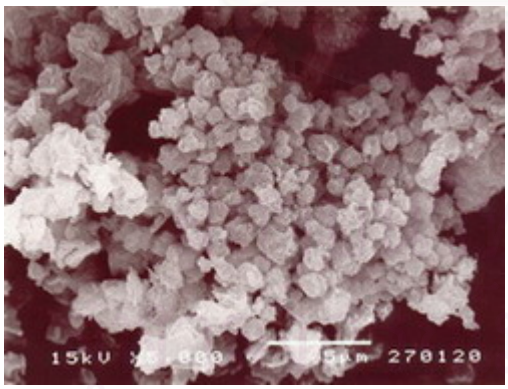

(E)

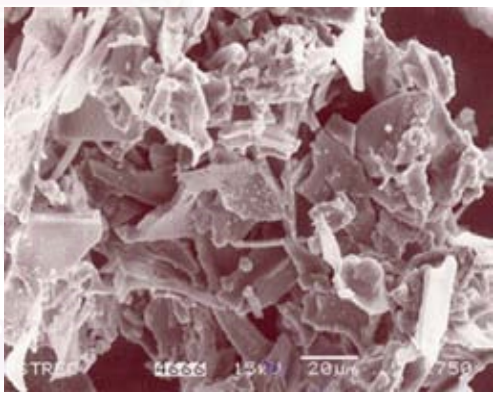

(F)

Figure 5 Photomicrographs of (A) RM (X750), (B) CD (X750) (C) RM (X5000), (D) SPCD (X5000), (E) SPRM (X5,000), and (F) FDCD/NaOH (X750).

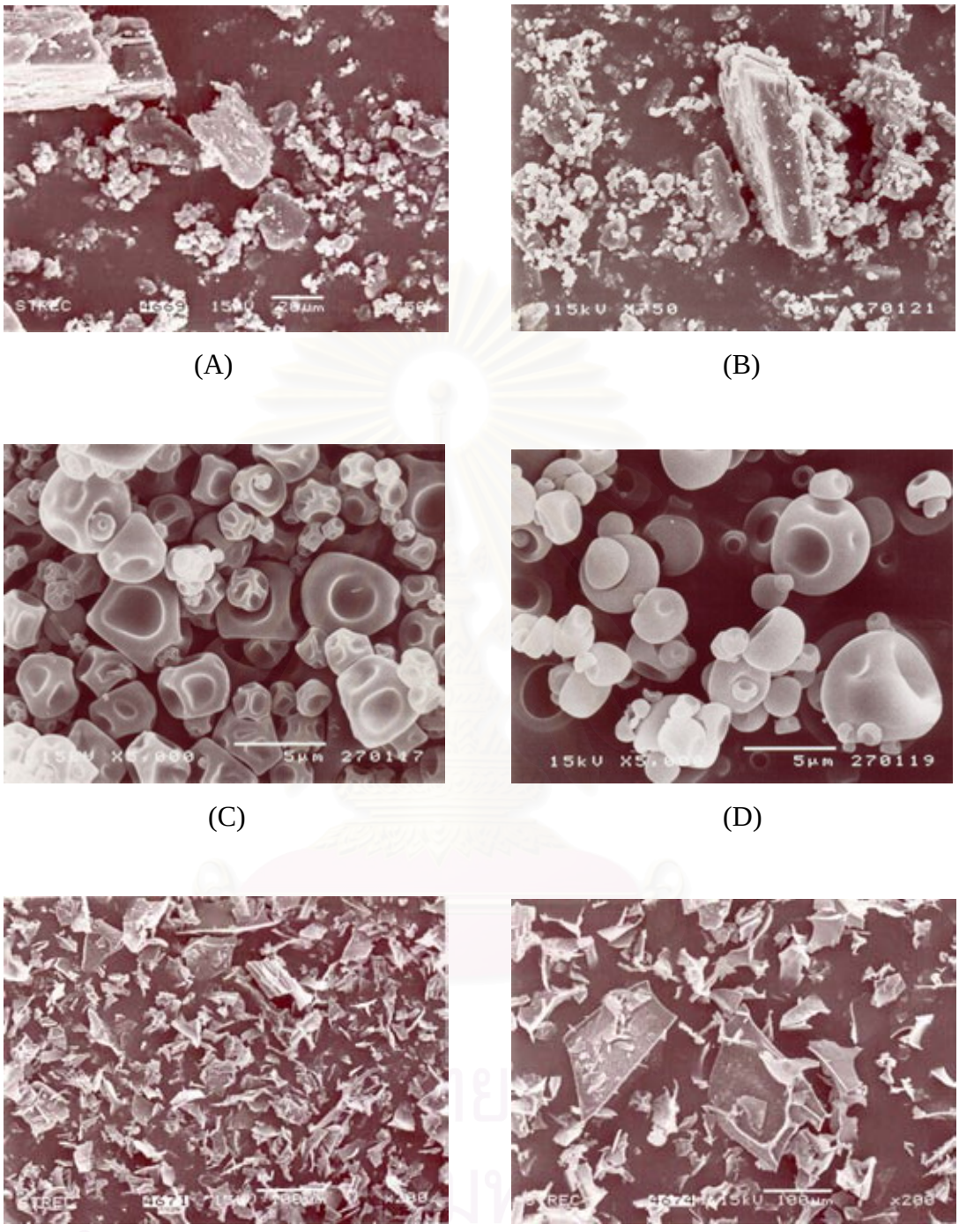

(A) (B)

(C) (D)

(E) (F)

Figure 6 Photomicrographs of (A) PM 1:1 (X750), (B) PM1:2 (X750), (C) SP 1:1 (X5,000), (D) SP 1:2 (X5,000), (E) FD 1:1 (X5,000), and (F) FD 1:2 (X5,000).

2.2 Particle size analysis

The particle size distribution of samples was shown in Table 6. Due to the fact that the formulation and spray drying had an effect on the particle size of spray dried products. In the other words, its particle size was affected by % solid content in the formulation and the droplet size during spray drying process. Since the freeze drying process generates solid bookies of components, the particle size of freeze dried products was controlled by sieving.

Table 6 The particle size distribution of RM, SPRM, CD, SPCD, FDCD, FDCD/NaOH, SP 1:1, SP 1:2, FD 1:1, and FD 1:2.

Samples	d_{10} (average ± SD) (μm)	d_{50} (average ± SD) (μm)	d_{90} (average ± SD) (μm)	Span (average ± SD)
RM	0.26 ± 0.01	7.64 ± 0.14	24.14 ± 0.16	3.126 ± 0.042
SPRM	0.35 ± 0.01	98.17 ± 12.45	266.15 ± 35.43	2.710 ± 0.197
CD	7.75 ± 0.17	76.12 ± 2.50	280.46 ± 16.42	3.586 ± 0.265
SPCD	0.99 ± 0.01	9.43 ± 0.05	25.92 ± 0.25	2.644 ± 0.014
FDCD	2.87 ± 0.02	18.43 ± 0.17	61.29 ±1.84	3.171 ± 0.078
FDCD/NaOH	19.05 ± 0.42	81.51 + 2.00	215.85 ± 4.33	2.415 ± 0.012
SP 1:1	0.50 ± 0.02	4.68 ± 0.05	14.38 ± 0.07	2.966 ± 0.024
SP 1:2	0.57 ± 0.02	4.10 ± 0.05	10.94 ± 0.03	2.529 ± 0.026
FD 1:1	9.14 ± 0.13	47.71 ± 0.33	147.61 ± 2.43	2.902 ± 0.049
FD 1:2	14.60 ± 0.22	60.61 ± 0.98	184.05 ± 4.08	2.796 ± 0.019

D_{10} The 10% volume or weight fractiles of the particle size distribution

D_{50} Mean particle size, the 50% volume or weight fractile

D_{90} The 90% volume or weight fractiles of the particle size distribution

Span A measure of size distribution narrowness calculated from the following equation:

$$Span = \frac{d_{90} - d_{10}}{d_{50}}$$

2.3 True density

The true density of pure materials, PM, SP, and FD was determined by using helium pycnometer; it is generally conceded that the helium method gives the closet approximation to true density. The true density of samples is shown in Table 7. The result showed that the density of SPRM was lower than that of RM even though SPRM had bigger size. These might be caused by the entrapment of air in the spray dried powder. The density of SPCD was lower than that of CD even though SPCD had bigger size. The density of FDCD/NaOH was higher than that of FDCD which might be attributed to the NaOH residual in the preparation.The density of PM both in the molar ratio 1:1 and 1:2 were higher than those of CD but lower than those of RM. The density of SPCD powder in the molar ratio 1:1 was higher than CD but lower than those of RM. The density of SP in the molar ratio 1:2 was lower than CD and RM. These might be due to the spray drying process, which affects the particle size of meloxicam as seen in the particle size distribution analysis. The density of FD both in the molar ratio 1:1and 1:2 was higher than those of CD and RM. These might be attributed to the effect of sodium hydroxide which still exist in the preparation after the freeze drying process.

Table 7 The true density of powder.

Samples	Apparent density (average ± SD)
RM	1.5178 ± 0.0017
SPRM	1.4227 ± 0.0032
CD	1.4570 ± 0.0018
SPCD	1.3802 ± 0.0071
FDCD	1.4485 ± 0.0040
FDCD/NaOH	1.6084 ± 0.0040
PM 1:1	1.4651 ± 0.0022
PM 1:2	1.4596 ± 0.0024
SP 1:1	1.4716 ± 0.0009
SP 1:2	1.4501 ± 0.0016
FD 1:1	1.5873 ± 0.0096
FD 1:2	1.8350 ± 0.0156

2.4 Moisture Content Determination

The moisture content of meloxicam intact, β-CD intact, spray dried powder, and freeze dried powder was presented in Table 8. β-CD itself had higher moisture content than meloxicam due to the fact that it was a hygroscopic substance. SP 1:2 contained higher moisture content than SP 1:1 according to the higher amount of β-CD. FD 1:2 also contained higher moisture content than FD 1:1 according to the higher the amount of β-CD. FD contained higher moisture content than SP. These phenomena might be caused by the effects of both β-CD and sodium hydroxide in the preparation.

Table 8 The moisture content of powder.

Samples	Weight (g)	% Moisture content
RM	0.0130	0.0354
CD	0.0125	9.2088
SP 1:1	0.0128	6.4164
SP 1:2	0.0130	7.9546
FD 1:1	0.0149	13.824
FD 1:2	0.0129	13.828

2.5 Powder X-ray diffractrometry (PXRD)

PXRD is a useful method for the detection of CD complexation in powder or microcrystalline states. The diffraction pattern of the complex should be clearly distinct from that of the superimposition of each component if a true inclusion complex has been formed.

The X-ray diffractograms of meloxicam systems are shown in Figure 7. SPRM exhibited considerable diminution of the diffraction peaks, suggesting that it is less crystalline than RM. This might due to either spray drying process or ammonium hydroxide or both.

The X-ray diffractograms of β-CD systems are shown in Figure 8. While SPCD and FDCD/NaOH showed a typical X-ray amorphous pattern, FDCD exhibited a similar diffraction pattern in comparison to that of CD. It might be concluded that the freeze drying process had no effect on β-CD; where as, either the spray drying process or ammonium hydroxide or sodium hydroxide affected β-CD.

The diffraction patterns of PM 1:1 and PM 1:2 Figure 9 show the sum of each component, indicating the presence of meloxicam and β-CD in the crystalline state. In contrast, the characteristic peaks of meloxicam are totally absent from the diffractograms of SP 1:1 and SP 1:2 (Figure 10) compared with those of PM 1:1 and PM 1:2, indicating a typical X-ray amorphous structure.

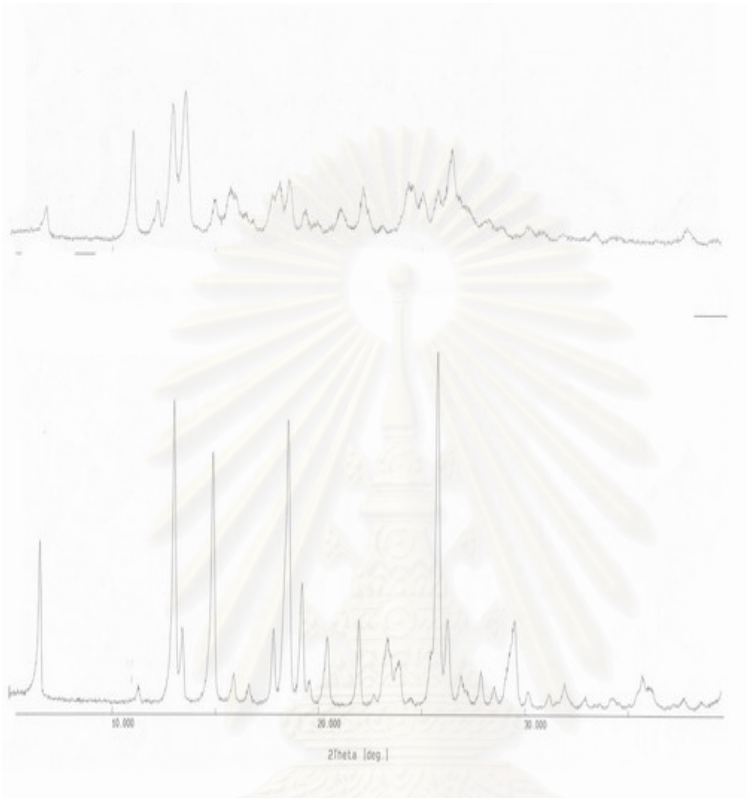

Figure 7 X-ray diffractograms of (A)RM and (B)SPRM.

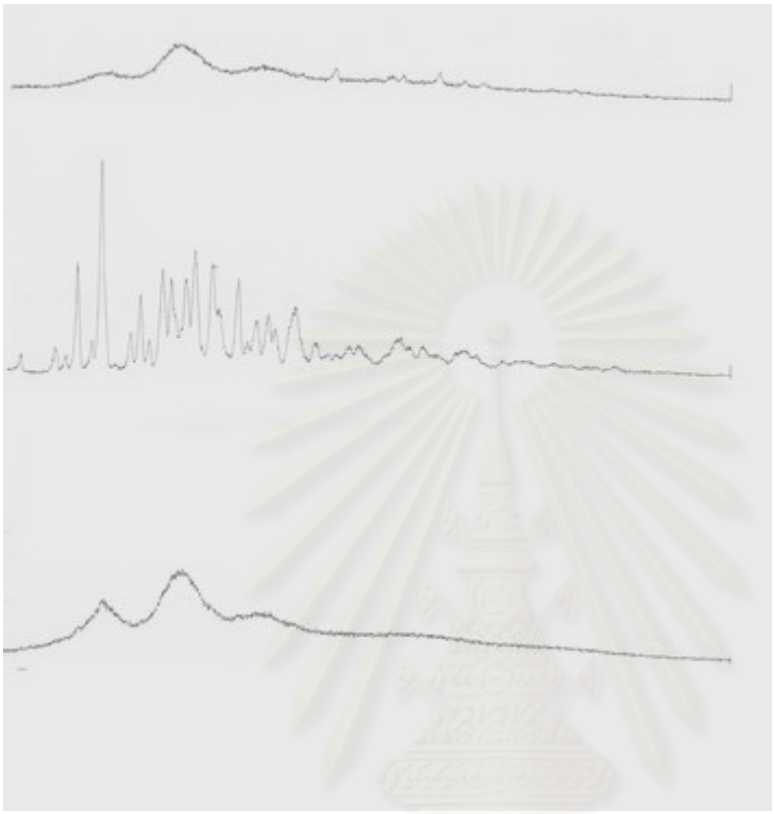

Figure 8 X-ray diffractograms of (A) CD, (B) SPCD, (C) FDCD, and (D) FDCD/NaOH.

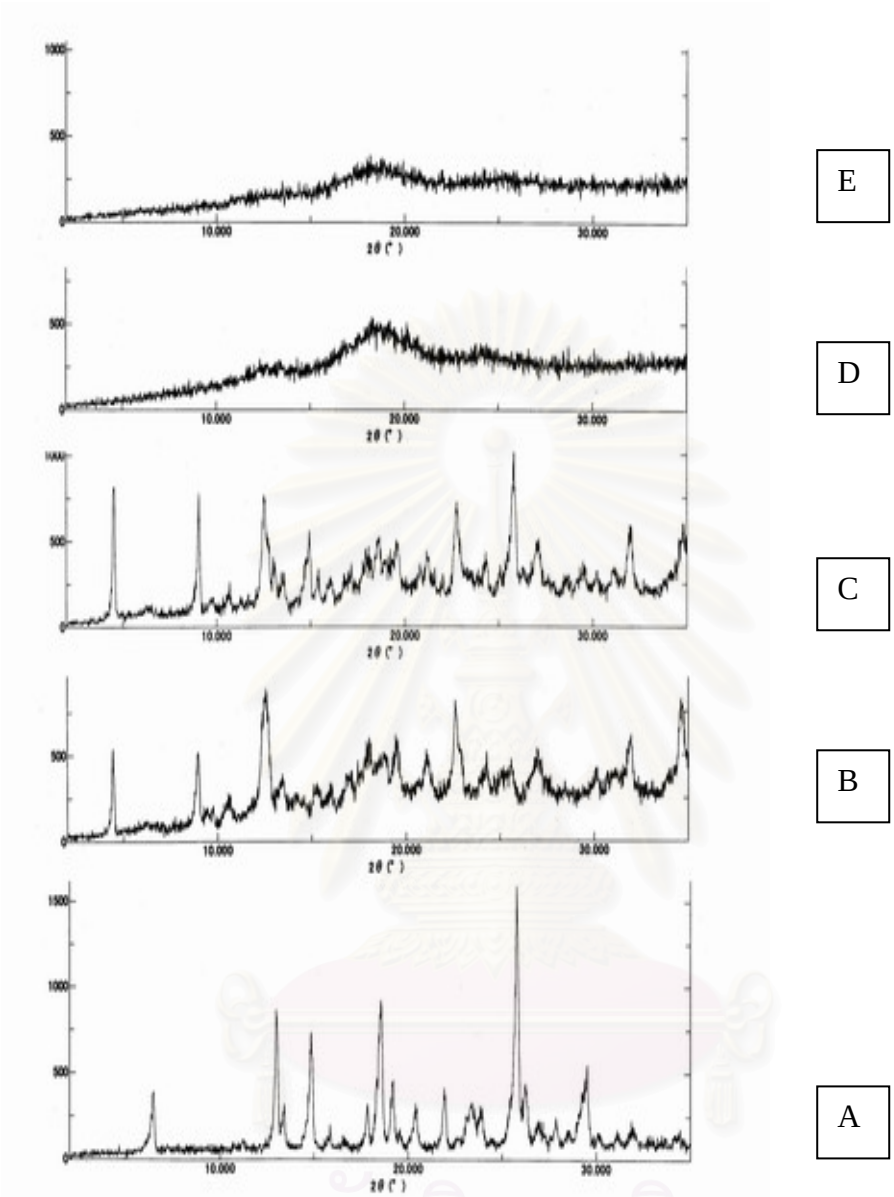

Figure 9 X-ray diffractograms of (A) RM, (B) CD, (C) PM 1:1, (D) SP 1:1, and (E) FD 1:1.

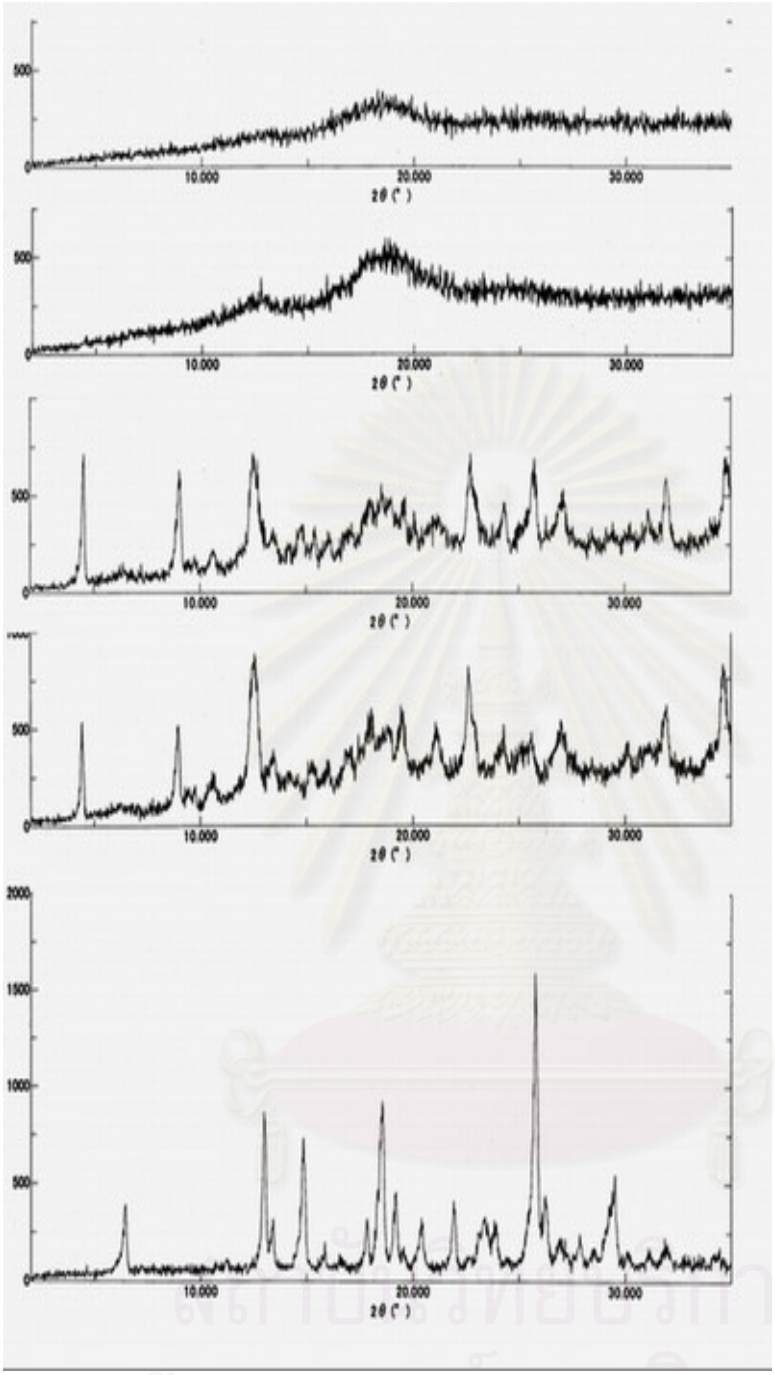

Figure 10 X-ray diffractograms of (A) RM, (B) CD, (C) PM 1:2, (D) SP 1:2, and (E) FD 1:2.

2.6 Fourier transform Infrared spectroscopy

IR proved to be very useful in analyzing the polymorphism of drug. The shifting or changing in the spectra was corresponding with the complexation.

The principle characteristic IR bands of meloxicam were:

3500-3060 cm^{-1}	- NH (amines, amides)
1580-1475 cm^{-1}	R - CO - NHR
1350-1250 cm^{-1}	aromatic amine C-N stretching
1335-1310 cm^{-1}	- SO_2 asymmetric stretching
1280-1180 cm^{-1}	C - N - (aromatic)
1230-1100 cm^{-1}	- C - N -
1200-1000 cm^{-1}	COH
1160-1130 cm^{-1}	- SO_2 symmetric stretching
1000-970 cm^{-1}	$CH = CH_2$
980-690 cm^{-1}	C = C – H
870-670 cm^{-1}	aromatic ring
835-800 cm^{-1}	CH = C (out-of-plane)
730-675 cm^{-1}	CH = CH (cis isomer)

The principle characteristic IR bands of β-CD were:

3500-3300 cm^{-1}	bonded O-H stretch in polymers
3000-2800 cm^{-1}	C -H stretch
1680-1580 cm^{-1}	C = C stretch
1600 cm^{-1} (Approx.)	aromatic ring
1420-1406 cm^{-1}	$C = CH_2$ (C – H in plane bond)
1380-1375 cm^{-1}	CH_3 symmetric (C-H bond)
1200-1000 cm^{-1}	COH
980-690 cm^{-1}	C = C – H
870-670 cm^{-1}	aromatic ring
835-800 cm^{-1}	CH = C (out-of-plane)
730-675 cm^{-1}	CH = CH (cis isomer)

The IR spectra of meloxicam systems were shown in Figure 11. RM and SPRM exhibit very pronounced difference in FT-IR spectra as shown in Figure 11A and Figure 11B, respectively. Main difference in the IR spectra of SPRM was observed at 3290.87 cm^{-1}, where the band for OH and NH stretching could not be found. This might be attributed to the presence of tertiary amide which caused by the attachment of H atom from ammonium hydroxide to the amide functional group.

The IR spectra of CD systems were shown in Figure 12. SPCD exhibited similar spectra in comparison to CD. A minor difference between FDCD and CD was observed from 1030 to 1028 cm^{-1}, where was sharper than those of CD which might be attributed to the temperature and pressure used in the freeze drying process. While, no change in absorption band position were observed in SPCD in comparison to CD, the presence of peak at 1450.88 cm^{-1} was observed in FDCD/NaOH which might be attributed to the sodium hydroxide in the preparation.

The IR spectra of meloxicam-β-CD systems in the molar ratio 1:1 and 1:2 were shown in Figure 13 and 14, respectively. According to the changing of the peaks especially at 3290.87 cm^{-1} and 1621-1240.72 cm^{-1}, the interaction between meloxicam and β-CD after the spray drying process and freeze drying might have occurred at amide group.

Figure 11 IR spectra of (A) RM and (B) SPRM.

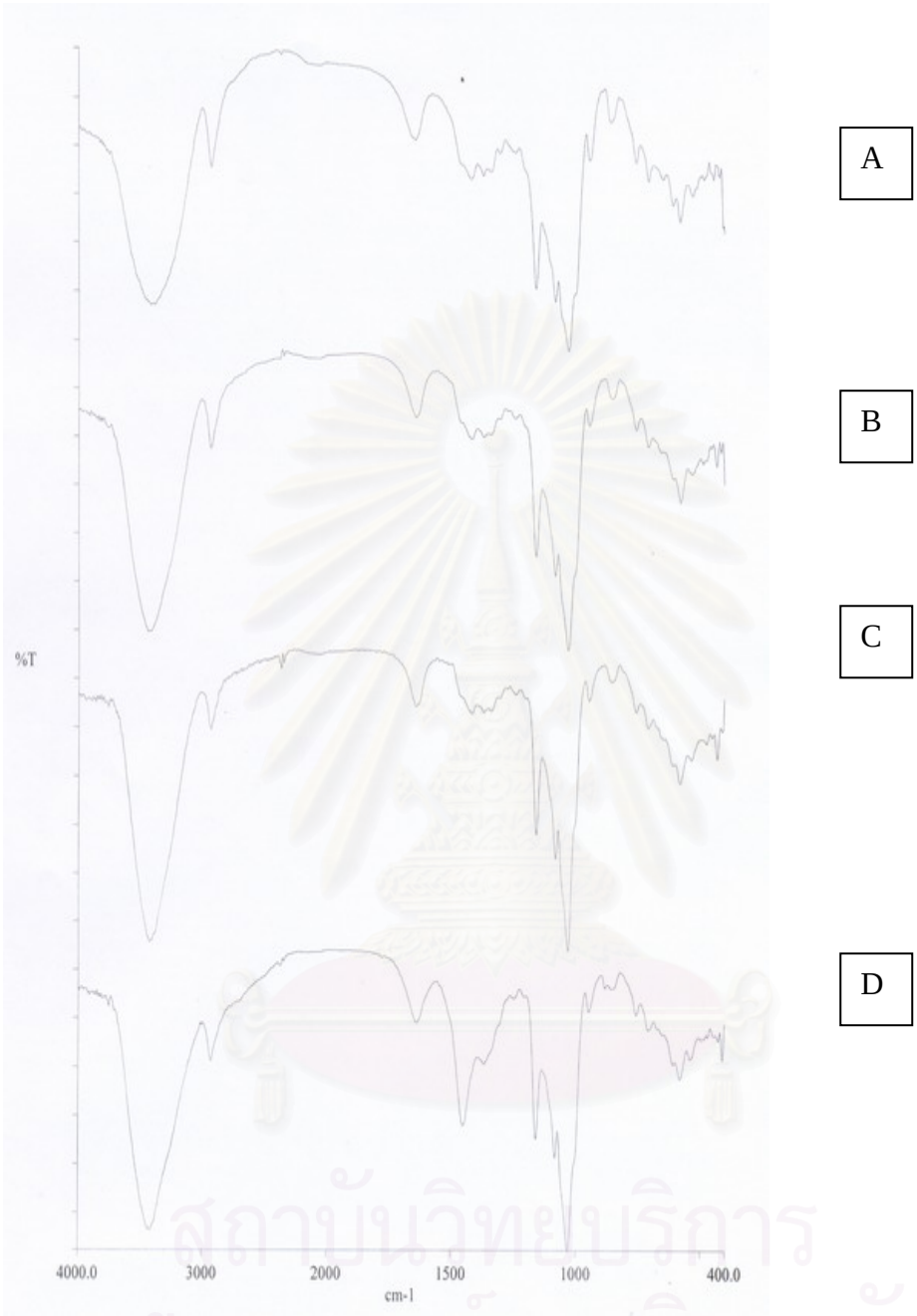

Figure 12 IR spectra of (A) CD, (B) SPCD, (C) FDCD, and ((D) FDCD/NaOH.

Figure 13 IR spectra of (A) RM, (B) CD, (C) PM 1:1, and (D) PM 1:2.

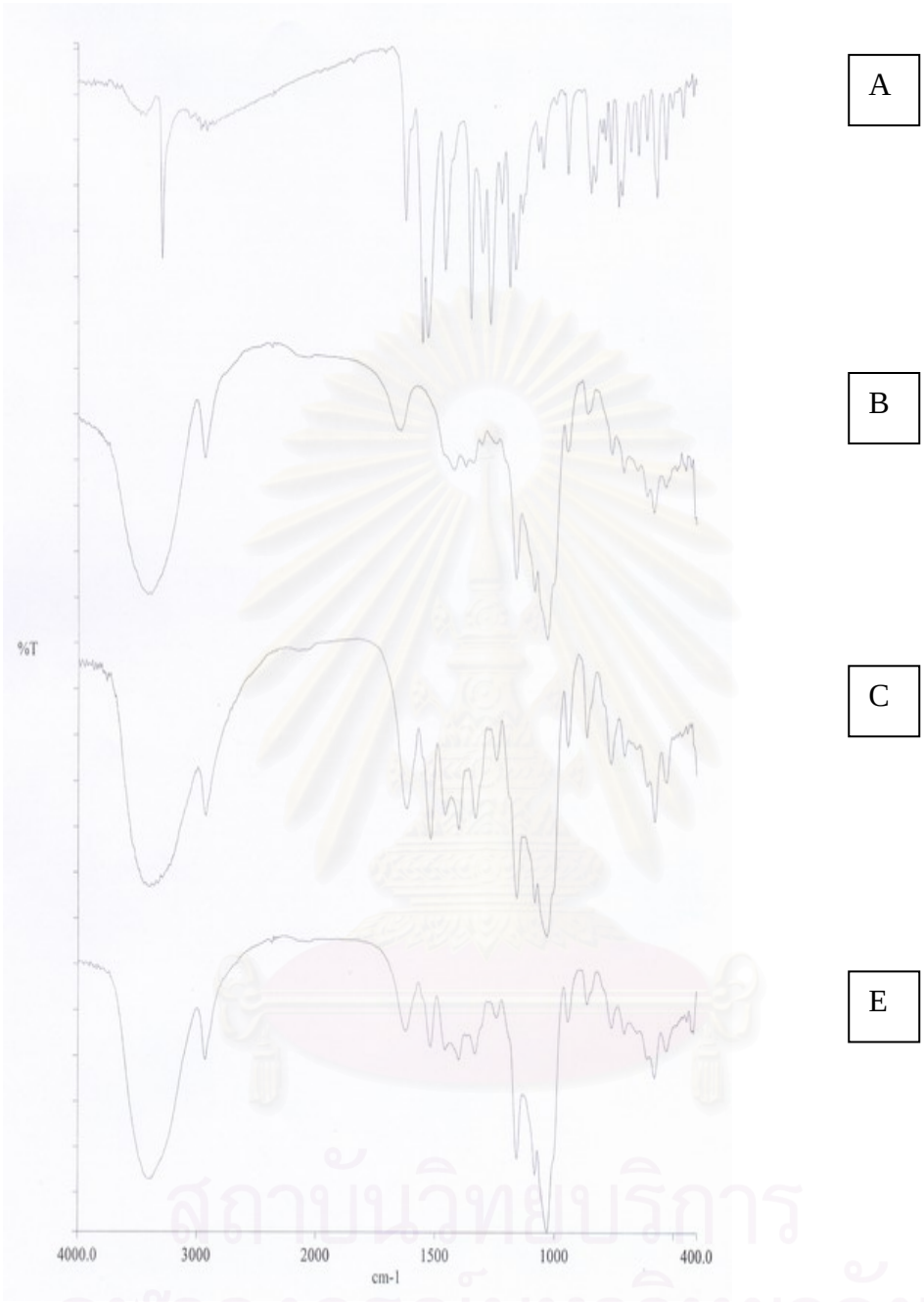

Figure 14 IR spectra of (A) RM, (B) CD, (C) SP 1:1, and (D) SP 1:2.

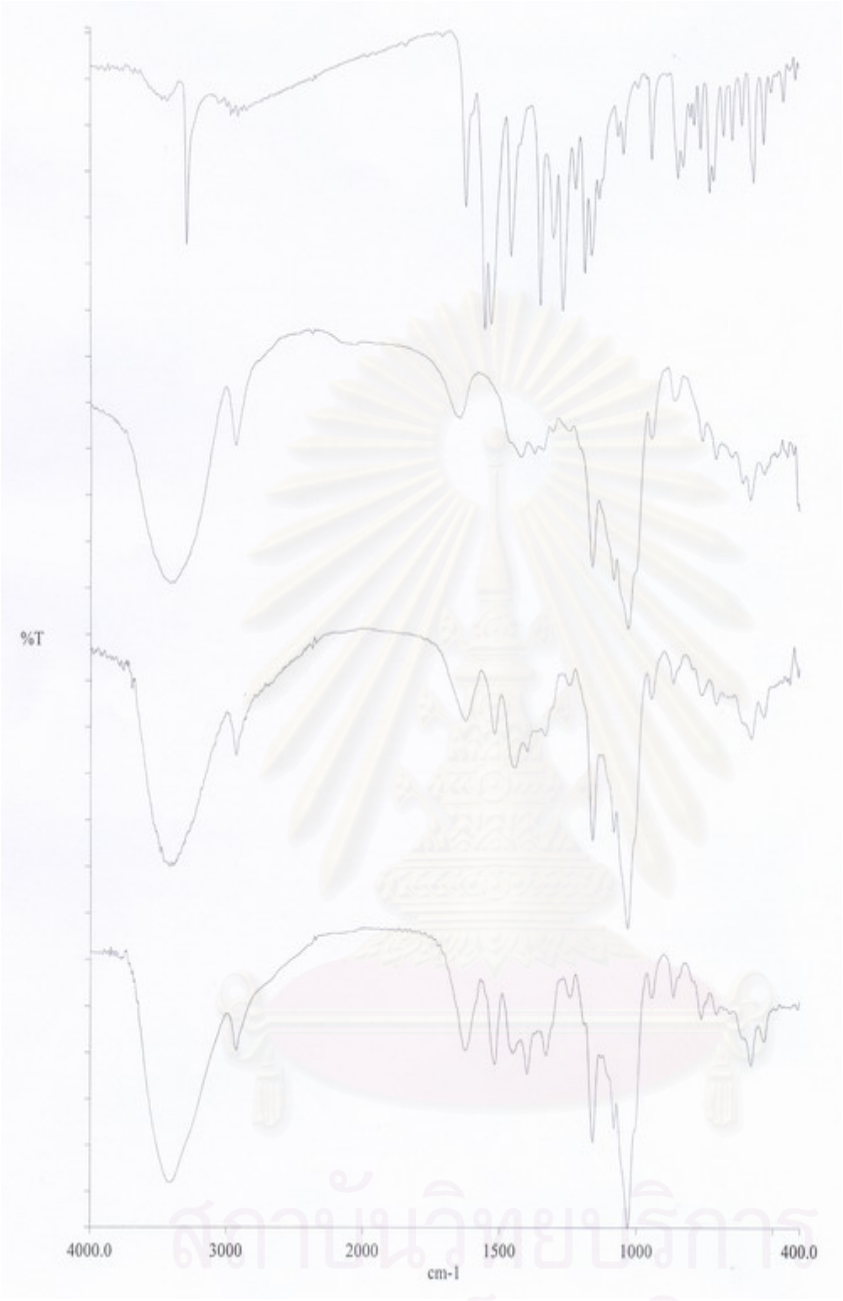

Figure 15 IR spectra of (A) RM, (B) CD, (C) FD 1:1, and (D) FD 1:2.

2.6 Differential scanning calorimetry (DSC)

DSC is a useful technique for drugs that form inclusion complex with CDs, being evidenced by the loss of the drug melting endotherm.

The DSC curves obtained from RM (Figure 16A) and SPRM (Figure 16B) show a double endothermic peak which could be attributed to the presence of two different polymorphisms in the samples. While, the DSC thermogram of RM exhibits a double endothermic effect at 267.64 °C and 272.60 °C, the DSC thermogram of SPRM exhibits a double endothermic effect at 257.60 °C and 268.50 °C. This observation could be concluded that SPRM might have higher entropy than RM, which resulted in lower melting point of SPRM in comparison to RM.

The thermoanalytical profile of *β*-CD can be generally divided into three parts: (1) water loss from ambient temperature up to 120°C depending on the experimental arrangements; (2) thermal degradation which accompanied by oxidation in air starting above 250°C in solid phase at first and continuing in liquid state after fusion which occurs approximately at 300 °C; (3) ignition takes place in air above 300°C (Giordano F., Novak C, and Moyano J.R., 2001). In this study, the loss of water was observed in the DSC thermogram of *β*-CD (Figure17A), as presented by the broad endothermic peaks between room temperature and 100°C (71.64°C). The endothermic peak exhibited at 316.74°C.

The DSC thermogram of SPCD (Figure 17B) presents the lower amount of water in comparison to CD which might be attributed to the dehydration during the spray drying process. The endothermic peak shifted to the higher temperature and exhibited the broader peak which might be assumed that SPCD consumed more enthalpy than CD.

The DSC thermogram of FDCD (Figure 17C) shows the dehydration period as similar to CD but presented the lower endothermic peak in comparison to CD in the same position as in SPCD.

The DSC thermogram of FDCD/NaOH (Figure 17D) exhibits only the dehydration period which might be due to the interruption of sodium hydroxide in the rearrangement of meloxicam and β-CD. That was the reason why X-ray detected them as amorphous and why DSC could not detect their melting points

The DSC thermograms of PM 1:1 and PM 1:2 (Figure 18) show the endothermic peaks of meloxicam which shift to the lower temperature in comparison to RM. This might be assumed that either the water in β-CD molecules or β-CD itself had an effect on the polymorphism of meloxicam. This assumption was approved by observing the DSC thermograms of physical mixture prepared from meloxicam intact and heated β-CD powder (100°C for 1 hr). The DSC thermograms of hPM 1:1 and hPM 1:2 show less endothermic peaks of β-CD, suggesting the less amount of water and present the endothermic peaks of meloxicam as similar to those of PM 1:1 and PM 1:2, respectively.

The inclusion was evidenced by the loss of the endothermal melting peak of crystalline meloxicam as shown in SP 1:1 and SP 1:2 (Figure 19).

FD 1:1 and FD 1:2 exhibit the DSC thermogram which is similar to those of FDCD/NaOH as shown in Figure 20.

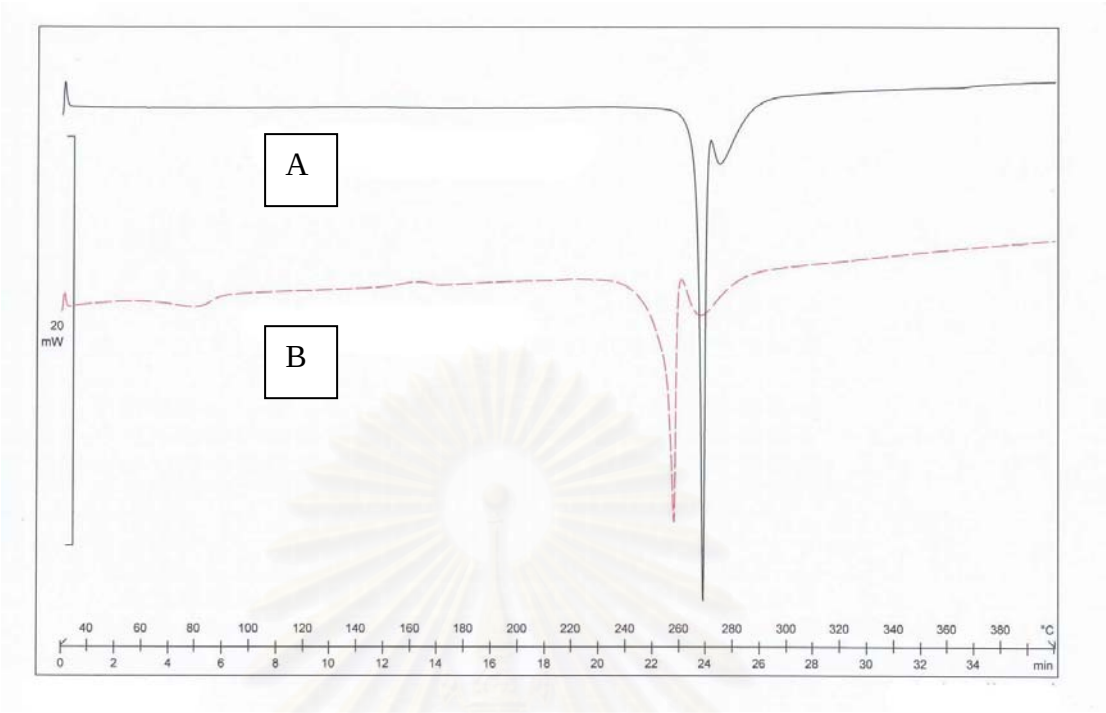

Figure 16 DSC thermograms of (A) RM, and (B) SPRM.

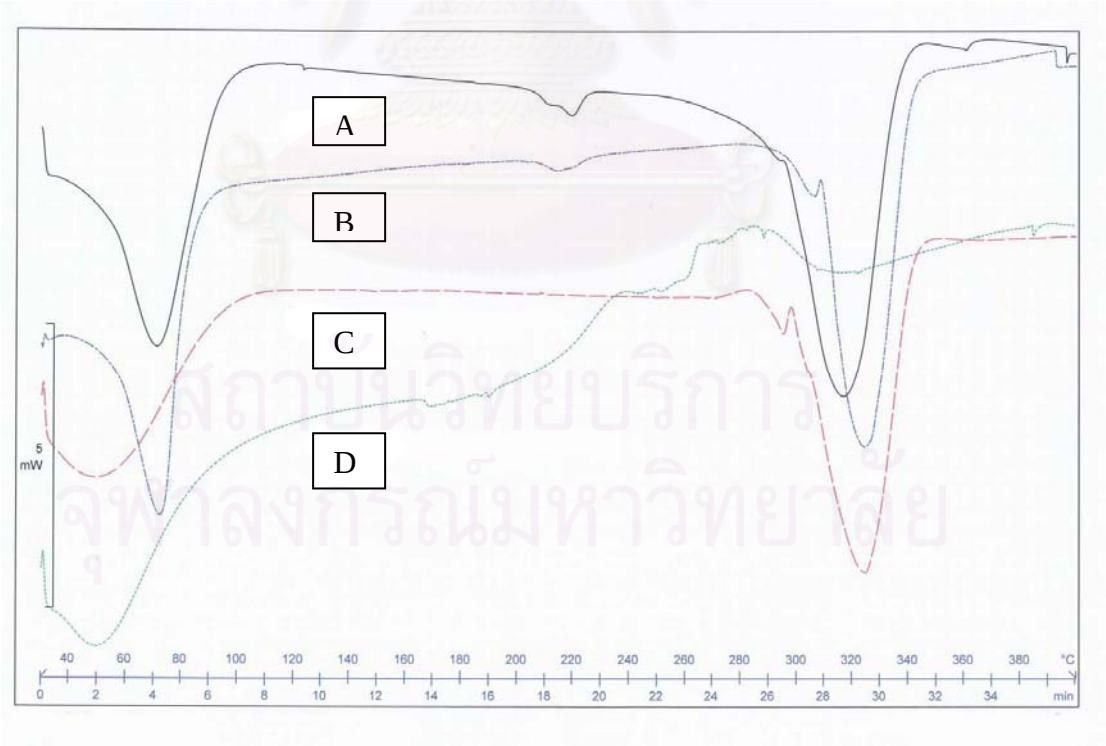

Figure 17 DSC thermograms of (A)CD, (B)FDCD, (C)SPCD, and (D)FDCD/NaOH.

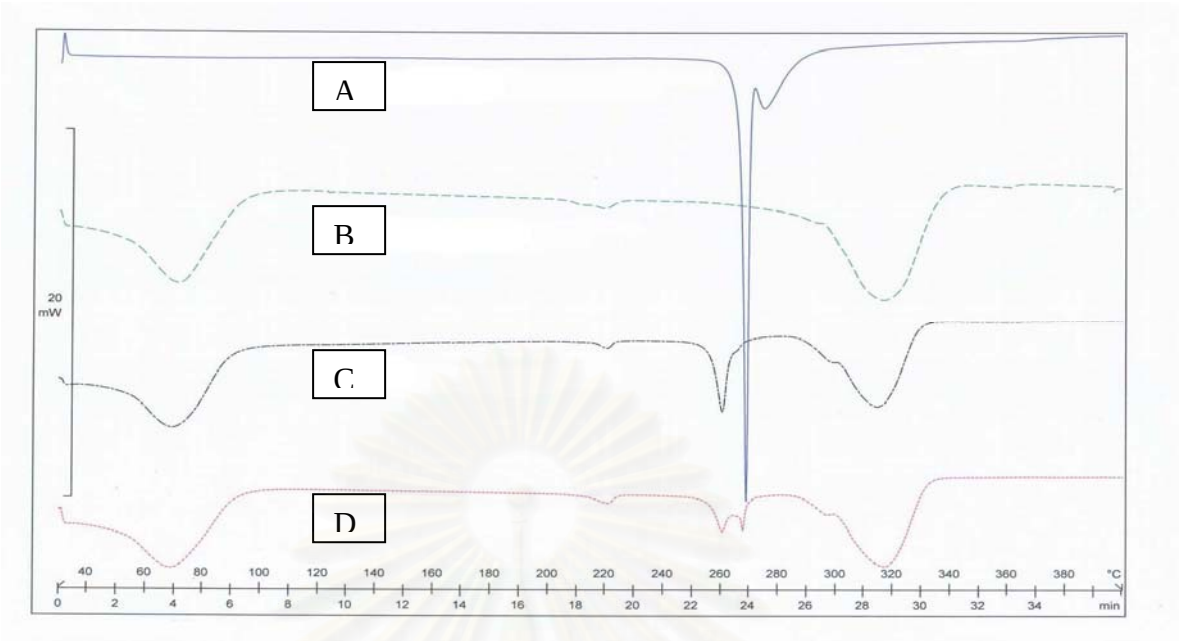

Figure 18 DSC thermograms of (A) RM, (B) SPRM, (C) PM 1:1, and (D) PM 1:2.

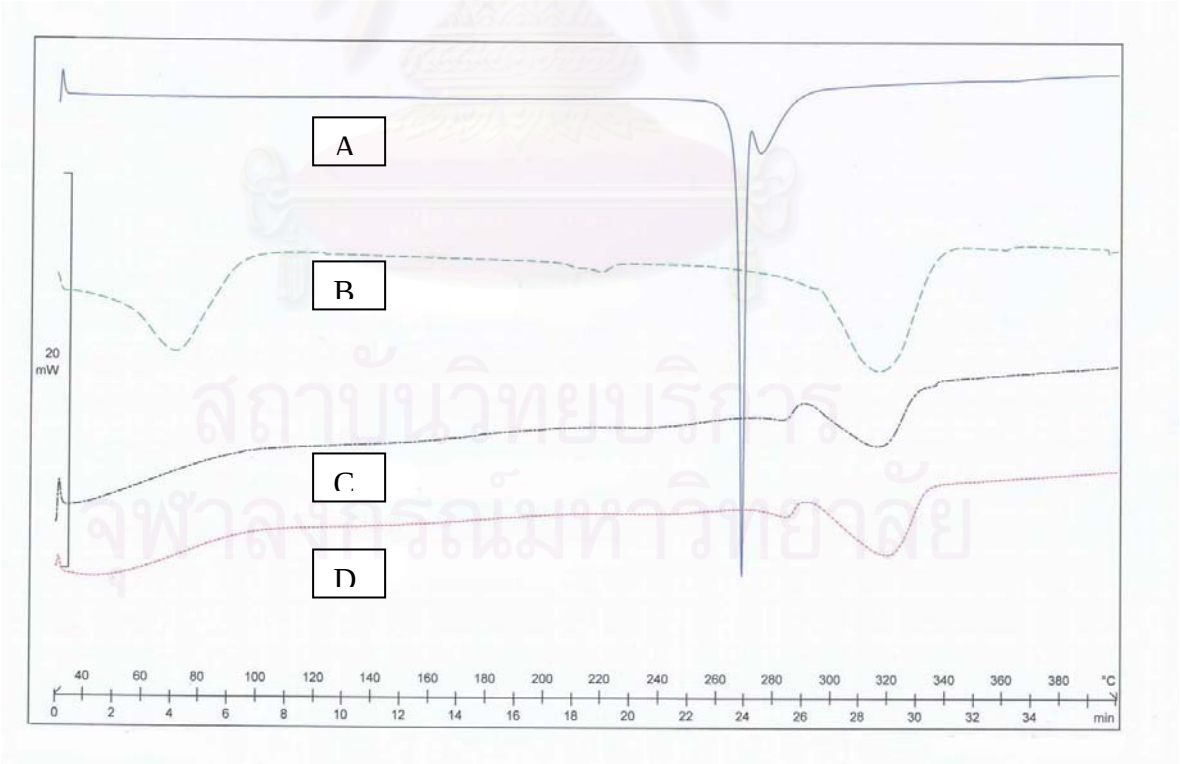

Figure 19 DSC thermograms of (A) RM, (B) SPRM, (C) SP 1:1, and (D) SP 1:2.

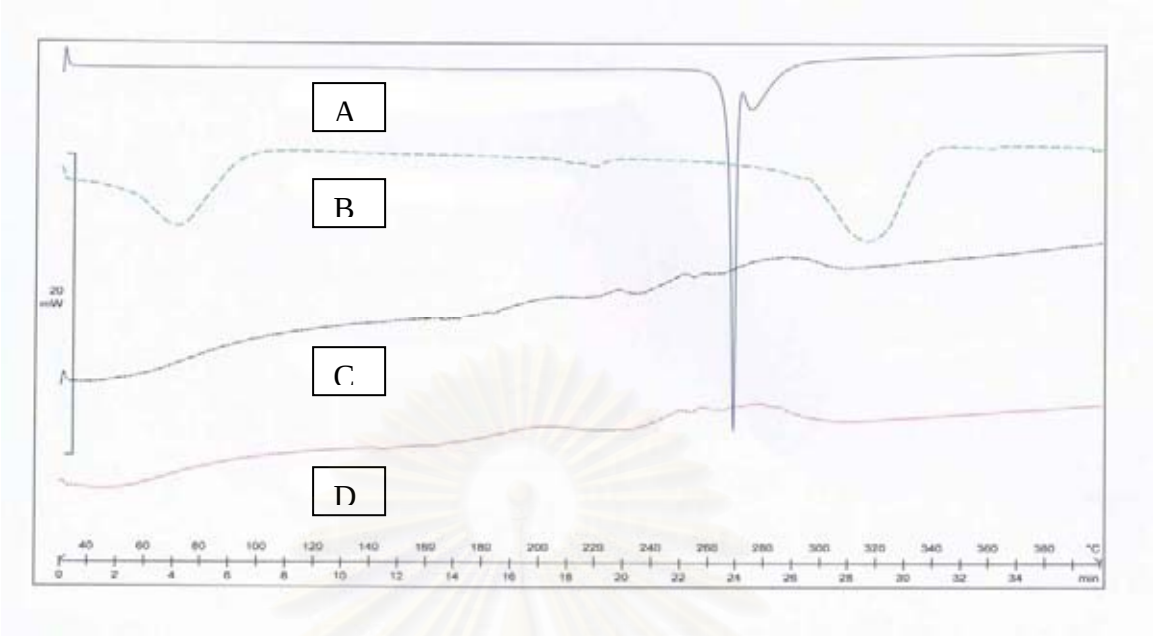

Figure 20 DSC thermograms of (A) RM, (B) CD, (C) FD 1:1, and (D) FD 1:2.

2.7 Quantitation of meloxicam in spray dried and freeze dried powder

The quantity of meloxicam found in spray dried and freeze dried powder were illustrated in Table 9. The data obtained from this section, were used for tablet formulation.

Table 9 Quantitation of meloxicam in spray and freeze dried powder.

Preparations	% meloxicam[a] (average ± SD)	% meloxicam[b] (average ± SD)
SP 1:1	18.75 ± 0.34	100.06 ± 1.83
SP 1:2	13.10 ± 0.23	97.28 ± 1.74
FD 1:1	21.88 ± 1.20	100.70 ± 5.53
FD 1:2	13.76 ± 0.39	113.02 ± 3.23

a) % meloxicam in powder

b) % theoretical amount of meloxicam

3. Evaluation of meloxicam tablets

3.1 Physical properties of meloxicam tablets

Tablet weight, hardness, friability, and disintegration time of meloxicam tablet are illustrated in Table 10.

3.1.1 Tablet weight

The tabletting process was operated one by one using a hydraulic press with a round flat faced punch-die assembly diameter of 10 mm. Each tablet weighed in the range of 178.44 – 181.46 mg.

3.1.2 Hardness

The hardness of meloxicam tablet was between 3.17 - 4.94 kp due to the differences of pressure used in the tabletting. The controlled hardness was ranging from 3 to 5 kp.

3.1.3 Thickness

The thickness of meloxicam tablet was between 3.45 - 4.52 mm. The rank of thickness of meloxicam tablet was as followed: RM < PM1:1 ≅ SPRM < PM1:2 < FD1:1 < SP1:1 < FD 1:2 < SP1:2. The pressure which used during tabletting, had an influence on thickness.

3.1.4 Friability

According to the sharp edge of meloxicam tablet, the friability was so high then lead to the failure to the USP 24 specification. The friability was ranged from 1.09 % to 1.67 %; whereas, the acceptable limit of friability conforming to the USP 24 was not more than 1%.

3.1.5 Disintegration time

The disintegration time of spray dried and freeze dried meloxicam-β-cyclodextrin tablet was longer than that of commercial tablet (Mobic®); whereas, that of meloxicam, spray dried meloxicam, physical mixture of meloxicam-β-cyclodextrin tablet were shorter.

Table 10 Physical properties of meloxicam tablets.

Preparations	Tablet Weight (mg) (average ± SD)	Hardness (kp) (average ± SD)	Thickness (mm) (average ± SD)	Friability (%)	Disintegration Time (minute)
RM	179.48 ± 0.80	4.53 ± 0.59	3.45 ± 0.03	1.32	0.48
SPRM	178.44 ± 0.86	4.26 ± 0.31	3.56 ± 0.04	1.38	0.24
PM 1:1	181.30 ± 1.07	4.80 ± 0.50	3.52 ± 0.02	1.09	0.45
PM 1:2	181.18 ± 1.56	4.39 ± 0.32	3.73 ± 0.04	1.66	0.52
SP 1:1	179.35 ± 0.46	4.92 ± 0.28	4.13 ± 0.05	1.15	4.10
SP 1:2	179.83 ± 0.77	4.40 ± 0.73	4.52 ± 0.02	1.29	5.41
FD 1:1	181.42 ± 0.64	4.12 ± 0.45	3.95 ± 0.09	1.65	5.05
FD 1:2	181.46 ± 1.56	4.94 ± 0.56	4.36 ± 0.03	1.67	4.30
Mobic	179.14 ± 1.76	7.97 ± 1.27	Nondetectable	0.27	1.19

3.1.6 The percentage labeled amount of meloxicam tablet

Since the acceptable limit of % LA conforming to the USP 24 was between 90-110%, the content of all meloxicam tablets passed the specification as shown in Table 11.

Table 11 The percentage labeled amount of meloxicam tablet.

Preparations	The percentage labeled amount of meloxicam tablet (average ± SD)
RM	95.12 ± 1.00
SPRM	90.57 ± 0.16
PM 1:1	94.42 ± 3.32
PM 1:2	93.99 ± 4.07
SP 1:1	96.28 ± 0.05
SP 1:2	101.44 ± 3.85
FD 1:1	98.90 ± 1.97
FD 1:2	96.44 ± 0.44

3.1.7 Dissolution studies of meloxicam tablets

The release profile of meloxicam was plotted between the percent of drug release against time. The dissolution profiles of meloxicam and commercial tablet in deionized water, 0.1 N HCl, and phosphate buffer pH 6.8 solutions are illustrated in Figure 21-25. Each point represented the average value which calculated from triplicate data at the given sampling time. From the data obtained, it was found that drug release at T_{30} in deionized water of meloxicam tablet prepared from RM (Figure 21A) showed significant difference from those of all preparations. It depicted the least % drug release which meant that combination with β-CD could improve the aqueous solubility of meloxicam. Moreover, the spray drying process and/or 30% concentrated ammonium hydroxide also increased the solubility in water of meloxicam which may caused by the changing in form of meloxicam.

There were no significant differences between the drug release at T_{30} in deionized water of t SPRM (Figure 21B) and that of tPM 1:1 (Figure 22A) and tPM 1:2 (Figure 22B). It indicated that the spray drying process and/or 30% concentrated ammonium hydroxide could enhance the aqueous solubility of meloxicam as well as the physical mixing with β-CD.

There were also no significant differences between the drug release at T_{30} in deionized water of t SPRM (Figure 21B) and those of meloxicam tSP 1:2 (Figure 23B) and tFD 1:1 (Figure 24(A)). There was a significant difference between the drug release at T_{30} in deionized water of tSP 1:1 (Figure 23A) and that of tSP 1:2 (Figure 23B) which were lower. There was also a significant difference between the drug release at T_{30} in deionized water of tFD 1:1 (Figure 24A) and that of tFD 1:2 (Figure 24B) which were higher. It indicated that the molar ratio of meloxicam and β-CD was important for spray drying and freeze drying processes. There were no significant differences between the drug release at T_{30} in deionized water of Mobic® and that of tPM 1:1 (Figure 22A) and tPM 1:2 (Figure 22B). It indicated that co-spray drying and co-freeze drying techniques with β-CD could improve aqueous solubility of meloxicam when comparing with Mobic®. The rank of the percentage of drug release in deionized water at T_{30} was as followed: RM < Mobic® < PM1:1 ≅ PM 1:2 ≅ SPRM ≅ FD 1:1 ≅ SP 1:2 ≅ SP 1:1 ≅ FD 1:2.

In this study, it was found that there were no significant differences between the drug release at T_{30} in 0.1 N HCl pH 1.2 of tRM (Figure 21A) and that of t PM 1:1 (Figure 22A) and PM 1:2 (Figure 22B). It indicated that physical mixing with β-CD could not improve the solubility of meloxicam in 0.1 N HCl. There were significant differences between the drug release at T_{30} in 0.1 N HCl pH 1.2 of t (Figure 21A) and that of tSP 1:1 (Figure 23A) and SP 1:2 (Figure 23B). It indicated that co-spray drying technique with β-CD could increase the solubility of meloxicam in 0.1 N HCl. However, there were no significant differences between the drug release at T_{30} in 0.1 N HCl pH 1.2 of tSPRM (Figure 21B) and that of tSP 1:1 (Figure 23A) and SP 1:2 (Figure 23B). It indicated that the spray drying process alone could enhance the solubility of meloxicam in 0.1 N HCl as well as co-using with β-CD. There were significant differences between the drug release at T_{30} in 0.1 N HCl pH 1.2 of tRM and that of tFD 1:1 (Figure 24A) and tFD 1:2 (Figure 24B). It indicated that co-freeze drying technique with β-CD could increase the solubility of meloxicam in 0.1 N HCl.

There was no significant difference between the drug release at T_{30} in 0.1 N HCl of tSP 1:1 (Figure 23A) and that of tSP 1:2 (Figure 23B). On the other hand, there was a significant difference between the drug release at T_{30} in 0.1 N HCl of tFD 1:1 (Figure 24A) and that of meloxicam tablet prepared from FD 1:2 (Figure 24B) which were higher. It indicated that the molar ratio of meloxicam and β-CD was not important for spray drying process but it was important for freeze drying process. There were significant differences between the drug release at T_{30} in 0.1 N HCl pH 1.2 of Mobic® (Figure 25) and those of all preparations. It indicated that co-spray drying and co-freeze drying techniques with β-CD could improve the solubility of meloxicam in 0.1 N HCl when comparing with Mobic®. The rank of % drug release in 0.1 N HCl pH 1.2 at T_{30} was as followed: Mobic® < RM ≅ PM1:2 ≅ PM 1:1 < SPRM ≅ SP 1:2 ≅ SP 1:1 ≅ FD 1:1 ≅ FD 1:2.

In this study, it was found that there were no significant differences between the drug release at T_{30} in phosphate buffer pH 6.8 of tRM and that of tPM 1:1 (Figure 22A), tPM 1:2, (Figure 22B), and tSPRM (Figure 21B). It indicated that physical mixing with β-CD and spray drying alone could not improve the solubility of meloxicam in phosphate buffer pH 6.8. There were significant differences between the drug release at T_{30} in phosphate buffer pH 6.8 of tRM (Figure 21A) and that of tSP 1:1 (Figure 23A) and tSP 1:2 (Figure 23B). Moreover, there were no significant differences between the drug release at T_{30} in phosphate buffer pH 6.8 of tRM and that of tFD 1:1 (Figure 24A) and tFD 1:2 (Figure 24B). It indicated that co-spray drying and co-freeze drying techniques with β-CD could enhance the solubility of meloxicam in phosphate buffer pH 6.8. There was no significant difference between the drug releases at T_{30} in phosphate buffer pH 6.8 of tSPRM (Figure 21B) and that of tSP 1:1 (Figure 23A) and tSP 1:2 (Figure 23B). It indicated that the spray drying process alone could enhance the solubility of meloxicam in phosphate buffer pH 6.8 as well as co-using with β-CD.

There was no significant difference between the drug release at T_{30} in phosphate buffer pH 6.8 of tSP 1:1 (Figure 23A) and that of tSP 1:2 (Figure 23B). Moreover, there was also no significant difference between the drug release at T_{30} in phosphate buffer pH 6.8 of tFD 1:1 (Figure 24A) and that of tFD 1:2 (Figure 24B). It indicated that the molar ratio of meloxicam and β-CD did not affect tSP. There was significant difference between the drug release at T_{30} in phosphate buffer pH 6.8 of Mobic® (Figure 25) and that of tSPRM (Figure 21B), tSP 1:1 (Figure 23A), tSP 1:2 (Figure 23B), tFD 1:1 (Figure 24A), and tFD 1:2 (Figure 24B). It indicated that spray drying process alone, co-spray drying, and co-freeze drying technique with β-CD could improve the solubility of meloxicam in phosphate buffer pH 6.8 in comparison to Mobic®. The rank of the percentage of drug release in phosphate buffer pH 6.8 at T_{30} was as followed: Mobic® ≅ PM1:2 ≅ RM ≅ PM 1:1 ≅ SP 1:2 ≅ FD 1:1 ≅ FD 1:2 ≅ SPRM ≅ SP 1:1. In conclusion, co-spray drying and co-freeze drying with β-CD could significantly enhance the solubility of meloxicam in deionized water, 0.1 N HCl pH 1.2, and phosphate buffer pH 6.8.

As shown in Table 13, it was found that all preparations provided the higher dissolution profiles than RM and Mobic® preparations; even though, the disintegration time of tSP and tFD preparations was longer than that of tRM and Mobic® preparations. The used time to reach 75 % drug release of preparation between the molar ratio 1:1 and 1:2 showed no significant differences. The particle size of SPRM was larger than RM; nevertheless, the used time to reach 75 % drug release was shorter. This might be caused by the increasing of wettability and porosity of spray dried powder. tPM preparation also showed the shorter time which might be attributed to the influence of β-CD on the increasing solubility. It was found that tSP and tFD preparations provided the higher dissolution profiles in both 0.1 N HCl and phosphate buffer pH 6.8 solutions than tRM and Mobic®.

It exhibited that co-spray drying and co-freeze drying with β-CD improved the solubility of meloxicam in 0.1 N HCl and in phosphate buffer pH 6.8; however, either tSPRM or tPM showed no significant differences in comparison to tRM. The used time to reach 75 % drug release of preparation between the molar ratio 1:1 and 1:2 also showed no significant differences.

Table 12 The percentage of drug release in deionized water, 0.1 N HCl, and phosphate buffer pH 6.8 solutions at T_{30}.

Preparations	Drug release at T_{30} (average ± SD)		
	Deionized water	0.1 N HCl	Phosphate buffer pH 6.8
RM	59.02 ± 0.72	15.57 ± 0.55	80.78 ± 0.63
SPRM	89.53 ± 2.21	51.26 ± 2.10	93.18 ± 2.56
PM 1:1	85.86 ± 2.12	17.34 ± 0.05	80.99 ± 2.85
PM 1:2	86.23 ± 2.13	16.03 ± 0.17	78.50 ± 0.33
SP 1:1	101.14 ± 0.62	56.65 ± 0.51	96.54 ± 0.78
SP 1:2	95.96 ± 1.05	56.62 ± 0.77	91.85 ± 0.55
FD 1:1	95.52 ± 0.84	69.38 ± 2.27	92.51 ± 1.23
FD 1:2	103.97 ± 2.84	78.82 ± 2.81	93.05 ± 1.05
Mobic®	79.91 ± 2.15	10.78 ± 0.11	73.66 ± 1.96

Table 13 The used time to reach 75 % drug release in deionized water, 0.1 N HCl, and phosphate buffer pH 6.8 solutions and the used time to reach 50 % drug release in 0.1 N HCl.

Preparations	The used time to reach 75 % drug release (min)			The used time to reach 50 % drug release (min)
	Deionized water	0.1 N HCl	Phosphate buffer pH 6.8	0.1 N HCl
RM	> 120	> 120	20	> 120
SPRM	10-15	> 120	3	30
PM 1:1	10-15	> 120	20	> 120
PM 1:2	10-15	> 120	20	> 120
SP 1:1	~ 5	> 120	5	17
SP 1:2	5-7	> 120	7	15
FD 1:1	3-5	> 120	3	5
FD 1:2	1-3	10	5	< 5
Mobic®	20-30	> 120	30	> 120

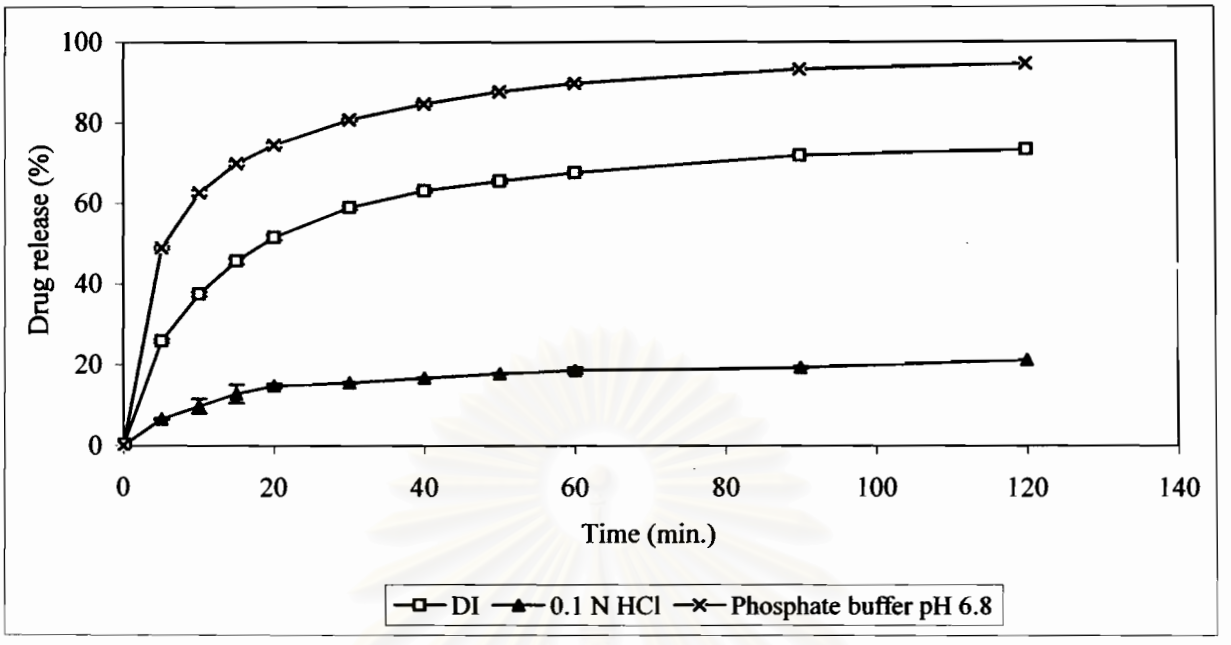

A

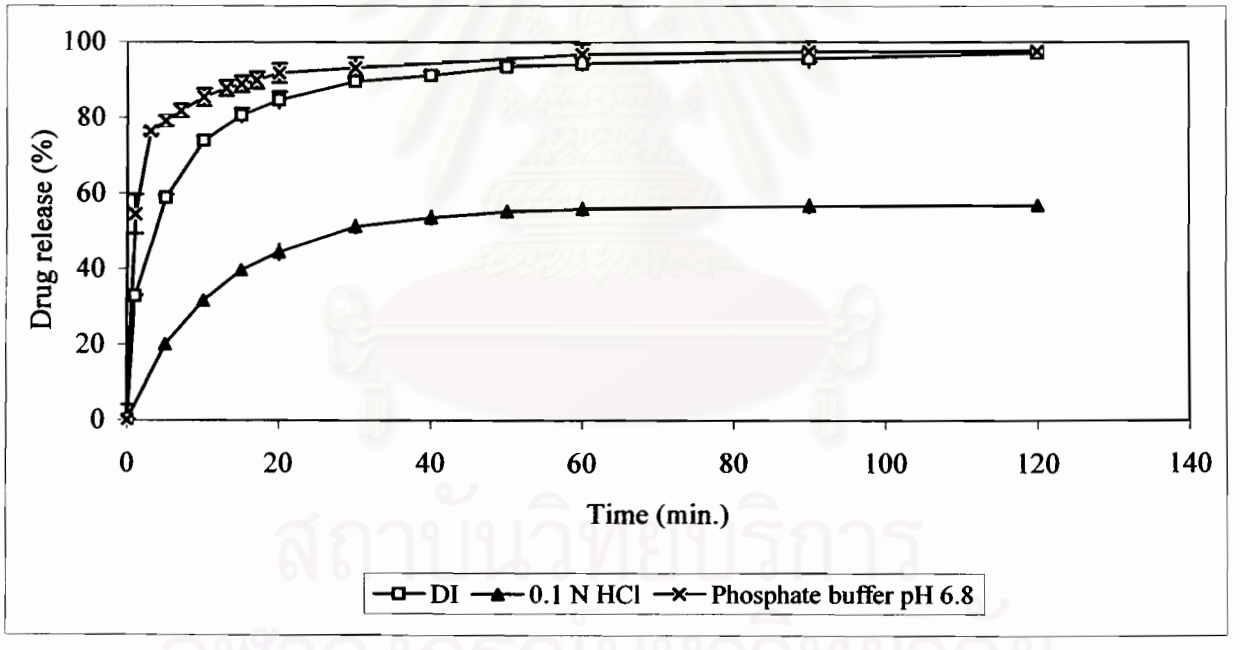

B

Figure 21 The release profiles of (A) tRM and (B) tSPRM in different media.

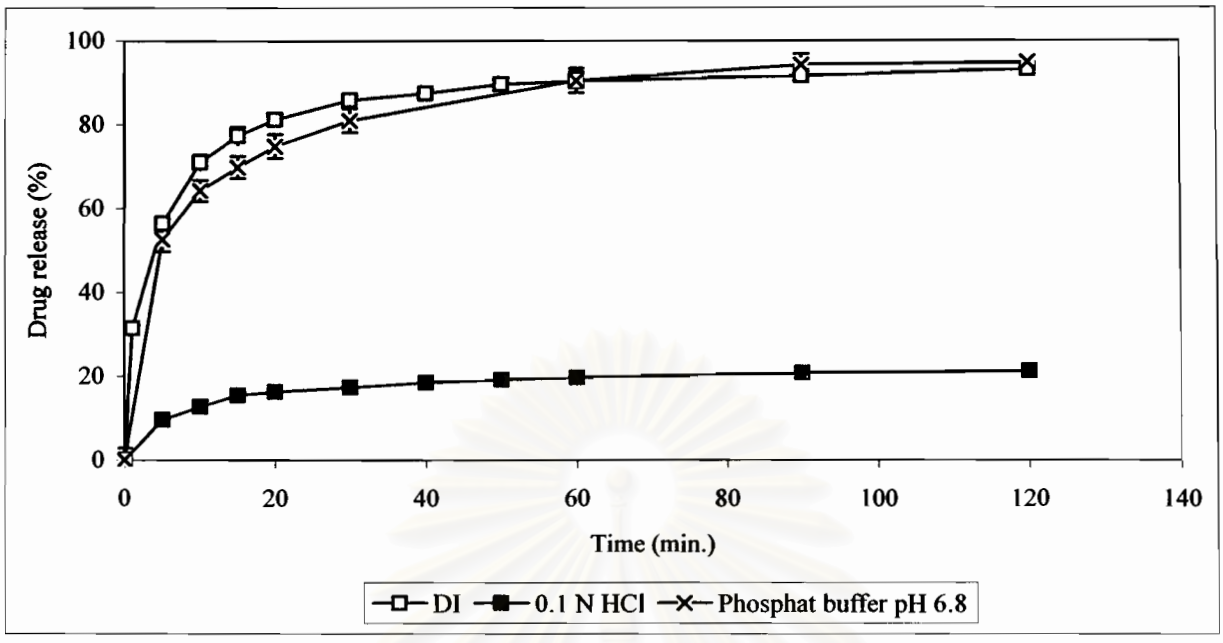

A

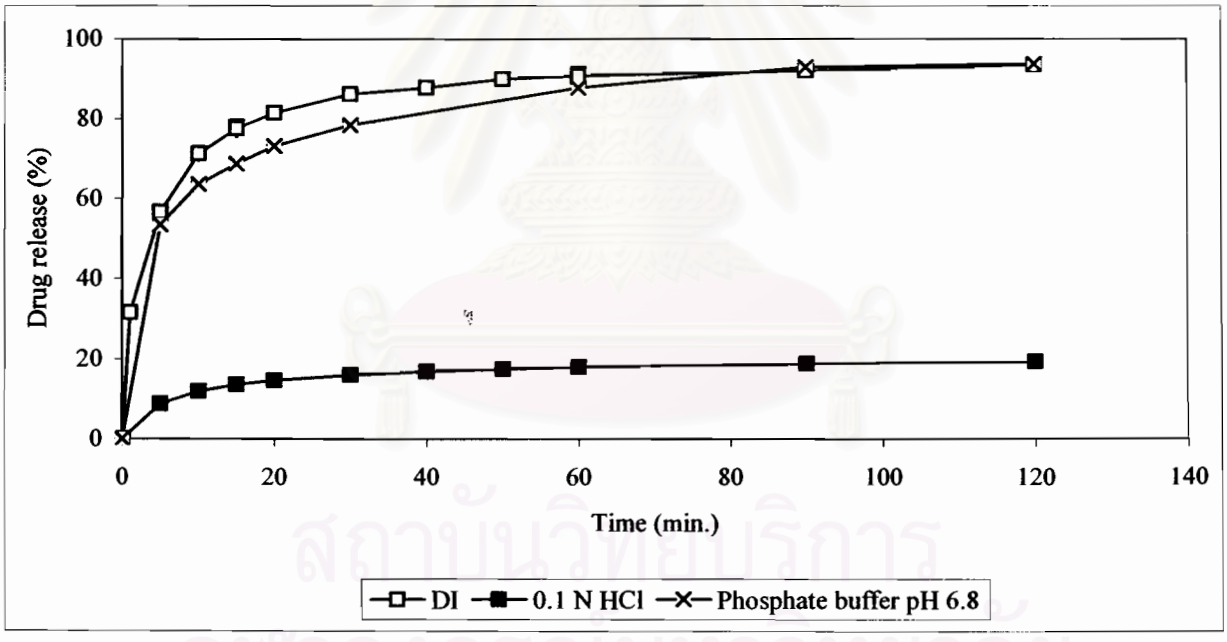

B

Figure 22 The release profiles of (A) tPM 1:1 and (B) tPM 1:2 in different media.

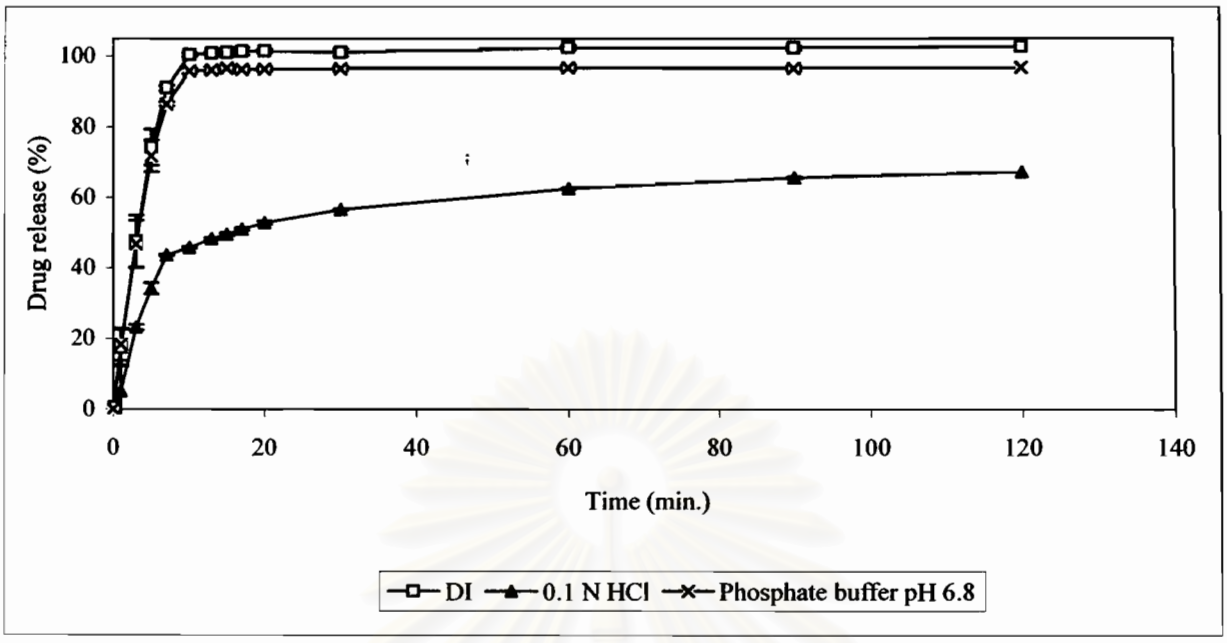

A

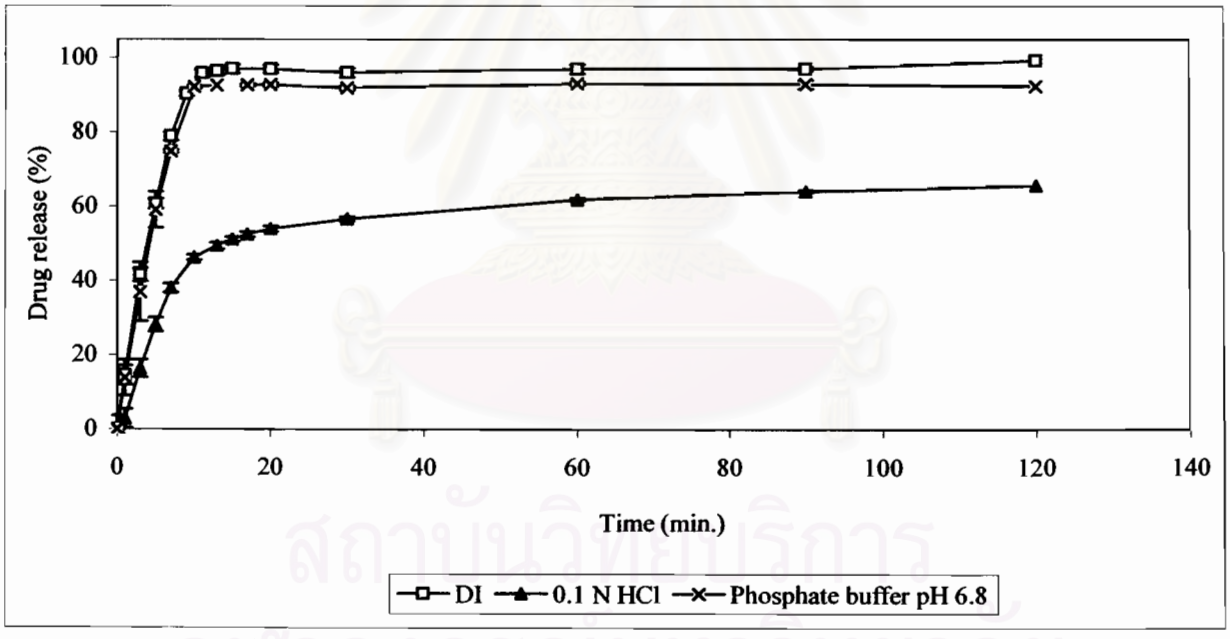

B

Figure 23 The release profiles of (A) tSP 1:1 and (B) tSP 1:2 in different media.

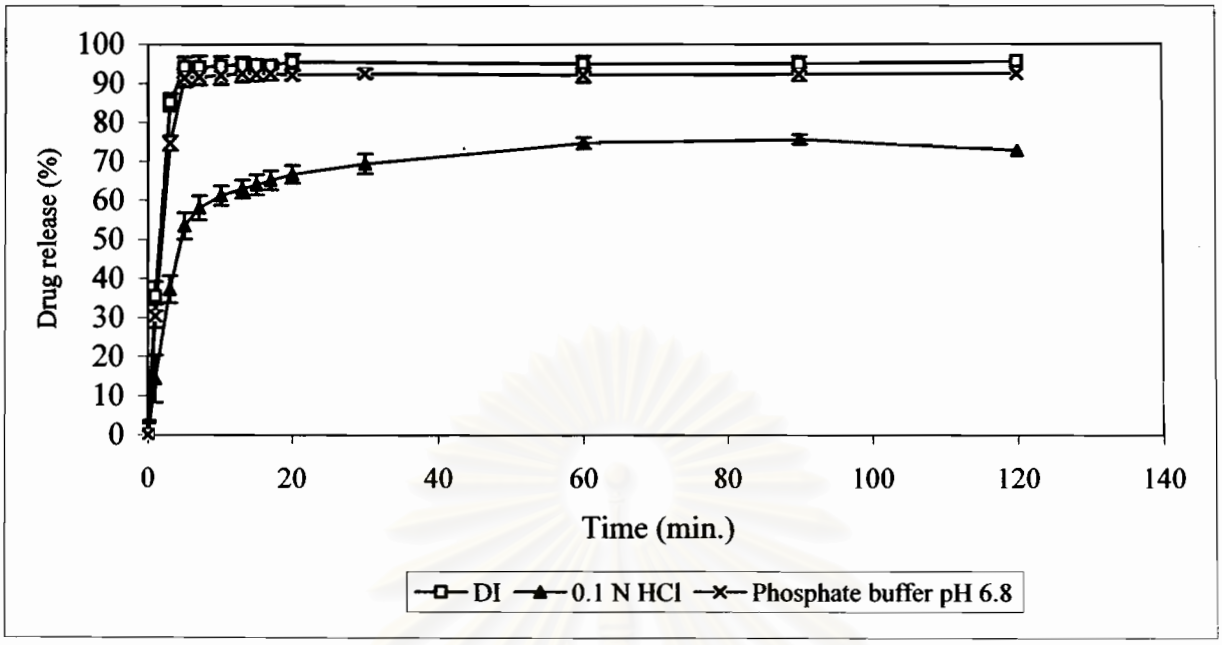

A

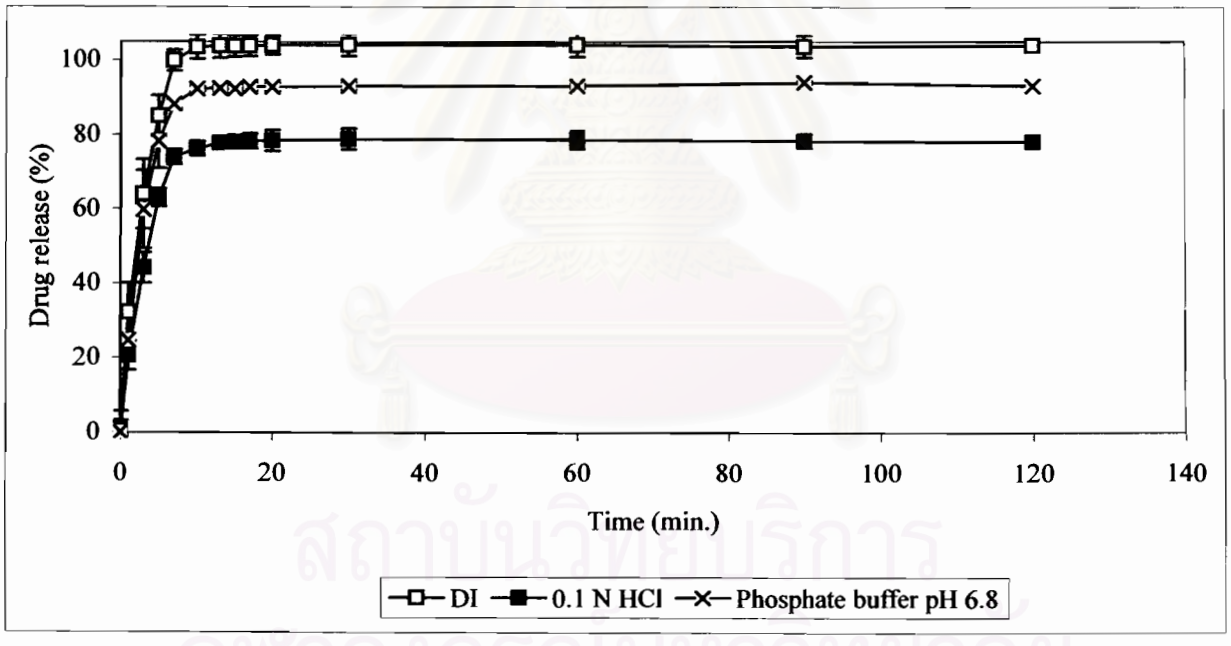

B

Figure 24 The release profiles of (A) tFD 1:1 and (B) tFD1:2 in different media.

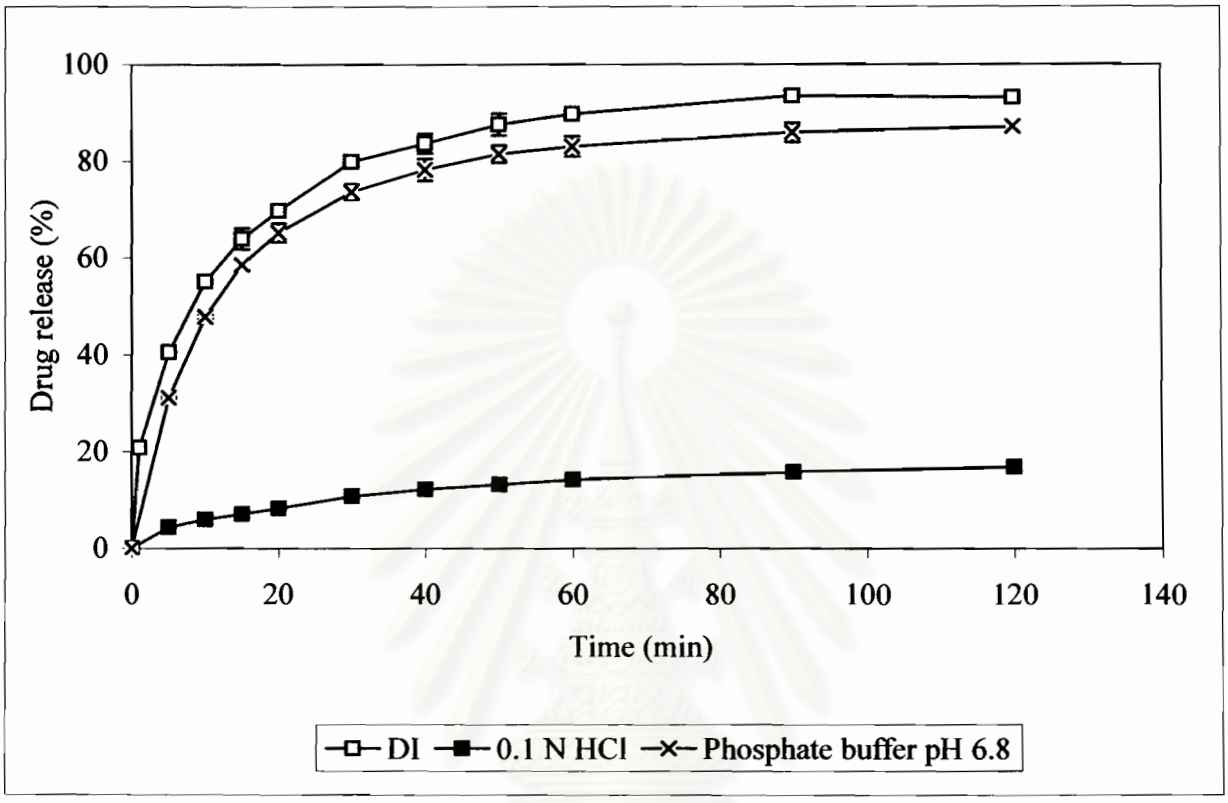

Figure 25 The release profiles of commercial meloxicam tablets.

CHAPTER V

CONCLUSIONS

The effects of co-spray and freeze drying with β-CD on the solubility of meloxicam were investigated and then summarized as followed:

1. The aqueous solubility of meloxicam increased linearly as function of β-CD concentration until it reached plateau due to the solubility limit of this complex. The further addition of β-CD resulted in formation of precipitated complexes. The phase solubility diagram of meloxicam-β-cyclodextrin system was classified as type B_S according to Higuchi and Connors (1965). The molar ratio of complex was 1:2.

2. The X-ray diffractrograms of SP and FD in the molar ratio 1:1 and 1:2 obviously showed the amorphous state; whereas, those of PM stated the crystalline state.

3. From FT-IR analysis, IR spectra of SPRM indicated the changing in form of meloxicam which might be caused by either the spray drying process or ammonium hydroxide. IR spectra of SP and FD, the changing of the peaks especially at 3290.87 cm^{-1} and 1621-1240.72 cm^{-1} after spray and freeze drying happened. It was found that the amide group might interact with β-CD.

4. The DSC thermograms of SPRM confirmed that meloxicam was changed it form after spray drying. The DSC thermograms of SP indicated the amorphous state which might be due to the spray drying process. The DSC thermograms of FD revealed the amorphous state which might be not true amorphous. Therefore, sodium hydroxide might interrupt the rearrangement of meloxicam and β-CD.

5. It was found that co-spray drying and co-freeze drying with β-CD could significantly enhance the solubility of meloxicam in deionized water, 0.1 N HCl pH 1.2, and phosphate buffer pH 6.8 at $T_{30.}$ This might be due to the changing in form of meloxicam; either the spray drying or the freeze drying or β-CD might changed the poor soluble form to be a soluble form of meloxicam.

6. In this study, β-CD was applied to meloxicam in an effort to improve drug solubility and dissolution rate. This improved characteristic might allowed more rapid drug absorption and more rapid onset of the analgesic effect

7. According to the X-ray diffractograms, FT-IR spectra, and DSC thermograms of meloxicam-β-CD systems, the changing in physicochemical properties of meloxicam existed. The stability study should be further investigated.

REFERENCES

[a]Acerbi, D., Bovis, G., Carli, F., Pasini, M., Pavesi, L., and Peveri, T. 1990. Biopharmaceutical optimisation of *β*-cyclodextrin inclusion compounds**.** Drug Investigation 2(Supplement 4): 29-36.

[b]Acerbi ,D., Lebacq, Jr.E., Rondelli, I., and Stockis, A. 1990. Rapid oral absorption profile of piroxicam from its *β*-cyclodextrin complex**.** Drug Investigation 2(Supplement 4): 50-55.

Baboota, S., and Agarwal, S.P. 2002. Inclusion complexation of meloxicam with *β* -cyclodextrin**.** Indian Journal of Pharmaceutical Sciences July-August: 408-410.

Backensfeld, T., Muller, B.W. and Kolter, K. 1991. Interaction of NSA with cyclodextrins and hydroxypropyl cyclodextrin derivatives. International Journal of Pharmaceutics 74: 85-93.

Bekers, O., Uijtendaal, E.V., Beijnen, J.H., Bult, A., and Underberg, W.J.M. 1991. Cyclodextrin and derivatives**.** Drug Development and Industrial Pharmacy 17(11):1503-1549.

Braibanti, A., Fisicaro, E., Ghiozzi, A., Compari, C., and Bovis, G. 1998. Host-guest interactions between *β*-cyclodextrin and piroxicam. Reactive & Functional Polymers 36: 251-255.

Cameron, P. 1997. Good pharmaceutical freeze-drying practice**.** USA. Interpharm press, Inc.

Duchene, D., Vaution, C., and Glomot, F. 1986. Cyclodextrins, their value in pharmaceutical technology. Drug Development and Industrial Pharmacy 12(11-13): 2193-2215

Duchene, D., and Wouessidjewe, D. 1990. Pharmaceutical uses of cyclodextrins and derivatives. Drug Development and Industrial Pharmacy 16(17): 2487-2499.

Giordano F., Novak C, and Moyano J.R. 2001.Thermal analysis of cyclodextrins and their inclusion compounds. Thermochimica Acta 380: 123-151.

Guo Xiliang, Yang Yu Zhao Guoyan, Zhang Guomei, Chao Jianbin, and Shuang Shaomin. 2003. Study on inclusion interaction of piroxicam with *β*-cyclodextrin derivatives. Spectrochimica Acta Part A 59:3386-3379

Hamada, Y., Nambu, N., and Nagai, T.1975. Inclusions of α- and β-cyclodextrins with several non-steroidal anti-inflammatory drugs in aqueous solution. Chemical Pharmaceutical Bulletin 23(6): 1205-1211.

Higuchi, T. and Connors, K.A. 1965. Phase solubility techniques. Advances in analytical chemistry and instrumentation 4: 117-212.

Killeen, J.M. 1996. Spray drying and spray congealing of pharmaceuticals. Encyclopedia of Pharmaceutical vol 14: 207-221.

Kurozumi, M., Nambu, N., and Nagai, T. 1975. Inclusion compounds of non-steroidal anti-inflammatory and other slightly water soluble drugs with α- and β-cyclodextrins in powdered form. Chemical Pharmaceutical Bulletin 23(12): 3062-3068.

Loftsson, T., Birna J. ÓlafsdÓttir, HafrÚn FriðriksdÓttir, and Sigriður JÓnsdÓttir. 1993. Cyclodextrin complexation of NSAIDs: physicochemical characteristics. European Journal of Pharmaceutical Sciences 1: 95-101.

Loftsson, T., and Marcus E. Brewster. 1996. Pharmaceutical applications of cylcodextrins. 1. Drug solubilization and stabilization. Journal of Pharmaceutical Sciences Oct, 85(10): 1017-1025.

Luger, P., Daneck, K., Engel, W., Trummlitz G., and Wagner, K. 1996. Structure and physicochemical properties of meloxicam, a new NSAID. European Journal of Pharmaceutical Science 4: 175-187.

Mamdouh M. Ghorab, Heba M. Abdel-Salam, Marwa A. ElpSayad, and Mohammed M. Melhel. 2004. Tablet formulation containing meloxicam and β-cyclodextrin: mechanical characterization and bioavailability evaluation. AAPS Pharmaceutical Science Technology 5(4) Article 59: 1-6.

Mark E. Davis and Marcus E. Brewster. 2004. Cyclodextrin-based pharmaceutics: past, present and future. Nature reviews 3: 1023-1035 .

Matin Del Valle E.M. 2004. Cyclodextrins and their uses: a review. Process Biochemistry 39: 1033-1046.

Mosher, G.,and Thompson, D. 2000. Complexation and cyclodextrins. In J. Swarbrick, and J.C. Boylan (eds.). Encyclopedia of pharmaceutical technology vol. 19 supplement 2, pp. 49-88. New York: Marcel Dekker.

Naidu, N.B., Chowdary, K.P.R., Murthy K.V.R., Satyanarayana, V., Hayman A.R., and Becket, G. 2004. Physiochemical characterization and dissolution properties of meloxicam-cyclodextrin binary systems. Journal of Pharmaceutical and Biomedical Analysis 35: 75-86.

Nath, B.S., and Shivakumar, H.N. 2000. A 2^3 factorial studies on factors influencing meloxicam β -cyclodextrin complexation for better solubility. Indian Journal Pharmaceutical Science 62:129-132.

Pikal, M.J. Freeze drying. Encyclopedia of pharmaceutical technology vol. 6, pp. 275-303. New York: Marcel Dekker.

Redenti, E., Peveri, T., Zanol, M., Ventura, P., Gnappi, G., and Montenero, A. 1996. A study on the differentiation between amorphous piroxicam: β-cyclodextrin complex and a mixture of the two amorphous components. International Journal of Pharmaceutics 129: 289-294.

Reuy-Shiunan Tsai, Pierre-Alain Carrupt, Nabil El Tayar, Yvan Giroud, Pedro Andrade, and Bernard Testa. 1993. Physicochemical and structural properties of non-steroidal anti-inflammatory oxicams. Helvetica Chimica Acta 76: 842-854.

Rey, L. and May, J.C. 1999. Freeze-drying / lyophilization of pharmaceutical and biological products. Drugs and the pharmaceutical sciences vol. 96. USA: Marcel Dekker.

Sanoferajan, A.M., Nanjundaswamy, N.G., Mahesh, S. and Moorthy, S.N. 2000. Formulation and Evaluation of β-cyclodextrin complexes of tenoxicam. Indian Journal Pharmaceutical Sciences 62:119.

Seedher N. and Bhatia S. 2003. Solubility enhancement of Cox-2 inhibitors using various solvent systems. AAPS Pharmaceutical Science Technology 4(3) Article 33: 1-9.

Shan-Yang Lin and Yuh-Horng Kao. 1989. Solid particulates of drug- β -cyclodextrin inclusion complexes directly prepared by a spray-drying technique. International Journal of Pharmaceutics 56: 249-259.

Szejtli, J. 1982. Cyclodextrins and their inclusion complexes Budapest, Akademiai Kiado.

Vrecer F., Vrbinc M., and Meden A. 2003. Characterization of piroxicam crystal modifications. International Journal of Pharmaceutics 256: 3-15.

APPENDICES

Appendix A

Calibration

Table 1A Absorbance of meloxicam in deionized water at 361 nm.

Concentration (mg/ml)	Abs (n 1)	Abs (n 2)	Abs (n 3)	Abs (av.± SD)
0.002595	0.1398	0.1392	0.1416	0.1402 ± 0.0012
0.005190	0.2721	0.2708	0.2704	0.2711 ± 0.0009
0.007785	0.4145	0.4110	0.4120	0.4125 ± 0.0018
0.010380	0.5440	0.5428	0.5476	0.5448 ± 0.0025
0.012975	0.6870	0.6900	0.6855	0.6875 ± 0.0023

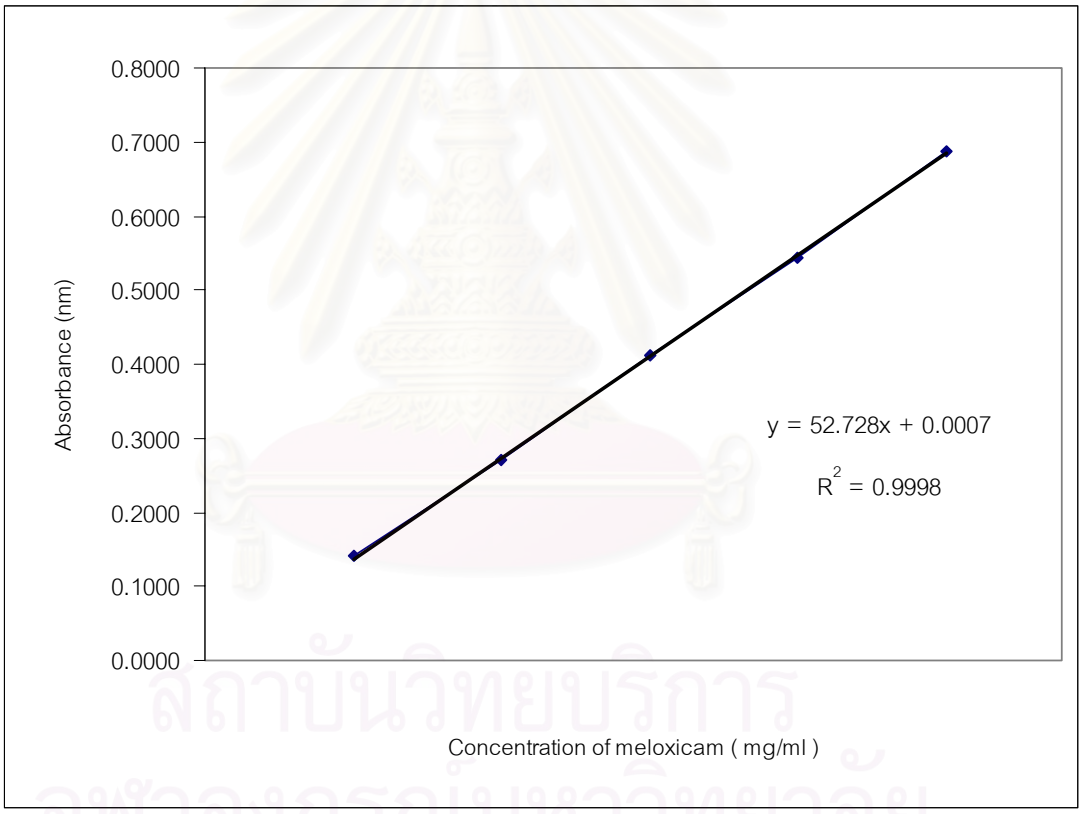

Figure 1A Calibration curve of meloxicam in deionized water at 361 nm.

Table 2A Absorbance of meloxicam in 0.1 N HCl at 361 nm.

Concentration (mg/ml)	Abs (n 1)	Abs (n 2)	Abs (n 3)	Abs (av. ± SD)
0.00277	0.1656	0.1531	0.1543	0.1577 ± 0.0069
0.00554	0.3108	0.3132	0.3195	0.3145 ± 0.0045
0.00831	0.4732	0.4708	0.4792	0.4744 ± 0.0043
0.01108	0.6301	0.6302	0.6347	0.6316 ± 0.0026
0.01385	0.7906	0.7922	0.8010	0.7946 ± 0.0056
0.01662	0.9631	0.9591	0.9605	0.9609 ± 0.0020
0.01939	1.1347	1.1252	1.1259	1.1286 ± 0.0053

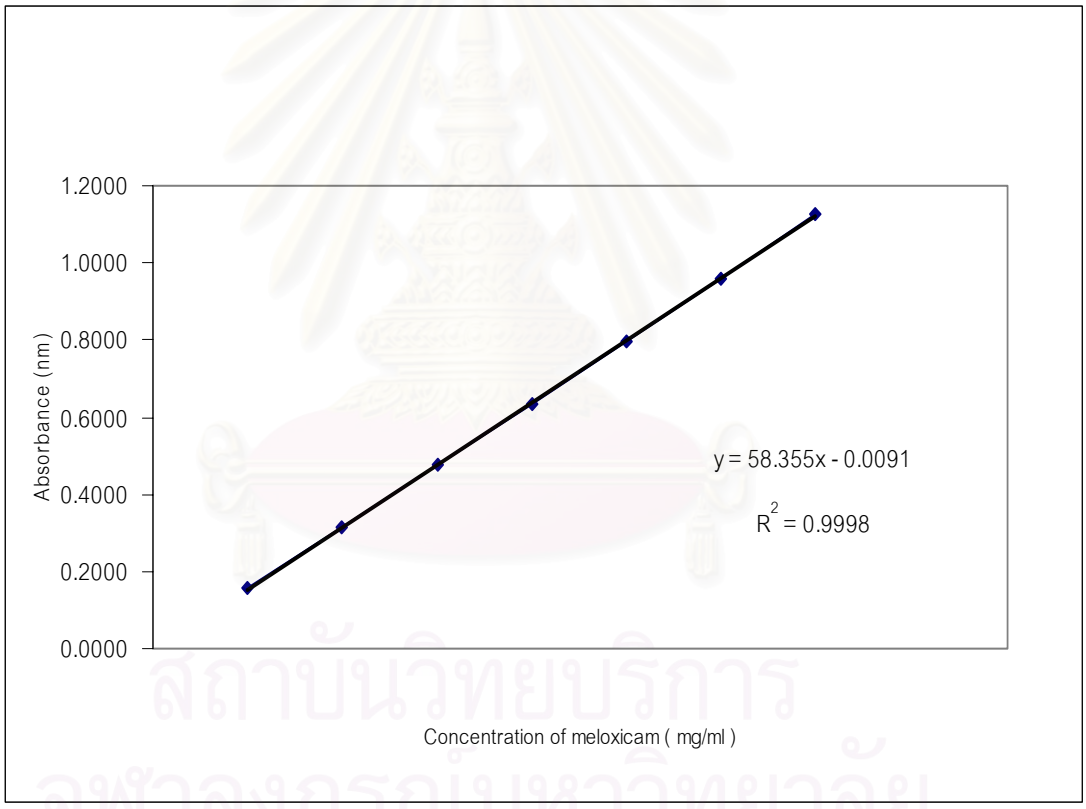

Figure 2A Calibration curve of meloxicam in 0.1 N HCl at 361 nm.

Table 3A Absorbance of meloxicam in phosphate buffer pH 6.8 at 361 nm.

Concentration (mg/ml)	Abs (n 1)	Abs (n 2)	Abs (n 3)	Abs (av. ± SD)
0.00277	0.1468	0.1452	0.1604	0.1508 ± 0.0084
0.00554	0.3055	0.3049	0.3091	0.3065 ± 0.0023
0.00831	0.4632	0.4674	0.4631	0.4644 ± 0.0025
0.01108	0.6060	0.6048	0.6096	0.6068 ± 0.0025
0.01385	0.7673	0.7638	0.7623	0.7645 ± 0.0026
0.01662	0.9094	0.9165	0.9178	0.9146 ± 0.0045
0.01939	1.0611	1.0648	1.0610	1.0623 ± 0.0022

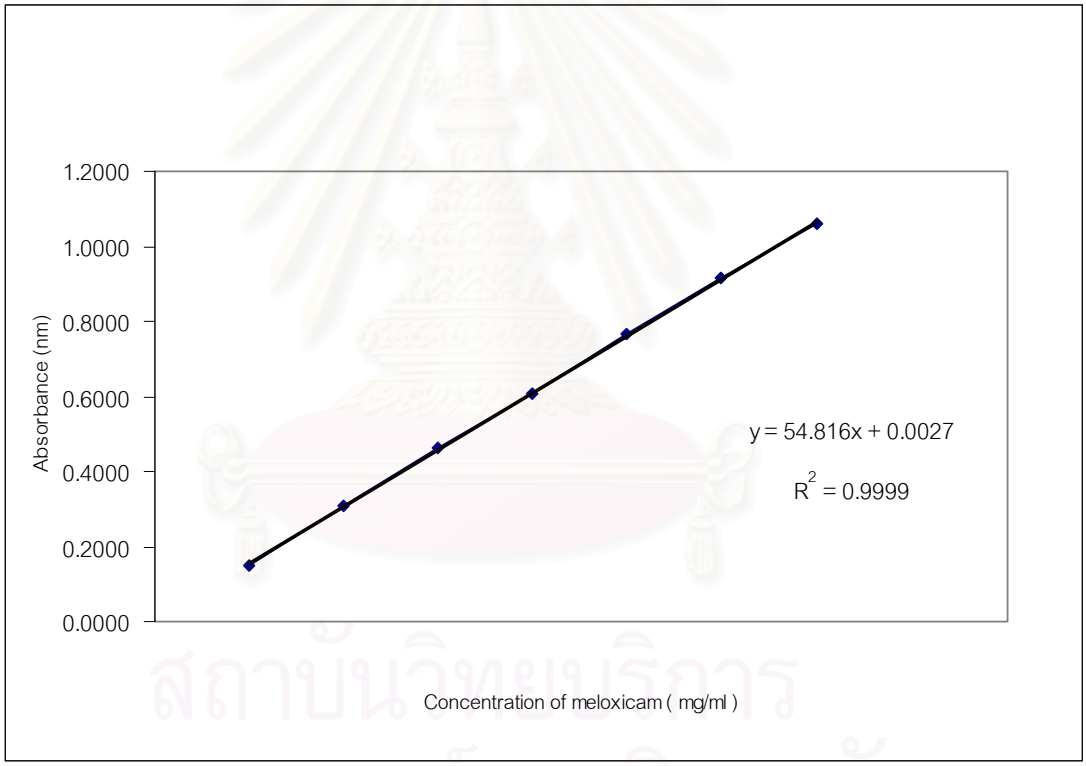

Figure 3A Calibration curve of meloxicam in phosphate buffer pH 6.8 at 361 nm.

Table 4A Absorbance of meloxicam in dimethylformamide at 361 nm.

Concentration (mg/ml)	Abs (n 1)	Abs (n 2)	Abs (n 3)	Abs (av. ± SD)
0.00320	0.1088	0.1083	0.1082	0.1085 ± 0.0003
0.00400	0.1383	0.1397	0.1387	0.1389 ± 0.0007
0.00640	0.2203	0.2228	0.2208	0.2213 ± 0.0013
0.00800	0.2732	0.2630	0.2744	0.2735 ± 0.0008
0.01200	0.4097	0.4084	0.4083	0.4088 ± 0.0008
0.02000	0.6852	0.6841	0.6842	0.6845 ± 0.0006
0.02400	0.8232	0.8249	0.8233	0.8238 ± 0.0010
0.02800	0.9621	0.9603	0.9606	0.9610 ± 0.0010

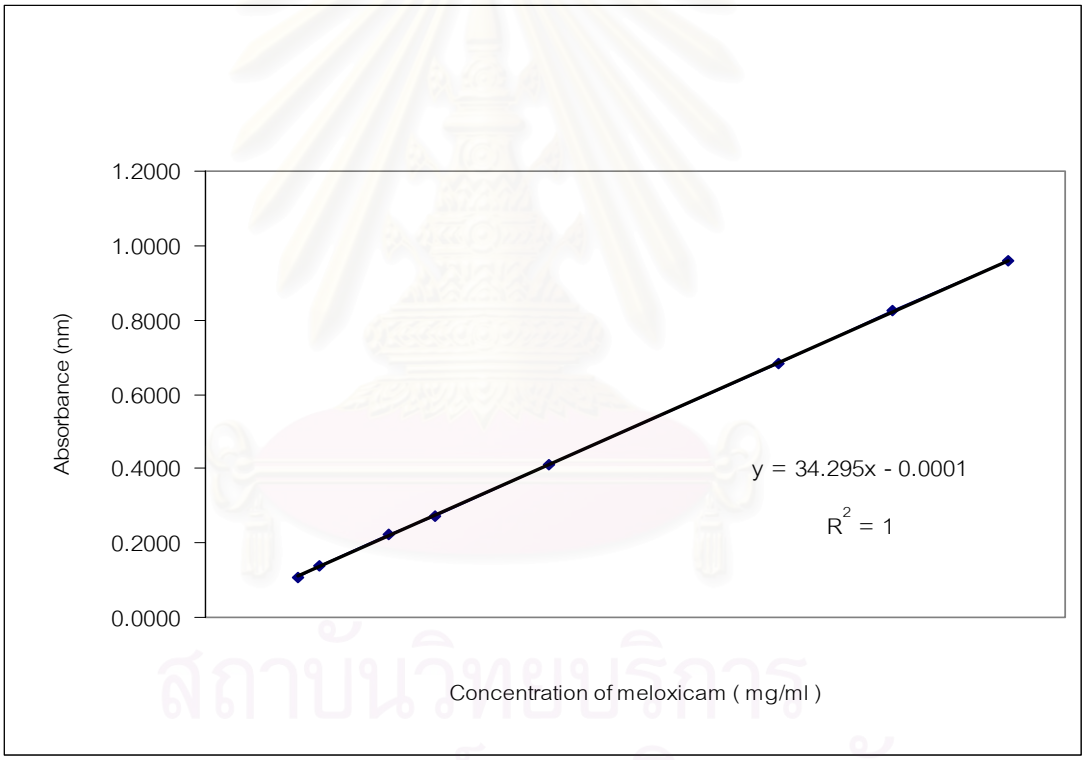

Figure 4A Calibration curve of meloxicam in dimethylformamide at 361 nm.

Appendix B

Solubility studies

Phase solubility studies were carried out according to Higuchi and Conners (1965). An excess amount of meloxicam was added into various concentrations of aqueous β-CD solution (0-14 mM). The mixture was equilibrated in the top-to-bottom rotating machine at 37 ± 1 ºC for 7 days.

Table 1B Solubility of meloxicam in various CD concentrations.

Conc. of CD	Day	Abs(361 nm)			Conc. (mM)			av.	SD
		1	2	3	1	2	3		
0	1	0.1169	0.2343	0.0766	0.0627	0.1261	0.0410	0.0766	0.04
0	2	0.1678	0.3129	0.0971	0.0902	0.1685	0.0520	0.1036	0.06
0	4	0.3004	0.4457	0.2034	0.1617	0.2402	0.1094	0.1704	0.07
0	7	0.3113	0.4670	0.3352	0.1676	0.2517	0.1805	0.1999	0.05
2	1	0.4688	0.1140	0.0766	0.2526	0.0611	0.0410	0.1182	0.12
2	2	0.6099	0.1616	0.1097	0.3288	0.0868	0.0588	0.1581	0.15
2	4	0.7359	0.2286	0.1809	0.3968	0.1230	0.0973	0.2057	0.17
2	7	0.4975	0.3368	0.2671	0.2681	0.1814	0.1438	0.1978	0.06
4	1	0.2496	0.1239	0.0533	0.1343	0.0665	0.0284	0.0764	0.05
4	2	0.3555	0.1913	0.0852	0.1915	0.1029	0.0456	0.1133	0.07
4	4	0.5176	0.2742	0.1994	0.2790	0.1476	0.1072	0.1779	0.09
4	7	0.6209	0.4609	0.3639	0.3347	0.2484	0.1960	0.2597	0.07
6	1	0.4295	0.0648	0.0691	0.2314	0.0346	0.0369	0.1010	0.11
6	2	0.5968	0.1160	0.0973	0.3217	0.0622	0.0521	0.1454	0.15
6	4	0.7942	0.2411	0.1635	0.4282	0.1297	0.0879	0.2153	0.19
6	7	0.7159	0.4810	0.2931	0.3860	0.2592	0.1578	0.2677	0.11
8	1	0.4283	0.2677	0.1667	0.2308	0.1441	0.0896	0.1548	0.07
8	2	0.5160	0.3205	0.2153	0.2781	0.1726	0.1158	0.1888	0.08
8	4	0.7465	0.3866	0.3037	0.4025	0.2083	0.1635	0.2581	0.13
8	7	0.8811	0.5341	0.4444	0.4751	0.2879	0.2395	0.3342	0.12
10	1	0.0595	0.1184	0.1895	0.0317	0.0635	0.1019	0.0657	0.04
10	2	0.0802	0.1776	0.2507	0.0429	0.0955	0.1349	0.0911	0.05
10	4	0.1351	0.2664	0.3512	0.0725	0.1434	0.1892	0.1350	0.06
10	7	0.4424	0.4596	0.2340	0.2384	0.2477	0.1259	0.2040	0.07
12	1	0.4704	0.0633	0.4983	0.2535	0.0338	0.2685	0.1853	0.13
12	2	0.5875	0.0906	0.6308	0.3167	0.0485	0.3401	0.2351	0.16
12	4	0.8146	0.1598	0.8060	0.4393	0.0859	0.4346	0.3199	0.20
12	7	0.5123	0.3367	0.9689	0.2761	0.1813	0.5225	0.3267	0.18
14	1	0.1949	0.1112	0.1179	0.1048	0.0596	0.0633	0.0759	0.03
14	2	0.2204	0.1592	0.1500	0.1186	0.0855	0.0806	0.0949	0.02
14	4	0.2336	0.2410	0.1966	0.1257	0.1297	0.1057	0.1204	0.01
14	7	0.5481	0.3909	0.3205	0.2954	0.2106	0.1726	0.2262	0.06

Appendix C

Particle size determination

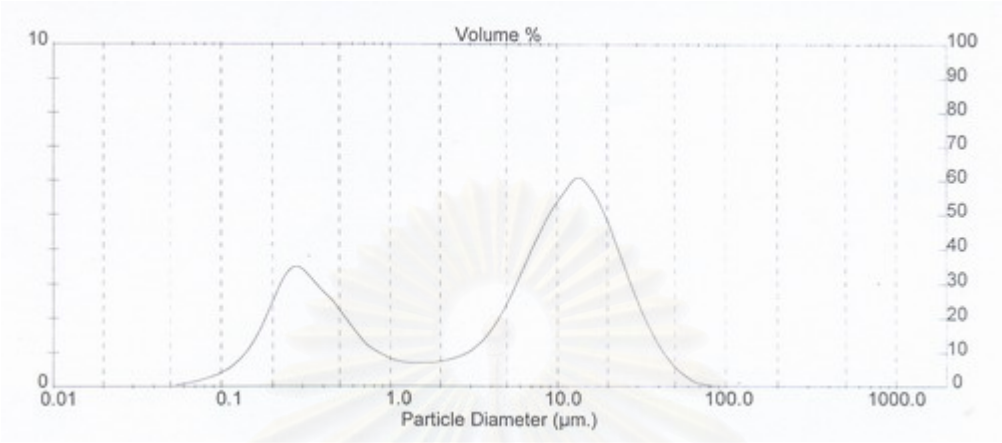

Figure 1C Particle size distribution of RM.

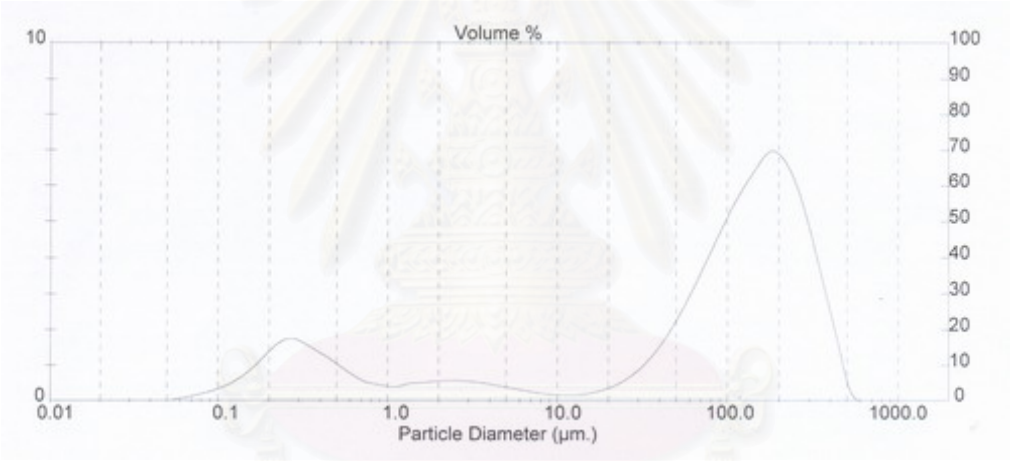

Figure 2C Particle size distribution of SPRM.

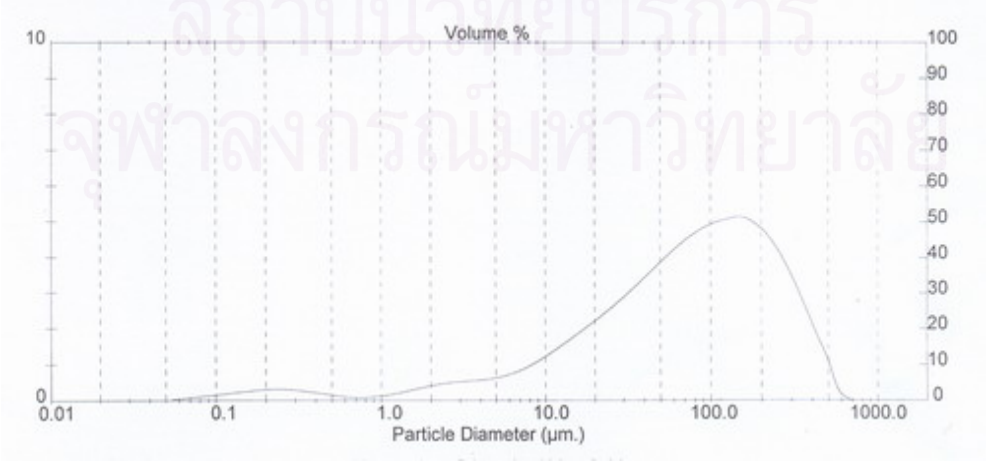

Figure 3C Particle size distribution of CD.

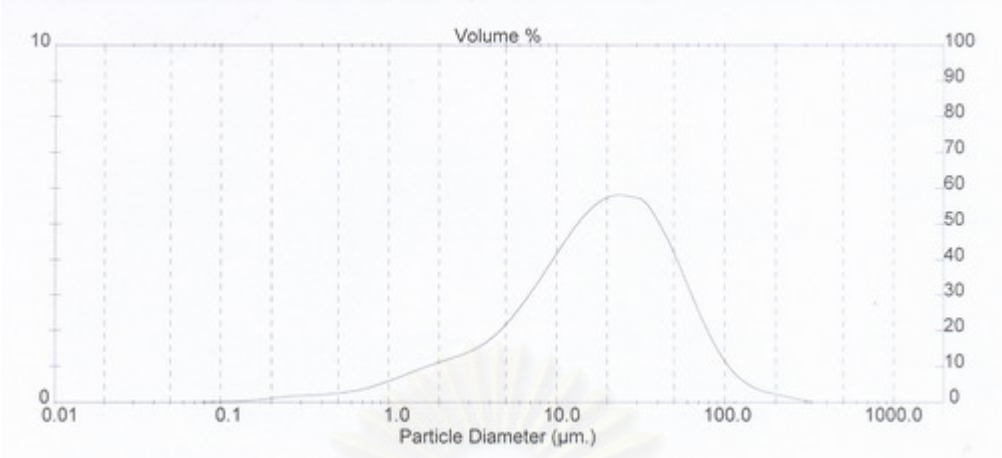

Figure 4C Particle size distribution of SPCD.

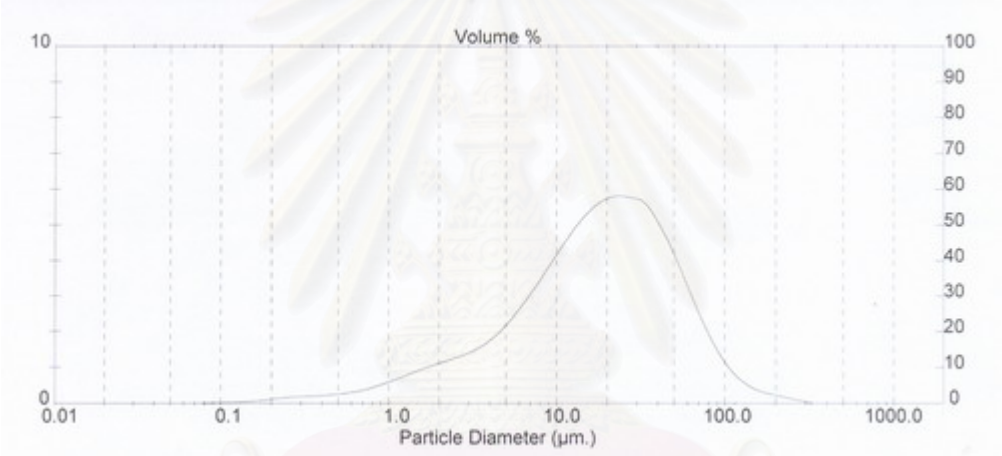

Figure 5C Particle size distribution of FDCD.

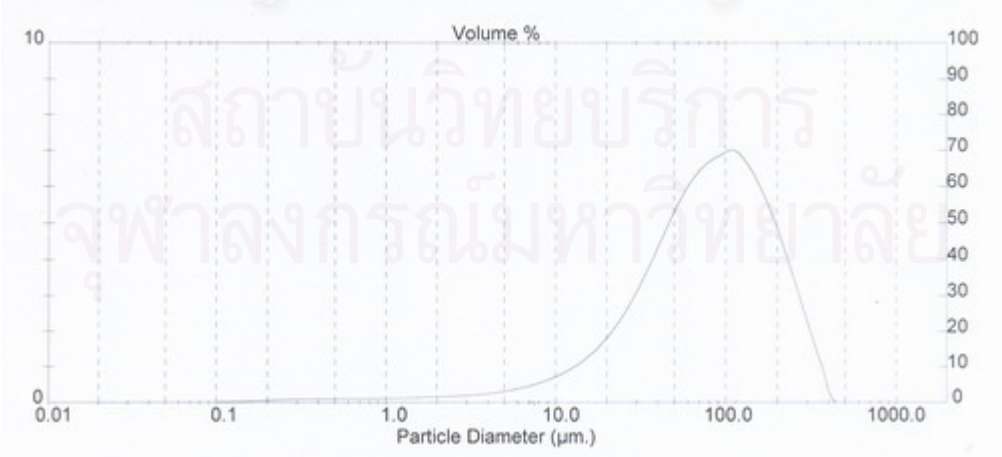

Figure 6C Particle size distribution of FDCD/NaOH.

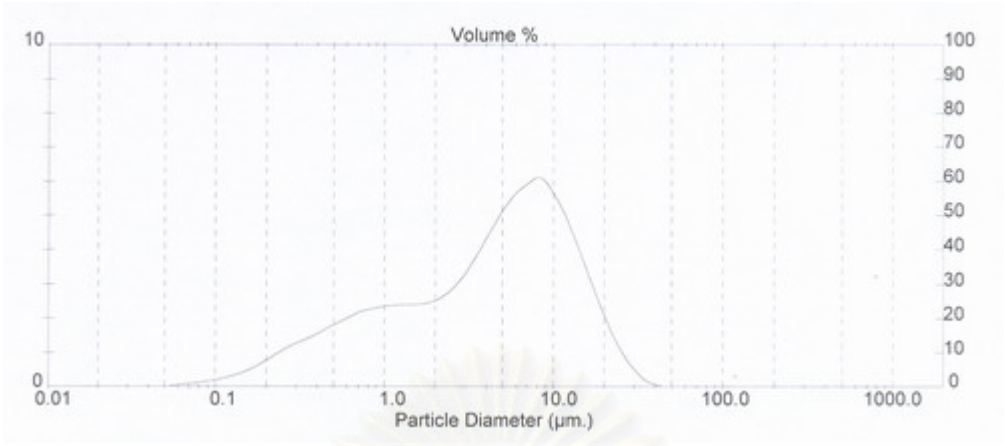

Figure 7C Particle size distribution of SP 1:1.

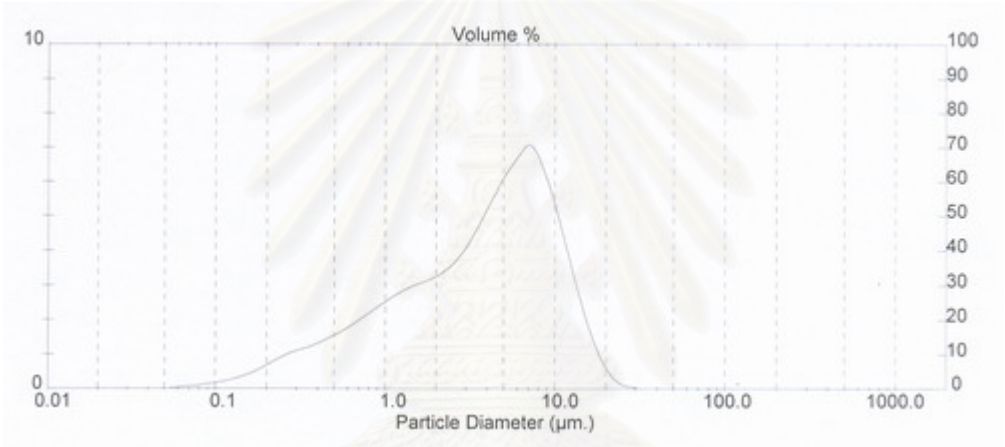

Figure 8C Particle size distribution of SP 1:2.

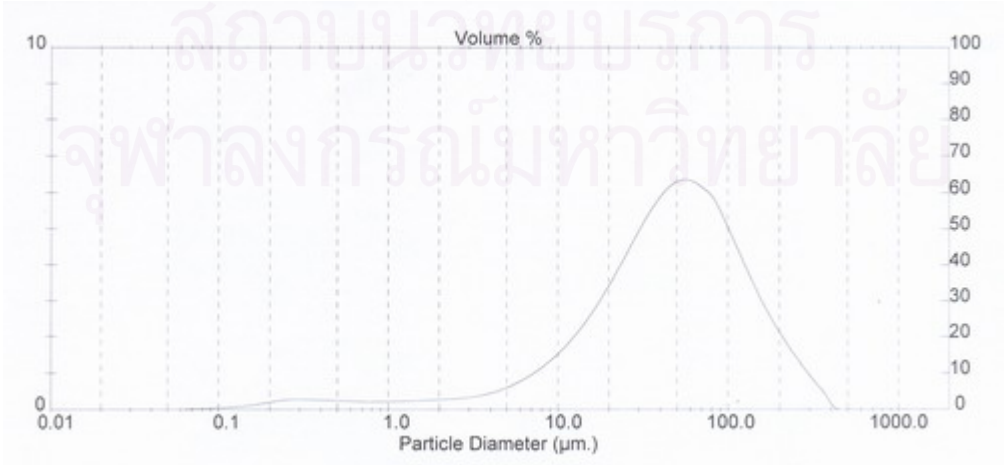

Figure 9C Particle size distribution of FD 1:1.

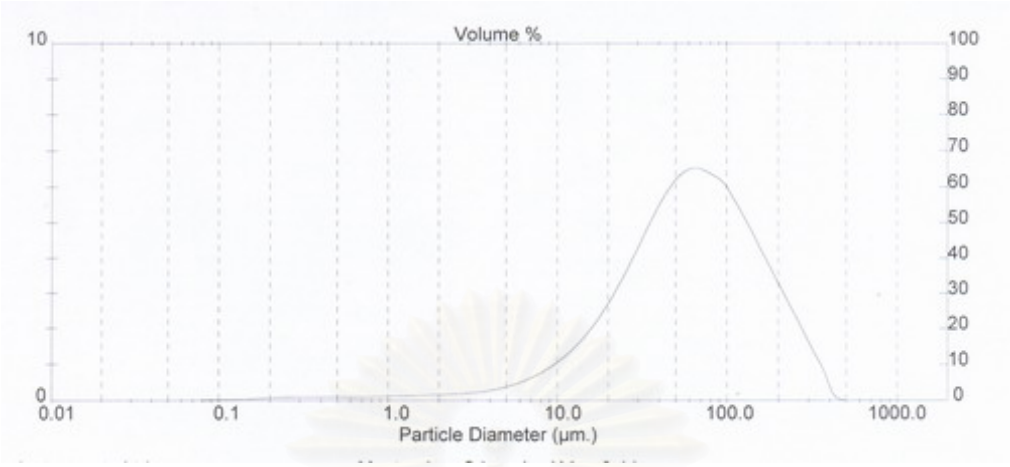

Figure 10C Particle size distribution of FD 1:2.

Appendix D

The percentage of drug release

Table 1D The percentage of drug release from tRM in deionized water.

Time	% Drug release of tRM in deionized water					
	1	2	3	Av.	stdev	%RSD
5	25.57	25.66	26.52	25.92	0.5274	2.0348
10	37.27	37.32	38.12	37.57	0.4764	1.2680
15	45.49	45.37	46.39	45.75	0.5601	1.2244
20	51.08	51.27	52.48	51.61	0.7558	1.4643
30	58.58	58.63	59.84	59.02	0.7168	1.2145
40	62.80	63.00	63.77	63.19	0.5122	0.8106
50	65.10	65.63	66.17	65.64	0.5370	0.8182
60	67.15	67.62	68.26	67.68	0.5570	0.8229
90	71.57	71.90	72.33	71.93	0.3820	0.5311
120	73.23	73.29	73.56	73.36	0.1790	0.2439

Table 2D The percentage of drug release from tRM in 0.1 N HCl.

Time	% Drug release of tRM in HCL					
	1	2	3	Av.	stdev	%RSD
5	6.45	6.40	6.88	6.58	0.2632	4.0018
10	9.74	9.93	9.59	9.76	0.1710	1.7522
15	11.84	11.80	14.85	12.83	1.7498	13.6413
20	13.35	13.63	17.43	14.81	2.2793	15.3938
30	15.21	15.30	16.20	15.57	0.5472	3.5155
40	16.58	16.76	16.93	16.76	0.1756	1.0478
50	17.75	17.85	18.04	17.88	0.1475	0.8250
60	18.48	18.75	18.67	18.63	0.1369	0.7345
90	19.85	19.88	18.47	19.40	0.8025	4.1369
120	21.22	20.97	21.52	21.24	0.2733	1.2868

Table 3D The percentage of drug release from tRM in phosphate buffer pH 6.8 solution.

Time	% Drug release of PM 1:2 in PB					
	1	2	3	Av	stdev	%RSD
5	52.49	53.24	54.82	53.52	1.1893	2.2223
10	62.62	63.87	64.49	63.66	0.9498	1.4920
15	68.13	68.95	69.25	68.78	0.5779	0.8402
20	71.88	74.03	73.66	73.19	1.1498	1.5710
30	78.20	78.44	78.86	78.50	0.3338	0.4252
60	87.33	87.36	88.79	87.83	0.8323	0.9477
90	92.64	92.25	93.99	92.96	0.9154	0.9847
120	94.51	92.99	93.81	93.77	0.7623	0.8129

Table 4D The percentage of drug release from tSPRM in deionized water.

Time	% Drug release of tSPRM in DI					
	1	2	3	Av	stdev	%RSD
1	32.83	32.45	32.93	32.74	0.2518	0.7691
5	58.96	58.48	58.96	58.80	0.2785	0.4736
10	74.92	73.81	73.29	74.01	0.8345	1.1276
15	81.73	80.55	79.52	80.60	1.1029	1.3684
20	86.26	85.09	82.60	84.65	1.8704	2.2096
30	92.01	88.82	87.76	89.53	2.2139	2.4727
40	92.79	90.60	90.08	91.16	1.4416	1.5814
50	94.55	93.39	92.38	93.44	1.0848	1.1609
60	95.36	93.46	93.80	94.21	1.0143	1.0766
90	97.38	94.35	95.00	95.58	1.5947	1.6685
120	99.81	95.67	95.80	97.09	2.3552	2.4257

Table 5D The percentage of drug release from tSPRM in 0.1 N HCl.

Time	% Drug release of tSPRM in HCl					
	1	2	3	Av	stdev	%RSD
5	20.56	19.78	19.87	20.07	0.4221	2.1030
10	31.28	31.82	31.79	31.63	0.3037	0.9602
15	39.60	39.78	39.66	39.68	0.0906	0.2283
20	44.35	44.64	44.53	44.50	0.1486	0.3340
30	50.05	50.03	53.69	51.26	2.1046	4.1060
40	52.43	52.82	55.61	53.62	1.7324	3.2309
50	54.15	54.22	57.29	55.22	1.7931	3.2472
60	54.90	55.07	57.63	55.87	1.5260	2.7315
90	55.59	55.85	58.68	56.71	1.7153	3.0248
120	55.83	55.84	58.93	56.87	1.7876	3.1435

Table 6D The percentage of drug release from tSPRM in phosphate buffer pH 6.8 solution.

Time	% Drug release of PM 1:2 in PB					
	1	2	3	Av	stdev	%RSD
5	52.49	53.24	54.82	53.52	1.1893	2.2223
10	62.62	63.87	64.49	63.66	0.9498	1.4920
15	68.13	68.95	69.25	68.78	0.5779	0.8402
20	71.88	74.03	73.66	73.19	1.1498	1.5710
30	78.20	78.44	78.86	78.50	0.3338	0.4252
60	87.33	87.36	88.79	87.83	0.8323	0.9477
90	92.64	92.25	93.99	92.96	0.9154	0.9847
120	94.51	92.99	93.81	93.77	0.7623	0.8129

Table 7D The percentage of drug release from tPM 1:1 in deionized water.

Time	% Drug release of tPM 1:1 in DI					
	1	2	3	Av	stdev	%RSD
1	31.49	31.12	31.58	31.40	0.2415	0.7691
5	56.55	56.08	56.55	56.39	0.2671	0.4736
10	71.85	70.78	70.29	70.97	0.8003	1.1276
15	78.38	77.25	76.26	77.30	1.0577	1.3684
20	82.73	81.61	79.21	81.18	1.7938	2.2096
30	88.24	85.19	84.16	85.86	2.1232	2.4727
40	88.99	86.89	86.39	87.42	1.3825	1.5814
50	90.68	89.57	88.60	89.62	1.0404	1.1609
60	91.46	89.63	89.96	90.35	0.9727	1.0766
90	93.39	90.49	91.11	91.66	1.5294	1.6685
120	95.72	91.75	91.87	93.12	2.2587	2.4257

Table 8D The percentage of drug release from tPM 1:1 in 0.1 N HCl.

Time	% Drug release of tPM 1:1 in HCL					
	1	2	3	Av.	stdev	%RSD
5	9.21	9.78	9.72	9.57	0.3099	3.2377
10	12.54	12.96	12.68	12.73	0.2144	1.6845
15	17.06	14.72	14.54	15.44	1.4063	9.1096
20	17.27	15.84	15.81	16.30	0.8344	5.1180
30	17.39	17.29	17.33	17.34	0.0486	0.2801
40	18.53	18.48	18.41	18.47	0.0624	0.3378
50	19.23	19.07	19.26	19.19	0.1026	0.5349
60	19.69	19.68	19.70	19.69	0.0090	0.0456
90	20.86	20.63	20.76	20.75	0.1148	0.5534
120	21.34	21.32	21.30	21.32	0.0191	0.0897

Table 9D The percentage of drug release from tPM 1:1 in phosphate buffer pH 6.8 solution.

Time	% Drug release of tPM 1:1 in PB					
	1	2	3	Av	stdev	%RSD
5	50.35	51.74	55.76	52.62	2.8132	5.3468
10	61.87	63.30	67.45	64.21	2.8951	4.5088
15	67.54	69.31	72.60	69.82	2.5684	3.6787
20	72.61	74.13	77.73	74.82	2.6301	3.5151
30	78.66	80.14	84.17	80.99	2.8476	3.5159
60	88.06	89.82	93.67	90.52	2.8708	3.1715
90	91.90	93.28	97.52	94.23	2.9273	3.1065
120	92.56	94.08	97.76	94.80	2.6714	2.8180

Table 10D The percentage of drug release from tPM 1:2 in deionized water.

Time	% Drug release of tPM 1:2 in DI					
	1	2	3	Av	stdev	%RSD
1	31.62	31.26	31.72	31.53	0.2425	0.7691
5	56.79	56.32	56.79	56.63	0.2682	0.4736
10	72.16	71.08	70.59	71.28	0.8037	1.1276
15	78.71	77.58	76.59	77.63	1.0622	1.3684
20	83.08	81.95	79.55	81.53	1.8014	2.2096
30	88.62	85.55	84.52	86.23	2.1322	2.4727
40	89.37	87.26	86.75	87.79	1.3884	1.5814
50	91.07	89.95	88.98	90.00	1.0448	1.1609
60	91.85	90.02	90.34	90.74	0.9769	1.0766
90	93.79	90.87	91.50	92.05	1.5359	1.6685
120	96.13	92.14	92.26	93.51	2.2683	2.4257

Table 11D The percentage of drug release from tPM 1:2 in 0.1 N HCl.

Time	% Drug release of tPM 1:2 in HCl					
	1	2	3	Av.	stdev	%RSD
5	9.58	8.25	8.38	8.74	0.7355	8.4191
10	12.34	11.73	11.84	11.97	0.3224	2.6936
15	13.98	13.46	13.44	13.62	0.3085	2.2646
20	14.92	14.61	14.55	14.69	0.2005	1.3648
30	16.18	16.08	15.84	16.03	0.1724	1.0752
40	16.94	16.76	16.93	16.88	0.1035	0.6132
50	17.54	17.59	17.57	17.57	0.0277	0.1578
60	18.03	17.91	18.04	17.99	0.0728	0.4045
90	18.98	18.80	18.86	18.88	0.0940	0.4977
120	19.35	19.19	19.52	19.35	0.1655	0.8553

Table 12D The percentage of drug release from tPM 1:2 in phosphate buffer pH 6.8 solution.

Time	% Drug release of tPM 1:2 in PB					
	1	2	3	Av	stdev	%RSD
5	52.49	53.24	54.82	53.52	1.1893	2.2223
10	62.62	63.87	64.49	63.66	0.9498	1.4920
15	68.13	68.95	69.25	68.78	0.5779	0.8402
20	71.88	74.03	73.66	73.19	1.1498	1.5710
30	78.20	78.44	78.86	78.50	0.3338	0.4252
60	87.33	87.36	88.79	87.83	0.8323	0.9477
90	92.64	92.25	93.99	92.96	0.9154	0.9847
120	94.51	92.99	93.81	93.77	0.7623	0.8129

Table 13D The percentage of drug release from tSP 1:1 in deionized water.

Time	% Drug release of tSP 1:1 in DI					
	1	2	3	Av.	stdev.	%RSD
1	17.14	18.49	16.29	17.31	1.1086	6.4062
3	42.67	53.07	46.87	47.54	5.2285	10.9988
5	68.42	82.50	71.72	74.21	7.3629	9.9216
7	87.04	96.78	89.36	91.06	5.0887	5.5881
10	99.77	101.29	100.39	100.48	0.7671	0.7634
13	100.42	101.49	100.95	100.96	0.5324	0.5274
15	100.70	101.63	101.00	101.11	0.4751	0.4699
17	100.32	101.69	102.49	101.50	1.0957	1.0795
20	100.97	102.84	101.01	101.61	1.0677	1.0508
30	100.53	101.78	101.12	101.14	0.6237	0.6166
60	102.84	103.27	101.23	102.45	1.0754	1.0497
90	102.52	102.94	101.55	102.34	0.7156	0.6993
120	102.81	103.43	102.02	102.76	0.7061	0.6871

Table 14D The percentage of drug release from tSP 1:1 in 0.1 N HCl.

Time	% Drug release of tSP 1:1 in HCl					
	1	2	3	Av.	stdev	%RSD
1	5.55	4.93	4.61	5.03	0.4778	9.4914
3	17.77	20.18	31.64	23.20	7.4139	31.9601
5	33.30	34.86	34.32	34.16	0.7913	2.3161
7	42.43	43.09	45.45	43.65	1.5861	3.6333
10	45.61	45.78	46.05	45.81	0.2226	0.4860
13	48.32	48.60	48.11	48.34	0.2496	0.5164
15	49.83	49.83	49.20	49.62	0.3641	0.7338
17	51.17	51.49	50.59	51.08	0.4547	0.8901
20	52.56	52.74	53.33	52.88	0.3999	0.7563
30	56.29	57.24	56.42	56.65	0.5145	0.9082
60	62.43	62.77	62.28	62.49	0.2500	0.4000
90	65.79	65.77	65.32	65.63	0.2667	0.4064
120	67.11	67.53	67.08	67.24	0.2559	0.3806

Table 15D The percentage of drug release from tSP 1:1 in phosphate buffer pH 6.8 solution.

Time	% Drug release of tSP 1:1 in PB					
	1	2	3	Av.	stdev	%RSD
1	19.72	16.01	19.10	18.28	1.9867	10.8706
3	50.45	41.66	48.22	46.78	4.5719	9.7742
5	79.23	66.27	69.65	71.72	6.7247	9.3768
7	90.27	81.48	87.79	86.51	4.5297	5.2358
10	95.28	96.38	95.91	95.86	0.5533	0.5772
13	95.58	96.95	95.88	96.14	0.7197	0.7487
15	95.49	97.28	97.22	96.67	1.0210	1.0562
17	95.54	97.07	96.50	96.37	0.7716	0.8007
20	95.58	97.36	96.42	96.45	0.8873	0.9199
30	95.73	97.28	96.60	96.54	0.7754	0.8032
60	96.05	97.41	96.84	96.77	0.6841	0.7069
90	95.84	97.44	96.41	96.56	0.8146	0.8436
120	96.16	97.56	96.56	96.76	0.7215	0.7457

Table 16D The percentage of drug release from tSP 1:2 in deionized water.

Time	% Drug release of tSP 1:2 in DI					
	1	2	3	Av.	stdev	%RSD
1	14.74	15.81	12.96	14.50	1.4383	9.9166
3	42.40	43.49	38.61	41.50	2.5597	6.1681
5	61.57	61.87	58.57	60.67	1.8224	3.0038
7	79.48	79.82	77.36	78.89	1.3292	1.6850
9	91.11	90.85	88.93	90.30	1.1905	1.3184
11	95.19	96.46	95.71	95.78	0.6342	0.6621
13	95.14	96.93	97.12	96.40	1.0912	1.1320
15	95.68	97.67	97.68	97.01	1.1514	1.1869
20	95.77	97.06	98.10	96.98	1.1707	1.2072
30	94.78	96.32	96.78	95.96	1.0476	1.0917
60	95.64	97.32	98.05	97.00	1.2357	1.2740
90	95.62	97.57	97.95	97.04	1.2471	1.2851
120	98.89	99.36	99.83	99.36	0.4687	0.4717

Table 17D The percentage of drug release from tSP 1:2 in 0.1 N HCl.

Time	% Drug release of tSP 1:2 in HCI					
	1	2	3	Av.	stdev	%RSD
1	2.68	2.61	3.30	2.86	0.3815	13.3187
3	13.79	16.20	18.82	16.27	2.5173	15.4699
5	25.39	28.93	30.02	28.11	2.4165	8.5957
7	35.81	38.99	39.20	38.00	1.9032	5.0082
10	45.10	46.11	47.56	46.25	1.2366	2.6735
13	48.55	49.73	49.88	49.39	0.7297	1.4775
15	50.21	51.28	52.02	51.17	0.9102	1.7788
17	51.70	52.96	52.75	52.47	0.6793	1.2946
20	53.10	54.13	54.53	53.92	0.7395	1.3716
30	55.73	57.01	57.12	56.62	0.7732	1.3655
60	61.19	61.82	62.43	61.81	0.6179	0.9996
90	63.67	64.17	64.51	64.12	0.4229	0.6597
120	65.64	65.47	66.02	65.71	0.2818	0.4288

Table 18D The percentage of drug release from tSP 1:2 phosphate buffer pH 6.8 solution.

Time	% Drug release of tSP 1:2 in PB					
	1	2	3	Av.	stdev	%RSD
1	11.35	12.10	17.93	13.79	3.6010	26.1066
3	32.70	35.86	42.18	36.92	4.8271	13.0754
5	52.18	57.27	67.72	59.06	7.9218	13.4135
7	69.43	76.16	78.82	74.80	4.8381	6.4677
10	91.79	92.59	91.91	92.10	0.4296	0.4665
13	92.53	92.93	92.18	92.54	0.3746	0.4048
17	92.47	93.19	92.19	92.62	0.5151	0.5562
20	92.44	93.13	92.59	92.72	0.3603	0.3885
30	91.53	92.48	91.53	91.85	0.5457	0.5941
60	93.00	93.74	92.45	93.06	0.6484	0.6968
90	92.86	93.37	92.38	92.87	0.4927	0.5306
120	91.11	93.39	92.80	92.43	1.1852	1.2823

Table 19D The percentage of drug release from tFD 1:1 in deionized water.

Time	% Drug release of tFD 1:1 in DI					
	1	2	3	Av.	stdev.	%RSD
0	0	0	0	0	0	0
1	32.65	38.88	34.70	35.41	3.1761	8.9688
3	80.89	88.11	86.32	85.11	3.7607	4.4187
5	93.75	96.57	92.23	94.19	2.2014	2.3373
7	93.86	96.99	91.87	94.24	2.5802	2.7379
10	94.83	96.91	91.55	94.43	2.7040	2.8636
13	95.47	97.02	92.22	94.90	2.4528	2.5845
15	95.42	96.14	92.70	94.75	1.8151	1.9156
17	94.98	95.80	93.15	94.64	1.3568	1.4336
20	94.69	96.37	95.51	95.52	0.8374	0.8766
60	94.60	97.12	93.30	95.01	1.9394	2.0413
90	95.23	97.63	93.89	95.01	1.9394	2.0413
120	96.02	96.72	93.25	95.58	1.8926	1.9801

Table 20D The percentage of drug release from tFD 1:1 in 0.1 N HCl.

Time	% Drug release of tFD 1:1 in HCl					
	1	2	3	Av.	stdev	%RSD
1	10.24	15.34	17.30	14.29	3.6446	25.5006
3	30.17	40.62	40.74	37.18	6.0680	16.3221
5	49.51	54.74	56.04	53.43	3.4563	6.4688
7	54.34	58.90	60.97	58.07	3.3886	5.8353
10	57.79	62.00	63.83	61.21	3.0925	5.0527
13	60.10	63.79	64.86	62.92	2.4939	3.9637
15	61.43	64.62	65.95	64.00	2.3244	3.6317
17	62.23	65.84	67.35	65.14	2.6316	4.0399
20	63.99	67.36	68.68	66.68	2.4153	3.6225
30	66.81	70.21	71.11	69.38	2.2689	3.2703
60	71.96	75.05	77.03	74.68	2.5547	3.4210
90	74.40	77.31	75.28	75.66	1.4923	1.9723
120	71.34	73.15	73.69	72.73	1.2287	1.6895

Table 21D The percentage of drug release from tFD 1:1 in phosphate buffer pH 6.8 solution.

Time	% Drug release of tFD 1:1 in PB					
	1	2	3	Av.	stdev	%RSD
1	31.95	26.93	32.13	30.34	2.9514	9.7279
3	78.11	72.92	72.91	74.65	2.9983	4.0165
5	89.38	92.17	92.75	91.43	1.8037	1.9728
7	89.01	92.70	93.36	91.69	2.3414	2.5536
10	89.64	93.23	93.44	92.10	2.1373	2.3205
13	89.83	93.60	94.35	92.59	2.4239	2.6179
15	89.87	93.80	93.51	92.39	2.1896	2.3698
17	90.50	93.72	93.43	92.55	1.7819	1.9254
20	90.07	93.01	93.10	92.06	1.7235	1.8721
30	91.13	92.94	93.47	92.51	1.2253	1.3245
60	90.85	92.32	93.23	92.14	1.2014	1.3039
90	90.33	93.20	93.72	92.42	1.8218	1.9713
120	90.48	93.31	93.49	92.43	1.6867	1.8250

Table 22D The percentage of drug release from tFD 1:2 in deionized water.

Time	% Drug release of tFD 1:2 in DI					
	1	2	3	Av.	stdev.	%RSD
1	31.98	29.12	35.52	32.21	3.2037	9.9478
3	59.41	59.49	72.95	63.95	7.7948	12.1894
5	78.19	81.03	95.61	84.94	9.3446	11.0009
7	94.76	99.08	105.72	99.85	5.5217	5.5298
10	100.25	104.79	105.44	103.49	2.8269	2.7314
13	100.14	105.57	105.70	103.81	3.1766	3.0601
15	99.99	105.71	105.54	103.75	3.2567	3.1391
17	100.49	105.20	105.75	103.81	2.8910	2.7848
20	100.80	104.82	106.28	103.97	2.8355	2.7273
30	101.38	104.48	106.34	104.07	2.5017	2.4039
60	100.99	104.28	106.96	104.08	2.9875	2.8705
90	100.38	103.88	106.70	103.65	3.1667	3.0551
120	100.62	104.90	106.34	103.95	2.9721	2.8592

Table 23D The percentage of drug release from tFD 1:2 in 0.1 N HCl.

Time	% Drug release of tFD 1:2 in HCl					
	1	2	3	Av.	stdev	%RSD
1	19.02	19.06	23.70	20.59	2.6882	13.0549
3	40.45	43.55	48.22	44.07	3.9080	8.8673
5	58.61	63.55	66.73	62.96	4.0914	6.4982
7	72.06	76.59	73.07	73.91	2.3812	3.2219
10	75.32	78.61	74.82	76.25	2.0611	2.7031
13	77.19	79.88	76.13	77.73	1.9333	2.4871
15	77.91	79.71	76.52	78.05	1.5995	2.0494
17	77.74	80.33	76.83	78.30	1.8142	2.3170
20	77.95	80.65	76.65	78.42	2.0367	2.5973
30	77.69	82.02	76.74	78.82	2.8147	3.5712
60	77.35	81.80	76.67	78.60	2.7881	3.5470
90	77.36	81.09	76.57	78.34	2.4152	3.0830
120	77.43	80.32	76.73	78.16	1.9054	2.4378

Table 24D The percentage of drug release from tFD 1:2 in phosphate buffer pH 6.8 solution.

Time	% Drug release of tFD 1:2 in PB					
	1	2	3	Av.	stdev	%RSD
1	18.12	28.08	27.84	24.68	5.6799	23.0147
3	51.25	60.94	67.02	59.74	7.9556	13.3175
5	66.51	81.40	86.73	78.21	10.4791	13.3984
7	79.76	91.45	93.23	88.15	7.3168	8.3005
10	91.06	92.27	93.36	92.23	1.1541	1.2513
13	91.60	92.53	93.02	92.38	0.7210	0.7804
15	91.58	92.03	93.01	92.21	0.7292	0.7908
17	91.71	92.80	93.88	92.80	1.0827	1.1667
20	91.63	92.80	93.75	92.73	1.0595	1.1426
30	91.94	93.20	94.03	93.05	1.0510	1.1294
60	92.04	93.22	94.01	93.09	0.9912	1.0647
90	93.39	94.18	94.64	94.07	0.6335	0.6734
120	92.65	93.08	93.51	93.08	0.4302	0.4621

Appendix E
Statistic analysis

The percentage of drug release at T_{30} of each preparation in different media was analyzed by using ANOVA to define the differences.

Table 1E ANOVA analysis of drug release at T_{30} in DI.

Multiple Comparisons

Dependent Variable: DI
Scheffe

(I) sample	(J) sample	Mean Difference (I-J)	Std. Error	Sig.	95% Confidence Interval	
					Lower Bound	Upper Bound
RM	SPRM	-30.5133*	1.47434	.000	-37.1202	-23.9065
	PM 11	-26.8467*	1.47434	.000	-33.4535	-20.2398
	PM 12	-27.2133*	1.47434	.000	-33.8202	-20.6065
	SP 11	-42.1267*	1.47434	.000	-48.7335	-35.5198
	SP 12	-36.9433*	1.47434	.000	-43.5502	-30.3365
	FD 11	-36.5067*	1.47434	.000	-43.1135	-29.8998
	FD 12	-44.9500*	1.47434	.000	-51.5568	-38.3432
	MOBIC	-20.8900*	1.47434	.000	-27.4968	-14.2832
SPRM	RM	30.5133*	1.47434	.000	23.9065	37.1202
	PM 11	3.6667	1.47434	.631	-2.9402	10.2735
	PM 12	3.3000	1.47434	.746	-3.3068	9.9068
	SP 11	-11.6133*	1.47434	.000	-18.2202	-5.0065
	SP 12	-6.4300	1.47434	.061	-13.0368	.1768
	FD 11	-5.9933	1.47434	.096	-12.6002	.6135
	FD 12	-14.4367*	1.47434	.000	-21.0435	-7.8298
	MOBIC	9.6233*	1.47434	.002	3.0165	16.2302
PM 11	RM	26.8467*	1.47434	.000	20.2398	33.4535
	SPRM	-3.6667	1.47434	.631	-10.2735	2.9402
	PM 12	-.3667	1.47434	1.000	-6.9735	6.2402
	SP 11	-15.2800*	1.47434	.000	-21.8868	-8.6732
	SP 12	-10.0967*	1.47434	.001	-16.7035	-3.4898
	FD 11	-9.6600*	1.47434	.001	-16.2668	-3.0532
	FD 12	-18.1033*	1.47434	.000	-24.7102	-11.4965
	MOBIC	5.9567	1.47434	.100	-.6502	12.5635
PM 12	RM	27.2133*	1.47434	.000	20.6065	33.8202
	SPRM	-3.3000	1.47434	.746	-9.9068	3.3068
	PM 11	.3667	1.47434	1.000	-6.2402	6.9735
	SP 11	-14.9133*	1.47434	.000	-21.5202	-8.3065
	SP 12	-9.7300*	1.47434	.001	-16.3368	-3.1232
	FD 11	-9.2933*	1.47434	.002	-15.9002	-2.6865
	FD 12	-17.7367*	1.47434	.000	-24.3435	-11.1298
	MOBIC	6.3233	1.47434	.068	-.2835	12.9302
SP 11	RM	42.1267*	1.47434	.000	35.5198	48.7335
	SPRM	11.6133*	1.47434	.000	5.0065	18.2202
	PM 11	15.2800*	1.47434	.000	8.6732	21.8868
	PM 12	14.9133*	1.47434	.000	8.3065	21.5202
	SP 12	5.1833	1.47434	.211	-1.4235	11.7902
	FD 11	5.6200	1.47434	.140	-.9868	12.2268
	FD 12	-2.8233	1.47434	.869	-9.4302	3.7835
	MOBIC	21.2367*	1.47434	.000	14.6298	27.8435
SP 12	RM	36.9433*	1.47434	.000	30.3365	43.5502
	SPRM	6.4300	1.47434	.061	-.1768	13.0368
	PM 11	10.0967*	1.47434	.001	3.4898	16.7035
	PM 12	9.7300*	1.47434	.001	3.1232	16.3368
	SP 11	-5.1833	1.47434	.211	-11.7902	1.4235
	FD 11	.4367	1.47434	1.000	-6.1702	7.0435
	FD 12	-8.0067*	1.47434	.010	-14.6135	-1.3998
	MOBIC	16.0533*	1.47434	.000	9.4465	22.6602
FD 11	RM	36.5067*	1.47434	.000	29.8998	43.1135
	SPRM	5.9933	1.47434	.096	-.6135	12.6002
	PM 11	9.6600*	1.47434	.001	3.0532	16.2668
	PM 12	9.2933*	1.47434	.002	2.6865	15.9002
	SP 11	-5.6200	1.47434	.140	-12.2268	.9868
	SP 12	-.4367	1.47434	1.000	-7.0435	6.1702
	FD 12	-8.4433*	1.47434	.006	-15.0502	-1.8365
	MOBIC	15.6167*	1.47434	.000	9.0098	22.2235
FD 12	RM	44.9500*	1.47434	.000	38.3432	51.5568
	SPRM	14.4367*	1.47434	.000	7.8298	21.0435
	PM 11	18.1033*	1.47434	.000	11.4965	24.7102
	PM 12	17.7367*	1.47434	.000	11.1298	24.3435
	SP 11	2.8233	1.47434	.869	-3.7835	9.4302
	SP 12	8.0067*	1.47434	.010	1.3998	14.6135
	FD 11	8.4433*	1.47434	.006	1.8365	15.0502
	MOBIC	24.0600*	1.47434	.000	17.4532	30.6668
MOBIC	RM	20.8900*	1.47434	.000	14.2832	27.4968
	SPRM	-9.6233*	1.47434	.002	-16.2302	-3.0165
	PM 11	-5.9567	1.47434	.100	-12.5635	.6502
	PM 12	-6.3233	1.47434	.068	-12.9302	.2835
	SP 11	-21.2367*	1.47434	.000	-27.8435	-14.6298
	SP 12	-16.0533*	1.47434	.000	-22.6602	-9.4465
	FD 11	-15.6167*	1.47434	.000	-22.2235	-9.0098
	FD 12	-24.0600*	1.47434	.000	-30.6668	-17.4532

*. The mean difference is significant at the .05 level.

Table 2E ANOVA analysis of drug release at T_{30} in 0.1 N HCl.

Multiple Comparisons

Dependent Variable: 0.1 N HCl
Dunnett C

(I) sample	(J) sample	Mean Difference (I-J)	Std. Error	95% Confidence Interval	
				Lower Bound	Upper Bound
RM	SPRM	-35.6867*	1.25706	-47.7212	-23.6521
	PM 11	-1.7667	.31740	-4.8053	1.2720
	PM 12	-.4633	.33178	-3.6396	2.7130
	SP 11	-41.0800*	.43397	-45.2347	-36.9253
	SP 12	-41.0500*	.54675	-46.2843	-35.8157
	FD 11	-53.8067*	1.34698	-66.7020	-40.9114
	FD 12	-63.2467*	1.65543	-79.0950	-47.3984
	MOBIC	4.7867*	.32323	1.6922	7.8811
SPRM	RM	35.6867*	1.25706	23.6521	47.7212
	PM 11	33.9200*	1.21703	22.2688	45.5712
	PM 12	35.2233*	1.22086	23.5354	46.9112
	SP 11	-5.3933	1.25250	-17.3841	6.5975
	SP 12	-5.3633	1.29590	-17.7696	7.0430
	FD 11	-18.1200*	1.78739	-35.2316	-1.0084
	FD 12	-27.5600*	2.02999	-46.9941	-8.1259
	MOBIC	40.4733*	1.21856	28.8074	52.1392
PM 11	RM	1.7667	.31740	-1.2720	4.8053
	SPRM	-33.9200*	1.21703	-45.5712	-22.2688
	PM 12	1.3033*	.10499	.2982	2.3084
	SP 11	-39.3133*	.29879	-42.1738	-36.4528
	SP 12	-39.2833*	.44708	-43.5634	-35.0032
	FD 11	-52.0400*	1.30969	-64.5784	-39.5016
	FD 12	-61.4800*	1.62524	-77.0392	-45.9208
	MOBIC	6.5533*	.07364	5.8484	7.2583
PM 12	RM	.4633	.33178	-2.7130	3.6396
	SPRM	-35.2233*	1.22086	-46.9112	-23.5354
	PM 11	-1.3033*	.10499	-2.3084	-.2982
	SP 11	-40.6167*	.31402	-43.6230	-37.6103
	SP 12	-40.5867*	.45740	-44.9656	-36.2078
	FD 11	-53.3433*	1.31325	-65.9158	-40.7709
	FD 12	-62.7833*	1.62810	-78.3700	-47.1966
	MOBIC	5.2500*	.12147	4.0871	6.4129
SP 11	RM	41.0800*	.43397	36.9253	45.2347
	SPRM	5.3933	1.25250	-6.5975	17.3841
	PM 11	39.3133*	.29879	36.4528	42.1738
	PM 12	40.6167*	.31402	37.6103	43.6230
	SP 12	.0300	.53616	-5.1029	5.1629
	FD 11	-12.7267	1.34271	-25.5812	.1278
	FD 12	-22.1667*	1.65196	-37.9818	-6.3516
	MOBIC	45.8667*	.30498	42.9470	48.7864
SP 12	RM	41.0500*	.54675	35.8157	46.2843
	SPRM	5.3633	1.29590	-7.0430	17.7696
	PM 11	39.2833*	.44708	35.0032	43.5634
	PM 12	40.5867*	.45740	36.2078	44.9656
	SP 11	-.0300	.53616	-5.1629	5.1029
	FD 11	-12.7567	1.38329	-25.9996	.4862
	FD 12	-22.1967*	1.68510	-38.3291	-6.0643
	MOBIC	45.8367*	.45123	41.5168	50.1566
FD 11	RM	53.8067*	1.34698	40.9114	66.7020
	SPRM	18.1200*	1.78739	1.0084	35.2316
	PM 11	52.0400*	1.30969	39.5016	64.5784
	PM 12	53.3433*	1.31325	40.7709	65.9158
	SP 11	12.7267	1.34271	-.1278	25.5812
	SP 12	12.7567	1.38329	-.4862	25.9996
	FD 12	-9.4400	2.08686	-29.4186	10.5386
	MOBIC	58.5933*	1.31111	46.0413	71.1453
FD 12	RM	63.2467*	1.65543	47.3984	79.0950
	SPRM	27.5600*	2.02999	8.1259	46.9941
	PM 11	61.4800*	1.62524	45.9208	77.0392
	PM 12	62.7833*	1.62810	47.1966	78.3700
	SP 11	22.1667*	1.65196	6.3516	37.9818
	SP 12	22.1967*	1.68510	6.0643	38.3291
	FD 11	9.4400	2.08686	-10.5386	29.4186
	MOBIC	68.0333*	1.62638	52.4631	83.6036
MOBIC	RM	-4.7867*	.32323	-7.8811	-1.6922
	SPRM	-40.4733*	1.21856	-52.1392	-28.8074
	PM 11	-6.5533*	.07364	-7.2583	-5.8484
	PM 12	-5.2500*	.12147	-6.4129	-4.0871
	SP 11	-45.8667*	.30498	-48.7864	-42.9470
	SP 12	-45.8367*	.45123	-50.1566	-41.5168
	FD 11	-58.5933*	1.31111	-71.1453	-46.0413
	FD 12	-68.0333*	1.62638	-83.6036	-52.4631

*. The mean difference is significant at the .05 level.

Table 3E ANOVA analysis of drug release at T_{30} in phosphate buffer pH 6.8.

Multiple Comparisons

Dependent Variable: PBS pH 6.4
Dunnett C

(I) sample	(J) sample	Mean Difference (I-J)	Std. Error	95% Confidence Interval	
				Lower Bound	Upper Bound
RM	SPRM	-12.4000	1.52206	-26.9715	2.1715
	PM 11	-.2100	1.68638	-16.3546	15.9346
	PM 12	2.2800	.41284	-1.6723	6.2323
	SP 11	-15.7567*	.57831	-21.2931	-10.2202
	SP 12	-11.0667*	.48323	-15.6929	-6.4405
	FD 11	-11.7333*	.79690	-19.3624	-4.1042
	FD 12	-12.2767*	.70879	-19.0622	-5.4911
	MOBIC	7.1233	1.18797	-4.2497	18.4964
SPRM	RM	12.4000	1.52206	-2.1715	26.9715
	PM 11	12.1900	2.21225	-8.9891	33.3691
	PM 12	14.6800*	1.49018	.4137	28.9463
	SP 11	-3.3567	1.54423	-18.1404	11.4271
	SP 12	1.3333	1.51120	-13.1341	15.8008
	FD 11	.6667	1.63867	-15.0212	16.3545
	FD 12	.1233	1.59768	-15.1721	15.4188
	MOBIC	19.5233*	1.86050	1.7117	37.3349
PM 11	RM	.2100	1.68638	-15.9346	16.3546
	SPRM	-12.1900	2.21225	-33.3691	8.9891
	PM 12	2.4900	1.65766	-13.3796	18.3596
	SP 11	-15.5467	1.70641	-31.8831	.7897
	SP 12	-10.8567	1.67658	-26.9074	5.1941
	FD 11	-11.5233	1.79233	-28.6822	5.6356
	FD 12	-12.0667	1.75493	-28.8675	4.7342
	MOBIC	7.3333	1.99717	-11.7866	26.4533
PM 12	RM	-2.2800	.41284	-6.2323	1.6723
	SPRM	-14.6800*	1.49018	-28.9463	-.4137
	PM 11	-2.4900	1.65766	-18.3596	13.3796
	SP 11	-18.0367*	.48827	-22.7112	-13.3622
	SP 12	-13.3467*	.37078	-16.8963	-9.7970
	FD 11	-14.0133*	.73417	-21.0420	-6.9847
	FD 12	-14.5567*	.63745	-20.6593	-8.4540
	MOBIC	4.8433	1.14684	-6.1360	15.8226
SP 11	RM	15.7567*	.57831	10.2202	21.2931
	SPRM	3.3567	1.54423	-11.4271	18.1404
	PM 11	15.5467	1.70641	-.7897	31.8831
	PM 12	18.0367*	.48827	13.3622	22.7112
	SP 12	4.6900	.54908	-.5666	9.9466
	FD 11	4.0233	.83846	-4.0037	12.0504
	FD 12	3.4800	.75522	-3.7501	10.7101
	MOBIC	22.8800*	1.21625	11.2362	34.5238
SP 12	RM	11.0667*	.48323	6.4405	15.6929
	SPRM	-1.3333	1.51120	-15.8008	13.1341
	PM 11	10.8567	1.67658	-5.1941	26.9074
	PM 12	13.3467*	.37078	9.7970	16.8963
	SP 11	-4.6900	.54908	-9.9466	.5666
	FD 11	-.6667	.77594	-8.0952	6.7619
	FD 12	-1.2100	.68514	-7.7692	5.3492
	MOBIC	18.1900*	1.17402	6.9505	29.4295
FD 11	RM	11.7333*	.79690	4.1042	19.3624
	SPRM	-.6667	1.63867	-16.3545	15.0212
	PM 11	11.5233	1.79233	-5.6356	28.6822
	PM 12	14.0133*	.73417	6.9847	21.0420
	SP 11	-4.0233	.83846	-12.0504	4.0037
	SP 12	.6667	.77594	-6.7619	8.0952
	FD 12	-.5433	.93325	-9.4778	8.3912
	MOBIC	18.8567*	1.33411	6.0845	31.6288
FD 12	RM	12.2767*	.70879	5.4911	19.0622
	SPRM	-.1233	1.59768	-15.4188	15.1721
	PM 11	12.0667	1.75493	-4.7342	28.8675
	PM 12	14.5567*	.63745	8.4540	20.6593
	SP 11	-3.4800	.75522	-10.7101	3.7501
	SP 12	1.2100	.68514	-5.3492	7.7692
	FD 11	.5433	.93325	-8.3912	9.4778
	MOBIC	19.4000*	1.28343	7.1131	31.6869
MOBIC	RM	-7.1233	1.18797	-18.4964	4.2497
	SPRM	-19.5233*	1.86050	-37.3349	-1.7117
	PM 11	-7.3333	1.99717	-26.4533	11.7866
	PM 12	-4.8433	1.14684	-15.8226	6.1360
	SP 11	-22.8800*	1.21625	-34.5238	-11.2362
	SP 12	-18.1900*	1.17402	-29.4295	-6.9505
	FD 11	-18.8567*	1.33411	-31.6288	-6.0845
	FD 12	-19.4000*	1.28343	-31.6869	-7.1131

*. The mean difference is significant at the .05 level.

All statistic analysis were calculated using SPSS version 11.1.

VITA

Miss Petcharat Kornanansiri was born on August 31st 1980, in Bangkok, Thailand. She received her Bachelor of Science in Pharmacy in 2001 from the Faculty of Pharmaceutical Sciences, Silpakorn University, Nakornpathom, Thailand. She continued studying in the Master's Degree in Industrial Pharmacy Program in the Faculty of Pharmaceutical Sciences, Chulalongkorn University, Bangkok, Thailand. During study in the Master's Degree, she received a grant from the Chulalongkorn-Chiba Pharmaceutical Student Exchange Program in 2004.